

ÁLVARO JAVIER ÁVILA DÍAZ

**ASSESSING CURRENT AND FUTURE CHANGES IN EXTREME CLIMATE
EVENTS IN BRAZIL**

Thesis submitted to the Applied Meteorology
Graduate Program of the Universidade Federal de
Viçosa in partial fulfillment of the requirements for
the degree of *Doctor Scientiae*.

Adviser: Flávio Barbosa Justino

Co-adviser: Roger Rodrigues Torres

**VIÇOSA - MINAS GERAIS
2020**

**Ficha catalográfica preparada pela Biblioteca Central da Universidade
Federal de Viçosa - Câmpus Viçosa**

T

Ávila Díaz, Álvaro Javier, 1990-
A958a Assessing current and future changes in extreme climate
2020 events in Brazil / Álvaro Javier Ávila Díaz. – Viçosa, MG, 2020.
112 f. : il. (algumas color.) ; 29 cm.

Texto em inglês.

Inclui anexos.

Orientador: Flávio Barbosa Justino.

Tese (doutorado) - Universidade Federal de Viçosa.

Referências bibliográficas: f. 104-112.

1. Mudanças climáticas - Brasil. 2. Extremos climáticos - Índices. 3. Bacias hidrográficas. I. Universidade Federal de Viçosa. Departamento de Engenharia Agrícola. Programa de Pós-Graduação em Meteorologia Aplicada. II. Título.

CDD 22. ed. 551.6981


ÁLVARO JAVIER ÁVILA DÍAZ

**ASSESSING CURRENT AND FUTURE CHANGES IN EXTREME CLIMATE
EVENTS IN BRAZIL**

Thesis submitted to the Applied Meteorology
Graduate Program of the Universidade Federal de
Viçosa in partial fulfillment of the requirements for
the degree of *Doctor Scientiae*.

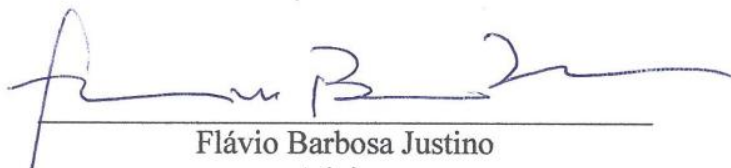
APPROVED: February 21, 2020.

Assent:



Alvaro Javier Avila Díaz

Author



Flávio Barbosa Justino

Adviser

ACKNOWLEDGEMENTS

To God for showing me the positive point of view of this complex world.

To the Federal University of Viçosa, for the opportunity to take the course.

This study was financed in part by the Coordenação de Aperfeiçoamento de Pessoal de Nível Superior – Brasil (CAPES) – Finance Code 001 and the Minas Gerais Research Foundation (FAPEMIG).

I greatly thank my advisor Flavio Barbosa Justino for his support and his patience. Many thanks for giving your guidance and for instilling in me the motivation to produce good science. Many thanks also go to my co-advisor Roger Rodrigues Torres, who explained to me a lot of things about the climate extremes chaotic world and for making me feel more confident with my work.

I sincerely thank Aaron B. Wilson and David Bromwich for the opportunity to learn more about atmospheric sciences during my visit to Ohio State University, USA.

To Graça Freitas, secretary of the Graduate Program in Applied Meteorology, for the assistance given during my graduate studies.

To my friends Wilmar Loiza and Cristian Zuluaga thanks for the critical reviews with my papers and for the friendship during my graduate studies. To my colleagues Alex Silva, Vanucia, and Hugo Thaner support me in many aspects as a graduate student. Special thanks to Gabriel Abrahão and Victor Benezoli for the dynamically-friendly working environment, always with exciting conversations and guidance with my code struggles. Also, to Guilherme Martins for developed the excellent guides to handle with CDO and NCL.

I own my deepest gratitude to my family, Elizabeth, Arnaldo, Fernando, Julian, Sandra, Valeria and Martin for their support and encouragement throughout over the last years. *“Gracias infinitas Chavita y Ara por todo el AMOR, paciencia y dedicación que tuvieron desde que nací, ahora lo comprendo, no es una tarea fácil, criar y dejar ir a un hijo”*. Special thanks goes to my “brothers” Alvaro and Santiago for their support during the last couple of decades.

I would like to show my appreciation to Marcia, Cláudio, Ana Cristina and Guilherme who supported in all aspects of my life (*Obrigado para sempre*).

To my wife Ana Claudia that helped me at crucial personal/professional times. Thank you for the comprehension at the moments when the struggles seemed too unbearable. But the most important, thanks for the good/excellent/wonderful moments that you and Lelete shared with me (*Obrigado meu amor*).

Finally, to all who directly/indirectly contributed to finished this journey.

“Promise me, boy, if thou get a master, work for him as hard as thou canst. If he does not appreciate all thou do, never mind. Remember, work, well-done, does good to the man who does it. It makes him a better man.”

George S. Clason

“All models are wrong, but some are useful”

George Edward Pelham Box

ABSTRACT

ÁVILA DÍAZ, Álvaro Javier, D.Sc., Universidade Federal de Viçosa, February, 2020. **Assessing Current and Future Changes in Extreme Climate Events in Brazil**. Adviser: Flávio Barbosa Justino. Co-adviser: Roger Rodrigues Torres.

Brazil is vulnerable to climatic variability, especially those related to climate extremes of the air temperature and precipitation because they provide expressive losses related to agricultural activities and the management of water resources. Climate change is expected to have a likely negative socio-economic impact, increasing the number of natural disasters in regions where climate change will be more pronounced. The main objective of this study was to evaluate the current and future changes of the climatic extremes in Brazil. To understand the magnitude of these changes, extremes of temperature and precipitation set by the team of experts from the climate extremes indices defined by the Expert Team on Climate Change Detection and Indices (ETCCDI) were selected. The first part of the research evaluated the performance of 25 Earth System Models (ESMs) in representing the variability of climatic extremes for the period between 1980 and 2005. ESMs use statistical and dynamic downscaling to reduce the original horizontal scale, which ranges from 1-3° for a spatial resolution of 0.25 ° (~ 25 km latitude/longitude). Statistical downscaling data were obtained from the National Aeronautics and Space Administration Earth Exchange Global Daily Downscaled Projections (NEX-GDDP). Dynamic downscaling data was provided by the National Institute for Space Research (INPE). The results showed that the obtained indices, using ESM downscaling, were similar to the observed climate indices, although the performance metrics revealed that climate extremes are not adequately represented in the Amazon basin. In addition, there are uncertainties in heat wave simulations for almost all models. In general, the average of the set of simulations of the ESMs, or multi-model ensemble (MME), that used statistical downscaling has the best results in comparison to any individual model. The second part of the work, aimed to assess the trend and magnitude of climate extremes in the last four decades (1980-2016) using several databases (e.g., observations and reanalysis). The projected changes in the extreme indices up to the middle of the 21st century (2046-2065) and the end of the 21st century (2081–2100) in relation to the 1986-2005 reference period were also analyzed. Future climate changes were analyzed from the ensemble of 20 downscaled ESMs of the NEX-GDDP dataset. For the historical period (1980-2016), temperature-related indices showed consistent heating patterns across Brazil with increasing trends on hot days/nights and decreasing trends for cold days/nights. Also, a similar warming pattern is projected for the mid and late 21st century. For precipitation-related

indices, observations show an increase in consecutive dry days and a reduction in consecutive wet days in almost all of Brazil from 1980-2016. Additionally, future scenarios indicate that the frequency and intensity of extremely wet days are likely to be more intense. The results of this research aim to contribute to the current understanding of extreme weather events in Brazil, in order to provide further essential insights for studies of impact, adaptation and vulnerability to climate change.

Keywords: Extreme climate indices. Hydrological Basins. Climate Change. Trends. CMIP5. Downscaling.

RESUMO

ÁVILA DÍAZ, Álvaro Javier, D.Sc., Universidade Federal de Viçosa, fevereiro de 2020. **Avaliação das mudanças atuais e futuras dos eventos climáticos extremos no Brasil.** Orientador: Flávio Barbosa Justino. Coorientador: Roger Rodrigues Torres.

O Brasil é vulnerável às variabilidades climáticas, principalmente àquelas relacionadas aos eventos extremos de temperatura do ar e precipitação, por propiciarem expressivas perdas relacionadas às atividades agrícolas e à gestão dos recursos hídricos. Adicionalmente, espera-se que as alterações no sistema climático relacionadas às mudanças climáticas tenham impactos socioeconômicos negativos por meio do aumento no número de desastres naturais em regiões onde tais alterações serão mais pronunciadas. O objetivo principal deste estudo foi avaliar as mudanças atuais e futuras dos extremos climáticos no Brasil. Para entender a magnitude dessas mudanças, foram selecionados extremos de temperatura e precipitação estabelecidos pela equipe de especialistas do Programa Mundial de Pesquisa Climática em Detecção e Índices de Mudanças Climáticas (ETCCDI). A primeira parte da pesquisa avaliou o desempenho de 25 modelos do sistema terrestre (ESMs) em representar a variabilidade dos extremos climáticos para o período entre 1980 e 2005. Os ESMs usam downscaling estatístico e dinâmico para reduzir a escala horizontal original, que oscila entre 1-3° para uma resolução espacial de 0,25° (~25 km de latitude/longitude). Os dados do downscaling estatístico foram obtidos da *National Aeronautics and Space Administration Earth Exchange Global Daily Downscaled Projections* (NEX-GDDP). Os dados do downscaling dinâmico foram fornecidos pelo Instituto Nacional de Pesquisas Espaciais (INPE). Os resultados mostraram que os índices obtidos, usando os downscaling dos ESMs, foram semelhantes aos índices climáticos observados, embora as métricas de desempenho revelaram que os extremos climáticos não são representados adequadamente na bacia Amazônica. Adicionalmente, existem grandes incertezas nas simulações de ondas de calor para quase todos os modelos. Em geral, a média do conjunto de simulações dos ESMs, ou multi-model ensemble (MME), que usaram downscaling estatístico tem os melhores resultados em comparação a qualquer modelo individual. A segunda parte do trabalho, teve como objetivo avaliar a tendência e a magnitude dos extremos climáticos nas últimas quatro décadas (1980-2016) usando vários bancos dados (e.g., observações e reanálises). Também foram analisadas as mudanças projetadas nos índices extremos até meados do século XXI (2046-2065) e final do século XXI (2081-2100) em relação ao período de referência 1986-2005. As mudanças climáticas futuras foram analisadas a partir da MME de 20 ESMs do conjunto de dados NEX-GDDP. Para o período histórico (1980-2016) os índices

relacionados à temperatura mostraram padrões de aquecimento consistentes em todo o Brasil com tendências de aumento nos dias/noites quentes e tendência decrescentes para dias/noites frias. Além disso, um padrão de aquecimento semelhante é projetado para meados e final do século XXI. Para os índices relacionados à precipitação, as observações mostram um aumento nos dias secos consecutivos e uma redução de dias úmidos consecutivos em quase todo o Brasil entre 1980-2016. Adicionalmente, as projeções dos cenários futuros indicam que a frequência e a intensidade de dias extremamente úmidos deverão ser mais intensos. Os resultados desta pesquisa almejam contribuir o atual entendimento dos eventos climáticos extremos no Brasil, no intuito de fornecer subsídios essenciais para os estudos de impacto, adaptação e vulnerabilidade às mudanças climáticas.

Palavras-chave: Bacias hidrográficas. Índices Climáticos Extremos. Mudanças Climáticas. Tendências. CMIP5. Downscaling.

LIST OF ILLUSTRATIONS

Figure 2.1 Geographical location of the eight hydrological basins in Brazil according to the Brazilian National Water Authority (ANA) classification-	31
Figure 2.2 Climatology bias for the annual maximum of daily maximum temperature - TXx (°C) for 21 statically (NEX-GDDP; models 1-21) and 4 dynamically (Eta-INPE; models 22-25) downscaled models, MME-Sta (26), MME-Dyn (27), and GMFD (28) from 1980 to 2005. Climatology for TXx in the observations dataset (OBS-BR; gray rectangle dataset 29) for 1980-2005.....	32
Figure 2.3 Statistics of performance obtained for annual temperature indices for statically (NEX-GDDP) and dynamically (Eta-INPE) downscaled models, MME-Sta, MME-Dyn, and GMFD from 1980 to 2005 over eight hydrological basins (Fig. 2.1). (a) Percent Bias (PBIAS); (b) RMSE-observations standard deviation ratio (RSR); (c) a refined index of model performance (dr); (d) Correlation coefficients (CORR; the diagonal lines indicate significant correlations at 95% level). The horizontal purple lines refer to Eta-INPE datasets. For PBIAS and RSR, dark colors indicate models that perform worse than others, on average, and light colors indicate models that perform better than others, on average. Furthermore, for dr and CORR, dark (light) colors show models that have better (worse) statistical metrics than others, on average	33
Figure 2.4 As in Fig. 2.2, but for extreme temperature indices in summer (DJF) and winter (JJA). The nomenclature of the ETCCDI indices was adapted to Index-“S” for summer and Index-“W” for winter	34
Figure 2.5 Trends per decade from 1980 to 2005 for temperature indices at the annual scale (a-h) for 21 NEX-GDDP climate models (1-21), 4 Eta-INPE climate models (22-25), MME-Sta (26), MME-Dyn (27), GMFD (28) and OBS-BR over eight hydrological regions in Brazil (Fig. 2.1). Diagonal lines indicate significant trends at 95% level. The vertical purple lines refer to ESMs from Eta-INPE datasets.	37
Figure 2.6 Trends (°C/decade) in hottest days (TXx) for 21 NEX-GDDP climate models (1-21), 4 Eta-INPE Models (22-25), MME-Sta (26), MME-Dyn (27), GMFD (28) and OBS-BR (29; gray rectangle) from 1980 to 2005. Hatching indicates where trends are significant at the 95% level.....	38
Figure 2.7 Climatology bias for the annual total wet-day precipitation - PRCPTOT (mm) for 21 statically (NEX-GDDP; models 1-21) and 4 dynamically (Eta-INPE; models 22-25) downscaled models, MME-Sta (26), MME-Dyn (27), and GMFD (28) from 1980 to 2005. Climatology for PRCPTOT in the observations dataset (OBS-BR; gray rectangle dataset 29) for 1980-2005.	39
Figure 2.8 Statistics of performance obtained for annual precipitation indices for statically (NEX-GDDP) and dynamically (Eta-INPE) downscaled models, MME-Sta, MME-Dyn, and GMFD from 1980 to 2005 over eight hydrological basins (Fig. 2.1). (a) Percent Bias (PBIAS); (b) RMSE-observations standard deviation ratio (RSR); (c) a refined index of model performance (dr); (d) Correlation coefficients (CORR; the diagonal lines indicate significant correlations at 95% level). The horizontal purple lines refer to Eta-INPE datasets. For PBIAS and RSR, dark colors indicate models that perform worse than others, on average, and light colors indicate models that perform better than others, on average. Furthermore, for dr and CORR, dark (light) colors show models that have better (worse) statistical metrics than others, on average	40

Figure 2.9 As in Fig. 2.8, but for extreme precipitation indices in summer (DJF) and winter (JJA). The nomenclature of the ETCCDI indices was adapted to Index-“S” for summer and Index-“W” for winter	42
Figure 2.10 Trends per decade from 1980 to 2005 for precipitation indices at the annual scale (a-h) for 21 NEX-GDDP climate models (1-21), 4 Eta-INPE climate models (22-25), MME-Sta (26), MME-Dyn (27), GMFD (28) and OBS-BR over eight hydrological regions in Brazil (Fig. 2.1). Diagonal lines indicate significant trends at 95% level. The vertical purple lines refer to ESMs from Eta-INPE datasets.	45
Figure 2.11 Trends (days/decade) in annual total wet-day precipitation - PRCPTOT (mm) for 21 NEX-GDDP climate models (1-21), 4 Eta-INPE climate models (22-25), MME-Sta (26), MME-Dyn (27), GMFD (28) and OBS-BR (29; gray rectangle) from 1980 to 2005. Hatching indicates where trends are significant at the 95% level.	46
Figure 2.12 Model rank (MR) value for temperature (a) and precipitation indices (b) at the annual scale. Each symbol represents a given basin. White, gray and yellow areas refer to 21 NEX-GDDP climate models, four (4) Eta-INPE climate models and multi-model ensembles (MMEs), respectively	48
Figure S2.1 Climatology for the coldest night – TNn for 21 NEX-GDDP climate models (1-21), 4 Eta-INPE models (22-25), MME-Sta (26), MME-Dyn (27), GMFD (28) and OBS-BR (29; gray rectangle) from 1980 to 2005. (b) Climatology bias for 1980-2005	52
Figure S2.2 Climatology for diurnal temperature range – DTR for 21 NEX-GDDP climate models (1-21), 4 Eta-INPE models (22-25), MME-Sta (26), MME-Dyn (27), GMFD (28) and OBS-BR (29; gray rectangle) from 1980 to 2005. (b) Climatology bias for 1980-2005	53
Figure S2.3 Climatology for cool nights – TN10p for 21 NEX-GDDP climate models (1-21), 4 Eta-INPE models (22-25), MME-Sta (26), MME-Dyn (27), GMFD (28) and OBS-BR (29; gray rectangle) from 1980 to 2005. (b) Climatology bias for 1980-2005	54
Figure S2.4 Climatology for warm nights – TN90p for 21 NEX-GDDP climate models (1-21), 4 Eta-INPE models (22-25), MME-Sta (26), MME-Dyn (27), GMFD (28) and OBS-BR (29; gray rectangle) from 1980 to 2005. (b) Climatology bias for 1980-2005	55
Figure S2.5 Climatology for cool days – TX10p for 21 NEX-GDDP climate models (1-21), 4 Eta-INPE models (22-25), MME-Sta (26), MME-Dyn (27), GMFD (28) and OBS-BR (29; gray rectangle) from 1980 to 2005. (b) Climatology bias for 1980-2005	56
Figure S2.6 Climatology for warm days – TX90p for 21 NEX-GDDP climate models (1-21), 4 Eta-INPE models (22-25), MME-Sta (26), MME-Dyn (27), GMFD (28) and OBS-BR (29; gray rectangle) from 1980 to 2005. (b) Climatology bias for 1980-2005	57
Figure S2.7 Climatology for warm spell duration indicator – WSDI for 21 NEX-GDDP climate models (1-21), 4 Eta-INPE models (22-25), MME-Sta (26), MME-Dyn (27), GMFD (28) and OBS-BR (29; gray rectangle) from 1980 to 2005. (b) Climatology bias for 1980-2005	58
Figure S2.8 Trends per decade from 1980 to 2005 for temperature indices at the seasonal scale (a-h) for 21 NEX-GDDP models, 4 Eta-INPE models, MME-Sta, and MME-Dyn over eight hydrological basins in Brazil (Fig. 2.1). Diagonal lines indicate significant trends at 5% level. The vertical purple lines refer to ESMs from Eta-INPE datasets. The nomenclature of the ETCCDI indices was adapted to Index-“S” for summer and Index-“W” for winter	59

Figure S2.9 Climatology for max 1-day precipitation – RX1day for 21 NEX-GDDP climate models (1-21), 4 Eta-INPE models (22-25), MME-Sta (26), MME-Dyn (27), GMFD (28) and OBS-BR (29; gray rectangle) from 1980 to 2005. (b) Climatology bias for 1980-2005	60
Figure S2.10 Climatology for max 5-day precipitation – RX5day for 21 NEX-GDDP climate models (1-21), 4 Eta-INPE models (22-25), MME-Sta (26), MME-Dyn (27), GMFD (28) and OBS-BR (29; gray rectangle) from 1980 to 2005. (b) Climatology bias for 1980-2005	61
Figure S2.11 Climatology for very wet days – R95p for 21 NEX-GDDP climate models (1-21), 4 Eta-INPE models (22-25), MME-Sta (26), MME-Dyn (27), GMFD (28) and OBS-BR (29; gray rectangle) from 1980 to 2005. (b) Climatology bias for 1980-2005.....	62
Figure S2.12 Climatology for simple daily intensity index – SDII for 21 NEX-GDDP climate models (1-21), 4 Eta-INPE models (22-25), MME-Sta (26), MME-Dyn (27), GMFD (28) and OBS-BR (29; gray rectangle) from 1980 to 2005. (b) Climatology bias for 1980-2005	63
Figure S2.13 Climatology for number of very heavy precipitation days – R20mm for 21 NEX-GDDP climate models (1-21), 4 Eta-INPE models (22-25), MME-Sta (26), MME-Dyn (27), GMFD (28) and OBS-BR (29; gray rectangle) from 1980 to 2005. (b) Climatology bias for 1980-2005.....	64
Figure S2.14 Climatology for consecutive wet days – CWD for 21 NEX-GDDP climate models (1-21), 4 Eta-INPE models (22-25), MME-Sta (26), MME-Dyn (27), GMFD (28) and OBS-BR (29; gray rectangle) from 1980 to 2005. (b) Climatology bias for 1980-2005	65
Figure S2.15 Climatology for consecutive dry days – CDD for 21 NEX-GDDP climate models (1-21), 4 Eta-INPE models (22-25), MME-Sta (26), MME-Dyn (27), GMFD (28) and OBS-BR (29; gray rectangle) from 1980 to 2005. (b) Climatology bias for 1980-2005	66
Figure S2.16 Trends per decade from 1980 to 2005 for precipitation indices at the seasonal scale (a-h) for 21 NEX-GDDP models, 4 Eta-INPE models, MME-Sta, and MME-Dyn over eight hydrological basins in Brazil (Fig. 2.1). Diagonal lines indicate significant trends at 5% level. The vertical purple lines refer to ESMs from Eta-INPE datasets. The nomenclature of the ETCCDI indices was adapted to Index-“S” for summer and Index-“W” for winter.	67
Figure 3.1 Hydrological basins in Brazil according to the Brazilian National Water Authority (ANA)	74
Figure 3.2 Evaluation metrics for temperature indices for ERA5 and GMFD with respect to the observational dataset (OBS-BR) from 1980 to 2016 over the eight hydrological basins in Brazil. (a) Bias in percentage (PBIAS) (b) RMSE-observations standard deviation ratio (RSR); (c) refined index of model performance (dr); (d) Pearson correlation coefficients (CORR); diagonal black lines indicate correlation values statistically significant correlations at 95% confidence level.....	75
Figure 3.3 The 1980-2016 climatology and bias for TXx (a-b) and TNn (c-d) for OBS-BR (black rectangle; gridded observations), ERA5, and GMFD. Figures for additional temperature indices are in Supplementary Material.....	77
Figure 3.4 Evaluation metrics for precipitation indices for ERA5 and GMFD with respect to the observational dataset (OBS-BR) from 1980 to 2016 over the eight hydrological basins in Brazil.	

(a) Bias in percentage (PBIAS) (b) RMSE-observations standard deviation ratio (RSR); (c) refined index of model performance (dr); (d) Pearson correlation coefficients (CORR); diagonal black lines indicate correlation values statistically significant correlations at the 95% confidence level. 78

Figure 3.5 The 1980-2016 climatology and bias for PRCPTOT (a-b) and CDD (c-d) for OBS-BR (black rectangle; gridded observations), ERA5, and GMFD. Figures for additional precipitation indices are in Supplementary Material. 79

Figure 3.6 Decadal trends in TXx (a), TNn (b), TN10p (c), and TX90p (d) during the period 1980–2016 for OBS-BR (black rectangle; gridded observations), ERA5, and GMFD. Hatching indicates where trends are significant at the 95% level. Trends for additional temperature indices are in Supplementary Material..... 81

Figure 3.7 Decadal trends in PRCPTOT (a), R95p (b), R20mm (c), and CDD (d) during the period 1980–2016 for OBS-BR (black rectangle; gridded observations), ERA5, GMFD, and MSWEP. Stippling indicates where trends are significant at the 95% level. Trends for additional precipitation indices are in Supplementary Material. 84

Figure 3.8 Projected changes in the hottest day–TXx (a-b), coldest night–TNn (c-d), cool nights – TN10p (e-f) and Warm days – TX90p (g-h) over the period 2046-2065 (white zone) and 2081-2100 (yellow zone) relative to the reference period (1986–2005) for RCP4.5 (black line) and RCP8.5 (red line). Regional mean changes are shown for each hydrological regions; the acronyms are defined in Fig. 3.1. The boxes indicate the variability of the ensemble of the downscaled models– MME (Table S3.1), which include the interquartile range (25th–75th percentiles), median (horizontal line), mean (black dots), maximum and minimum values (black circles). 85

Figure 3.9 Future changes of multi-model ensemble in temperature extremes indices under the (a-h) RCP4.5 and (i-p) RCP8.5 scenarios for the period 2046-2065 relative to the reference period (1986–2005). Stippling indicates grid-points where more than 66 percent of the models agreed in change signal and in which more than 50 percent of the models show a significant change. 86

Figure 3.10 As Fig. 3.7 but for the annual total wet-day precipitation - PRCPTOT (a-b), very wet days–R95p (c-d), Number of heavy precipitation days–R20mm (e-f), and consecutive dry days–CDD (h-g)..... 88

Figure 3.11 Future changes of multi-model ensemble in precipitation extremes indices under the (a-h) RCP4.5 and (i-p) RCP8.5 scenarios for the period 2046-2065 relative to the reference period (1986–2005). Stippling indicates grid-points where more than 66 percent of the models agreed in change signal and in which more than 50 percent of the models show a significant change 89

Figure S3.1 The 1980-2016 climatology and bias of the DTR (a-b), TN10p (c-d), TN90p (e-f), TX10p (g-h), TX90p (i-j) and WSDI (k-l) for OBS-BR (black rectangle; gridded observations), ERA5 and GMFD 93

Figure S3.2 The 1980-2016 climatology and bias of the RX1day (a-b), RX5day (c-d), R95p (e-f), SDII (g-h), R20mm (i-j) and CWD (k-l) for OBS-BR (black rectangle; gridded observations), ERA5, GMFD and MSWEP 94

Figure S3.3 Decadal trends in DTR (c), TN90p (d), TX10p (a), and WSDI (b) during the period 1980–2016 for OBS-BR (black rectangle; gridded observations), ERA5 and GMFD. Hatching indicates where trends are significant at the 95% level.....	95
Figure S3.4 Decadal trends in RX1day (a), RX5day (b), R95p (c), and SDII (d) during the period 1980–2016 for OBS-BR (black rectangle; gridded observations), ERA5 and GMFD. Hatching indicates where trends are significant at the 95% level.....	96
Figure S3.5 Projected changes in temperature indices (a-f) over the period 2046-2065 (white zone) and 2081-2100 (yellow zone) relative to the reference period (1986–2005) for RCP4.5 (black line) and RCP8.5 (red line). Regional mean changes are shown for each hydrological regions (Fig 1).....	97
Figure S3.6 Future changes of multi-model ensemble in temperature extremes indices under the (a-h) RCP4.5 and (i-p) RCP8.5 scenarios for the period 2081-2100 relative to the reference period (1986–2005). Stippling indicates grid-points where more than 66 percent of the models agreed in change signal and in which more than 50 percent of the models show a significant change	98
Figure S3.7 Projected changes in precipitation indices (a-f) over the period 2046-2065 (white zone) and 2081-2100 (yellow zone) relative to the reference period (1986–2005) for RCP4.5 (black line) and RCP8.5 (red line). Regional mean changes are shown for each hydrological regions (Fig. 3.1)	99
Figure S3.8 Future changes of multi-model ensemble in precipitation extremes indices under the (a-h) RCP4.5 and (i-p) RCP8.5 scenarios for the period 2081-2100 relative to the reference period (1986–2005). Stippling indicates grid-points where more than 66 percent of the models agreed in change signal and in which more than 50 percent of the models show a significant change	100

LIST OF TABLES

Table 2.1 The extreme temperature and precipitation indices used in this study recommended by the ETCCDI. More details on definitions of the core indices given at http://etccdi.pacificclimate.org/list_27_indices.shtml	26
Table 2.2 Information on the 25 general circulation models used in the present analysis. (a) ESMs used for generating the NEX-GDDP dataset through statistical downscaling. (b) ESMs used as boundary conditions to generate the Eta-INPE dataset through dynamical downscaling	28
Table 2.3 Ranking of downscaled ESMs and MMEs for temperature and precipitation indices at the annual scale over Brazil. Downscaled models or MMEs in bold achieve a skill score ≥ 0.85 . The optimal value of M_R is 1.0	47
Table S2.1 Ranking of downscaled ESMs and MMEs for temperature and precipitation indices at seasonal scale over Brazil. Downscaled models or MMEs in bold achieve a skill score ≥ 0.85 . The optimal value of M_R is 1.0.	51
Table 3.1 Extreme climate indices employed in this study as recommended by ETCCDI. The full list of indices and precise definitions are provided at http://etccdi.pacificclimate.org/list_27_indices.shtml . Abbreviations are as follows: TX (TN), daily maximum (maximum) temperature. A wet (dry) day is defined when precipitation ≥ 1 mm (PR<1mm).	70
Table 3.2 Characteristics of (a) gridded observations, (b) reanalyses, and (c) merged datasets. Variables are precipitation (PR), maximum temperature (TX) and minimum temperature (TN)	71
Table 3.3 Decadal trends in temperature indices over the period 1980-2016. Values in bold indicate trends are significant at the 95% level. Colors signify cooling (blue), warming (red), or no trend (white)	80
Table 3.4 Decadal trends in precipitation indices over the period 1980-2016. Values in bold indicate trends are significant at 95% level. Colors signify wetting (blue), drying (yellow), or no trend (white).	82
Table S3.1 The downscaled Earth System Models (ESMs) with a statistical downscaling ..	92

LIST OF ACRONYMS AND ABBREVIATIONS

AMZ	Amazon River
CAR	Central Atlantic Region
CDD	Consecutive dry days
CMIP5	Coupled Model Intercomparison Project Phase 5
CWD	Consecutive wet days
DTR	Diurnal temperature range
ERA	The fifth European Centre for Medium-Range Weather Forecasts Reanalysis
ESM	Earth system model
ETCCDI	Expert Team on Climate Change Detection and Indices
GMFD	Global Meteorological Forcing Dataset
INPE	National Institute for Space Research
IPCC	Intergovernmental Panel on Climate Change
MME	multi-model ensemble
MSWEP	Multi-Source Weighted-Ensemble Precipitation
NAR	North Atlantic Region
NASA	National Aeronautics and Space Administration
NEX-GDDP	NASA Earth Exchange Global Daily Downscaled Projections
OBS-BR	Observational dataset for Brazil
PAR	Parana River
PRCPTOT	Annual total wet-day precipitation
R20mm	Number of very heavy precipitation days
R95p	Very wet days
RCP	Representative Concentration Pathway
RX1day	Max 1-day precipitation amount
RX5day	Max 5-day precipitation amount
SAR	South Atlantic Region
SDII	Simple daily intensity index

SFR	São Francisco River
TN10p	Cool nights
TN90p	Warm nights
TNn	Coldest nights
TOC	Tocantins River
TX10p	Cool days
TX90p	Warm days
TXx	Hottest day
URU	Uruguay River
WSDI	Warm spell duration indicator

SUMMARY

1.	GENERAL INTRODUCTION	19
1.1.	Research questions and objectives	19
1.2.	Structure and organization of the thesis.....	20
1.3.	Relation to published work	22
CHAPTER 2.....		24
2.	Extreme Climate Indices in Brazil: Evaluation of Downscaled Earth System Models at High Horizontal Resolution	24
2.1.	Introduction	24
2.2.	Data and methods	26
2.2.1.	Extreme climate indices.....	26
2.2.2.	Observed datasets	27
2.2.3.	Earth System Model data	28
2.2.4.	Evaluation metrics and trend calculation.....	29
2.3.	Results and discussion	31
2.3.1.	Temperature indices	31
2.3.1.1.	Evaluation metrics	31
2.3.1.2.	Trend analysis in temperature indices	36
2.3.2.	Precipitation indices	39
2.3.2.1.	Evaluation metrics	39
2.3.2.2.	Trend analysis in precipitation indices	44
2.3.3.	The comprehensive model rank (M_R).....	46
2.4.	Summary and conclusions	49
2.5.	Acknowledgments	50
2.6.	Supplementary material	51
CHAPTER 3.....		68
3.	Assessing Current and Future Trends of Climate Extremes Across Brazil Using Reanalyses and Earth System Model Projections	68
3.1.	Introduction	68
3.2.	Data and Methodology.....	69
3.2.1.	Extreme Climate Indices.....	69
3.2.2.	Observation and reanalysis datasets	71
3.2.3.	Climate change projections	72
3.2.4.	Performance and trend analysis.....	73

3.3.	Results and analysis	74
3.3.1.	Metrics analysis of datasets performance	74
3.3.1.1.	Temperature indices	74
3.3.1.2.	Precipitation indices	76
3.3.2.	Historical changes in climate extremes	79
3.3.2.1.	Observed trends in temperature indices.....	79
3.3.2.2.	Observed trends in precipitation indices.....	82
3.2.3.	Future projections in climate extremes.....	85
3.2.3.1.	Changes in future temperature indices.....	85
3.2.3.2.	Changes in future precipitation indices	87
3.4.	Discussion and Concluding remarks	90
3.5.	Acknowledgments	91
3.6.	Supplementary material	92
4.	GENERAL CONCLUSIONS	101
5.	REFERENCES	104

1. GENERAL INTRODUCTION

1.1. Research questions and objectives

Extreme events, in meteorological or climatological terms, are associated with large deviations from mean climate state that could occur in different ranges, and the frequency vary from days to millennia (Fundação Brasileira para o Desenvolvimento Sustentável - FBDS 2009; McPhillips et al. 2018). Extreme events have a negative effect on society and mainly contribute to the increase in the frequency and severity of hydrometeorological hazards, especially with regard to floods, flash floods, heat waves, landslides and droughts (Avila et al. 2016; Debortoli et al. 2017; Marengo et al. 2017; Santos et al. 2017; Geirinhas et al. 2018). There is an increase in the number of hydrometeorological hazards worldwide (Hoeppe 2016), these positive trends have been linked with climate change and human activities resulting in increased frequency of the hazards as the climate warms up (Grant 2017; IPCC 2018).

In this sense, the current thesis contributes to solving some research questions relating to having a better understanding of the past and future occurrences of extreme climate events over Brazil. Below are key questions: Can the uncertainty be quantified in statistical quantities for observational, reanalyses, and downscaled model data? Which Brazilian hydrological basins have experienced significant warming/cooling or wetting/drying in recent decades? How well do downscaled products and reanalyses simulate the variability and trends of observed climate extreme events? Does increasing resolution improve the simulation (e.g., reanalyses and model data) in daily climate extremes? How can the performance evaluation of downscaled models and reanalyses improve the interpretation of the current climate trends and future changes? Considering the current limitations of downscaled Earth System Models (ESMs), how can one optimally evaluate the uncertainty in climate extreme projections of future emissions scenarios

adopted by the Intergovernmental Panel on Climate Change (IPCC)? Is the climate warming or cooling in future climate projections?

This research seeks to enhance the scientific understanding of the historical and projected changes in daily climate extremes of temperature and precipitation across Brazil. The specific objectives of this thesis are:

1. To evaluate how well the current climate model downscaling products can simulate the variability and trends of climate extremes of temperature and precipitation over the major Brazilian watersheds during 1980-2005.
2. To analyze the current state of climate extremes of temperature and precipitation over Brazil during 1980-2016 using several gridded datasets (e.g., Observations and reanalysis)
3. To investigate the projected changes in extreme climate indices over the mid-21st century (2046-2065) and end-of-21st century (2081–2100) relative to the reference period 1986–2005.

Eight hydrological basins (Fig. 2.1 and Fig 2.2) under heterogeneity of climates over Brazil are selected for all analyses in this thesis as a way to divide the country in a limited number regions to study the historical/future changes of climate extremes.

1.2. Structure and organization of the thesis

This thesis primarily consists of two individual manuscripts, though related to the analyzes of the historical patterns and future changes of extreme climate events over Brazil through the indices defined by the World Climate Research Program's Expert Team on Climate Change Detection and Indices (ETCCDI) framework. Chapter 1 presents a general introduction. Chapters 2 and 3 correspond to original research papers submitted for publication in the

international journal Climate Dynamics (<https://www.springer.com/journal/382>). Finally, Chapter 4 presents the general conclusions and future research.

Chapter 2 is entitled “Assessing current and future trends of climate extremes across Brazil using reanalyses and Earth System Model projections ”. The reference number for this manuscript is CLDY-D-19-00584. The authors are Alvaro Avila (AA), Gabriel Abrahão (GA), Flávio Justino (FJ), Roger Rodrigues (RR), and Aaron Wilson (AW). Author Contributions: Conceptualization, AA, FJ, and RR; methodology, AA, FJ, and RR; software was managed by AA and GA; visualization AA, GA, and AW; original draft preparation, AA, and reviewing and editing, AA, GA, FJ, RR, and AW.

Chapter 3 is entitled “Extreme climate indices in Brazil: Evaluation of downscaled Earth System Models at high horizontal resolution ”. The reference number for this paper is CLDY-D-19-00921. The authors are Alvaro Avila (AA), Victor Benezoli (VB), Flávio Justino (FJ), Roger Rodrigues (RR), and Aaron Wilson (AW). Author Contributions: Conceptualization, AA, FJ, and RR; methodology, AA, FJ, and RR; software was managed by AA and VB; visualization AA and VB; original draft preparation, AA, and AW; reviewing and editing, AA, VB, FJ, RR, and AW.

For both manuscripts first, second, and third authors are from the Department of Agricultural Engineering of the Universidade Federal de Viçosa (Brazil). The fourth author is a professor at the Natural Resources Institute from the Universidade Federal de Itajubá (Brazil). The last author works at the Polar Meteorology Group in the Byrd Polar and Climate Research Center of The Ohio State University (USA).

1.3. Relation to published work

During the doctoral studies, I have worked on the variations in frequency, intensity, and duration of climate extremes over regions with unusual or severe weather conditions such as tropical regions (e.g., Colombia and Brazil) and North America Arctic Region. Besides, I evaluated the performance of global/regional reanalyses in estimating observed climate extremes over the North American Arctic at Ohio State University with the Byrd Polar and Climate Research Center, from June to December 2019. Thus, I published the following papers to scientific journals relative to the climate area:

1. **Avila, A.**, Justino, F., Lindemann, D., Rodrigues, J., and Ferreira, G. 2020. Climatological aspects and changes in temperature and precipitation extremes in Viçosa - Minas Gerais. (*Accepted*). *Anais da Academia Brasileira de Ciências* (ISSN: 2073-4441). Manuscript ID: AABC-2019-0388
2. Loaiza, W., Kayano., M., Andreoli, R., **Avila., A**, Canchala, T., Francés, F., Ayes, I., Alfonso-Morales, W., Ferreira de Souza, R., Carvajal, Y. 2020. Streamflow Intensification Driven by the Atlantic Multidecadal Oscillation (AMO) in the Atrato River Basin, Northwestern Colombia. *Water*, v. 12, 216. <https://doi.org/10.3390/w12010216>
3. Justino, F., Wilson, A., Bromwich, David., **Avila, A.**, Bai, L., and Wang, Sheng-Hung. 2019. Northern Hemisphere Extratropical Turbulent Heat Fluxes in ASRv2 and Global Reanalyses. *Journal of Climate.* , v.32, p.2145 – 2166. <https://doi.org/10.1175/JCLI-D-18-0535.1>
4. **Avila, A.**, Cardona, F., Carvajal, Y., and Justino, F. 2019. Recent Precipitation Trends and Floods in the Colombian Andes. *Water.* , v.11, 379. <https://doi.org/10.3390/w11020379>

5. **Avila, A.**, Justino, F., Wilson, A., Bromwich, D. and Amorim, M. 2016. Recent precipitation trends, flash floods and landslides in southern Brazil. *Environmental Research Letters*, v.11, p.114029, 2016. <https://doi.org/10.1088/1748-9326/11/11/114029>

CHAPTER 2

2. Extreme Climate Indices in Brazil: Evaluation of Downscaled Earth System Models at High Horizontal Resolution

Alvaro Avila; Gabriel Abrahão; Flavio Justino; Roger Torres; Aaron Wilson.

Climate Dynamics. Manuscript number: CLDY-D-19-00584

Abstract:

This study evaluated the performance of 25 Earth System Models (ESMs), statistically and dynamically downscaled to a high horizontal resolution (0.25° of latitude/longitude), in simulating extreme climate indices of temperature and precipitation for 1980-2005. Datasets analyzed include 21 statistically downscaled ESMs from the National Aeronautics and Space Administration (NASA) Earth Exchange Global Daily Downscaled Projections (NEX-GDDP) and dynamically downscaled Eta Regional Climate Model simulations driven by 4 ESMs generated by the Brazilian National Institute for Space Research (INPE). Downscaled outputs were evaluated against observational gridded datasets at 0.25° resolution over Brazil, quantifying the skill in simulating the observed spatial patterns and trends of climate extremes. Results show that the downscaled products are generally able to reproduce the observed climate indices, although most of them have poorest performance over the Amazon basin for annual and seasonal indices. We find larger discrepancies in the warm spell duration index for almost all downscaled ESMs. The overall ranking shows that three downscaled models (CNRM-CM5, CCSM4, and MRI-CGCM3) perform distinctively better than others. In general, the ensemble mean of the statistically downscaled models achieves better results than any individual models at the annual and seasonal scales. This work provides the largest and most comprehensive intercomparison of statistically and dynamically downscaled extreme climate indices over Brazil and provides a useful guide for researchers and developers to select the models or downscaling techniques that may be most suitable to their applications of interest over a given region.

Key Words: CMIP5; Model evaluation; Climate extremes; Performance metrics; Trends

2.1. Introduction

The attention of global climate change impacts is progressively moving from the assessments of mean (or climatology) patterns to assessments of present and future trends of climate extreme events, such as the warmest day of the year, heat/cold waves, heavy or very heavy precipitation events, consecutive dry or wet spells (Burger et al. 2011; Alexander and Arblaster 2017). In this sense, the Expert Team on Climate Change Detection and Indices (ETCCDI) have been developing and publicizing a set of internationally-accepted indices based on daily measures of air temperature and precipitation (Alexander et al. 2006; Donat et al. 2013a; Sillmann et al. 2013a, b).

Many studies around the world have applied the ETCCDI climate indices to analyze the risk of climate extremes to human and natural systems, for past events using historical data (e.g., Aguilar et al. 2005; Santos et

al. 2017), and for future trends in extremes using climate models projections (e.g., Debortoli et al. 2017; Mysiak et al. 2018; Alexander and Arblaster 2017). Despite all efforts, investigations on future climate extremes have been frequently constrained by coarse resolutions in climate models, that lead to results that can not be assumed to reproduce local weather extremes. For instance, using General Circulation Models (GCMs) from the Coupled Model Intercomparison Project Phase 3 (CMIP3), Rusticucci et al. (2010) and Marengo et al. (2010b) found that those models exhibit a higher frequency of some climate extremes compared to observations over South America. Additionally, Sillmann et al. (2013a) evaluated the CMIP3 and CMIP5 models over the South American region and noted that many models overestimate the total precipitation in wet days, underestimate the maximum consecutive dry days and generally overestimate temperature extremes.

In light of an increasing need for finer resolution information of climate change projections (horizontal resolution less than 100 km), statistical and dynamical downscaling techniques provide more details of climatic patterns over a particular region, improving the accuracy and relevance of simulations and projections for climate impact studies (Burger et al. 2011; Ambrizzi et al. 2019). Although such research efforts are relatively rare in Brazil, several regionally/locally downscaled projections have been developed using various methodologies in recent years (Boulanger et al. 2006, 2007; Marengo et al. 2010a, 2012; Thrasher et al. 2012; Chou et al. 2014a; Valverde and Marengo 2014). For example, Valverde and Marengo (2014) and Chou et al. (2014a) assessed regional climate simulations applying dynamical downscaling using the Eta model and noted that the model reproduced reasonably well the extreme climatic events; although, simulations contain more extreme values than the observations.

The Brazilian economy has been highly vulnerable to climatic variability, especially to climate extremes of air temperature and precipitation, that can lead to considerable losses in agricultural activities and problems in the management of water resources (Tomasella et al. 2013; Ray et al. 2015; Debortoli et al. 2017; Marengo et al. 2017). In this way, current climate change projections are likely to have negative socio-economic impacts on the country, increasing the number of natural disasters in regions where climate change will be more pronounced (Torres and Marengo 2014; Darela-Filho et al. 2016).

In recent years, impactful natural hazards related to climate extremes have affected Brazil, such as droughts in the Northeast from 2012 to 2016 (Marengo et al. 2017, 2018a; Brito et al. 2018) or dry and warmer summers (December-March) in 2014 and 2015 in Southeast Brazil (Coelho et al. 2016a, b). However, at the same time, unprecedented floods were reported in the summer of 2014 in the southwestern Amazon Basin (Espinoza et al. 2014). The frequency of such catastrophes spurs the need for reliable simulations of climate extremes on local to regional scales that can inform the development of public policies, proper management of hydrological resources, and the mitigation of their impacts on human activity and the environment (Marengo et al. 2009).

Therefore, current impact projections rely on climate models with coarse resolutions (>100km), thus lacking the detail needed for regionally relevant impact assessments. The main goal of this work is to evaluate how well the current climate model downscaling products can simulate variability and trends of climate extremes events in Brazil. We investigate the performance of 25 statistically and dynamically downscaled ESMs to a high horizontal resolution in capturing the observed behavior of extreme temperature and precipitation events over the major Brazilian watersheds. Two main downscaled ESMs data sources were analyzed. First, 21 statistically

downscaled ESMs with a horizontal resolution of $0.25^\circ \times 0.25^\circ$ of latitude/longitude (approximately 25 km x 25 km) were taken from National Aeronautics and Space Administration (NASA) Earth Exchange Global Daily Downscaled Projections (NEX-GDDP). Second, 4 dynamically downscaled ESMs using the Eta model at a 20-km spatial resolution were provided by the Brazilian National Institute of Spatial Research (INPE). These two data sources, with relatively high spatial and temporal resolutions, have greatly captured the observed climatic patterns and have been used in studies of climate change impacts on a regional/local scale (Debortoli et al. 2017; Missirian and Schlenker 2017; Lyra et al. 2018; Raghavan et al. 2018; Liao et al. 2019).

The paper is organized as follows: Section 2 describes the different data sources and methodology used; results focused on observations and model evaluations are presented in Section 3; and finally, summaries, discussions and concluding remarks are presented in Section 4.

2.2. Data and methods

2.2.1. Extreme climate indices

Twenty-seven extreme climate indices are recommended by the ETCCDI and are calculated using daily maximum (TX) and minimum temperature (TN) and daily precipitation (PR). In this study, some ETCCDI indices are excluded, because their definitions are not appropriate across Brazil. For instance, the index was excluded if the study area has few records of extremely low temperatures as frost days (FD), ice days (ID), cold spell duration indicator (CSDI), and the common magnitude of growing season length is nearly 365 days (GSL). In addition, coldest day (TXn), warmest night (TNx), annual counts of daily minimum temperature greater than 20°C (tropical nights–TR), the maximum temperature greater than 25°C (summer days–SU), and days with rainfall greater than 1/10 mm (R1mm/R10mm) were excluded from this analysis, because these thresholds are not relevant to describe extreme climate events in Brazil.

We evaluate 16 extreme climate indices at the annual scale, 8 are associated with temperature and 8 with precipitation. Detailed descriptions are provided in Table 2.1, and further details may also be found in Zhang and Yang (2004) and Zhang et al. (2011), or at http://etccdi.pacificclimate.org/list_27_indices.shtml.

Table 2.1 The extreme temperature and precipitation indices used in this study recommended by the ETCCDI. More details on definitions of the core indices given at http://etccdi.pacificclimate.org/list_27_indices.shtml

Index	Indicator name	Indicator Definitions	Units
TXx	Hottest day	Monthly maximum value of daily maximum temp	°C
TNn	Coldest nights	Monthly minimum value of daily minimum temp	°C
DTR	Diurnal temperature range	Monthly mean difference between TX and TN	°C
TN10p	Cool nights	Percentage of days when TN<10th percentile	%
TN90p	Warm nights	Percentage of days when TN>90th percentile	%
TX10p	Cool days	Percentage of days when TX<10th percentile	%
TX90p	Warm days	Percentage of days when TX>90th percentile	%
WSDI	Warm spell duration indicator	Annual count of days with at least 6 consecutive days when TX>90th percentile	days
PRCPTOT	Annual total wet-day precipitation	Annual total precipitation (PR) in wet days (PR>=1mm)	mm
RX1day	Max 1-day precipitation amount	Monthly maximum 1-day precipitation	mm
RX5day	Max 5-day precipitation amount	Monthly maximum consecutive 5-day precipitation	mm
R95p	Very wet days	Annual total precipitation from days > 95th percentile	mm
SDII	Simple daily intensity index	The ratio of annual total precipitation to the number of wet days* (≥ 1 mm)	mm/day
R20mm	Number of very heavy precipitation days	Annual count of days when PR>=20mm	days
CWD	Consecutive wet days	Maximum number of consecutive days with PR>=1mm	days
CDD	Consecutive dry days	Maximum number of consecutive days with PR<1mm	days

*The ETCCDI defined a wet (dry) day when precipitation ≥ 1 mm (PR<1mm)

The extreme climate indices chosen can be calculated seasonally or monthly, albeit most of the impactful extreme events mentioned in the previous section can be described by annual indices (Aerenson et al. 2018). However, the seasonal analysis was done for the two extreme climate seasons over Brazil: austral summer (December, January, and February – DJF) and winter (June, July, and August – JJA), representing the wet and dry seasons, respectively, for the most of the country (Marengo et al. 2010a; Torres and Marengo 2014; Rao et al. 2016; Lyra et al. 2018). For this purpose, seasonal analysis was carried out for selected warm extremes (TXx, TX90P), cold extremes (TNn, TN10P), wet extremes precipitation (PRCPTOT, RX1day, RX5day) and the maximum number of consecutive dry days (CDD), which is associated with dry conditions (Zhang et al. 2011) and also indicative of potential water stress (Aerenson et al. 2018).

The climate indices were chosen, because they allow the assessment of intensity, frequency, and duration of extreme climate events. Also, this set of indices has been used to describe hydrometeorological hazards such as droughts, floods, heavy rains, and heat waves in Brazilian climate conditions (Alexander et al. 2006; Sillmann et al. 2013a, b; Skansi et al. 2013; Avila et al. 2016, 2019). Noteworthy, the ETCCDI indices are widely used to evaluate the capability of Earth System Models in simulating the observed climate extremes of temperature and precipitation (Marengo et al. 2010b; Rusticucci et al. 2010; Alexander and Arblaster 2017; Nguyen et al. 2017; Lyra et al. 2018; Dosio et al. 2019).

All extreme indices were calculated using gridded datasets (observational and reanalysis) and 25 downscaled ESMs that are shown in section 2.2 and 2.3, respectively. The calculations are performed with the `climindex.pcic.ncdf` package maintained by the Pacific Climate Impacts Consortium (PCIC), which runs on R software and is freely available at <https://github.com/pacificclimate/climindex.pcic.ncdf>.

2.2.2. Observed datasets

We examine the daily records from two gridded datasets. The first observational dataset (OBS-BR) contains daily fields of temperature and precipitation interpolated from 9259 rain gauges and 735 weather stations gridded to a regular grid of $0.25^\circ \times 0.25^\circ$ latitude/longitude covering all of Brazil territory over the period 1980–2015 (Xavier et al. 2015). The dataset is available at <https://utexas.app.box.com/v/Xavier-et-al-IJOC-DATA>. Noteworthy, daily fields of the observations and simulations covered 1980–2005, because the historical experiment for each downscaled model are only available through 2005 (see Section 2.3). The second dataset used is from Global Meteorological Forcing Dataset (GMFD) (Sheffield et al. 2006), which consists of 3-hourly, 0.25° -resolution fields of near-surface meteorological variables for global land areas for 1948–2016, available at the Terrestrial Hydrology Research Group website at Princeton University (<http://hydrology.princeton.edu/data/GMFD.php>). The GMFD is a merge of several datasets from the National Centers for Environmental Prediction - National Center for Atmospheric Research reanalysis (NCEP-NCAR), the satellite-based Global Precipitation Climatology Project (GPCP), Tropical Rainfall Monitoring Mission (TRMM) and interpolated ground observations from Climatic Research Unit (CRU).

The OBS-BR and GMFD employ different interpolation methods, quality control, and station networks in their development. GMFD was designed for pixel-scale hydrological consistency and has to rely on the NCEP reanalysis as the basis for daily weather variability (Sheffield et al. 2006). The use of a reanalysis product

introduces an additional error source, and can lead to smoother meteorological series in comparison to what is observed in the weather stations, which can dampen the magnitude of extreme climate events (Zhang et al. 2011). OBS-BR, on the other hand, directly interpolates the daily observations of its larger weather station/rain gauge network. For these reasons, we considered OBS-BR as the reference daily gridded dataset for meteorological variables (TN, TX, and PR) in Brazil. Special attention was given to the comparison between GMFD and OBS-BR datasets, because the National Aeronautics and Space Administration (NASA) Earth Exchange Global Daily Downscaled Projections (NEX-GDDP) dataset (Thrasher et al. 2012) used GMFD as the observational reference for its statistical downscaling technique. The following subsection describes the NEX-GDDP dataset.

2.2.3. Earth System Model data

For each dynamical and statistical dataset (see Table 2.2 for the list of models), we used the daily output of maximum and minimum temperature, and daily precipitation to study extreme climate indices from 1980–2005.

Table 2.2 Information on the 25 general circulation models used in the present analysis. (a) ESMs used for generating the NEX-GDDP dataset through statistical downscaling. (b) ESMs used as boundary conditions to generate the Eta-INPE dataset through dynamical downscaling

Model	Modeling center	Resolution (lat. × lon.)	VL*
(a) Statistical downscaled models			
1. ACCESS1-0	Commonwealth Scientific and Industrial Research Organization and Bureau of Meteorology, Australia	1.25°×1.875°	38
2. BCC-CSM1-1	Beijing Climate Center, China Meteorological Administration, China	2.8°×2.8°	26
3. BNU-ESM	Beijing Normal University, China	2.8°×2.8°	26
4. CanESM2	Canadian Centre for Climate Modeling and Analysis, Canada	2.8°×2.8°	35
5. CCSM4	National Center for Atmospheric Research (NCAR), USA	0.9°×1.25°	27
6. CESM1-BGC	National Science Foundation, Department of Energy and NCAR, USA	0.9°×1.25°	27
7. CNRM-CM5	Centre National de Recherches Météorologiques and Centre Européen de Recherche et Formation Avancée en Calcul Scientifique, France	1.4°×1.4°	31
8. CSIRO-MK3-6-0	Commonwealth Scientific and Industrial Research Organization, Australia	1.875°×1.875°	18
9. GFDL-CM3	NOAA Geophysical Fluid Dynamics Laboratory, USA	2.0°×2.5°	48
10. GFDL-ESM2G	NOAA Geophysical Fluid Dynamics Laboratory, USA	2.0°×2.5°	24
11. GFDL-ESM2M	NOAA Geophysical Fluid Dynamics Laboratory, USA	2.0°×2.5°	24
12. INMCM4	Institute for Numerical Mathematics (INM), Russia	~1.5°×2°	21
13. IPSL-CM5A-LR	Institut Pierre-Simon Laplace, France	1.895°×3.75°	39
14. IPSL-CM5A-MR	Institut Pierre-Simon Laplace, France	1.27°×2.5°	39
15. MIROC5	Atmosphere and Ocean Research Institute (The University of Tokyo), National Institute for Environmental Studies, and Japan Agency for Marine- Earth Science and Technology	1.4°×1.4°	40
16. MIROC-ESM	Japan Agency for Marine-Earth Science and Technology, Atmosphere and Ocean Research Institute (The University of Tokyo), and National Institute for Environmental Studies	2.8°×2.8°	80
17. MIROC-ESM-CHEM	Japan Agency for Marine-Earth Science and Technology, Atmosphere and Ocean Research Institute (The University of Tokyo), and National Institute for Environmental Studies	2.8°×2.8°	80
18. MPI-ESM-LR	Max Planck Institute for Meteorology, Germany	1.875°×1.875°	47
19. MPI-ESM-MR	Max Planck Institute for Meteorology, Germany	1.875°×1.875°	95
20. MRI-CGCM3	Meteorological Research Institute, Japan	1.125°×1.125°	48
21. NorESM1-M	Norwegian Climate Centre, Norway	~1.89°×2.5°	26
(b) Dynamical downscaled models			
22. BESM	Brazilian Earth System Model version (Version 2.3.1), Brazil	1.875° × 1.875°	28
23. CanESM2	Canadian Centre for Climate Modeling and Analysis, Canada	2.8°×2.8°	35
24. HadGEM2-ES	Met Office Hadley Centre, UK	1.25°×1.875°	38
25. MIROC5	Atmosphere and Ocean Research Institute (The University of Tokyo), National Institute for Environmental Studies, and Japan Agency for Marine- Earth Science and Technology	1.4°×1.4°	40

*Vertical Layers

The 21 statistically downscaled CMIP5 ESMs were obtained from the NEX-GDDP dataset (Thrasher et al. 2012). This dataset is available at <https://nex.nasa.gov/nex/projects/1356/>. It consists of the results of 21 CMIP5 models, bias-corrected and disaggregated to a grid of horizontal resolution of 0.25 degrees of latitude/longitude using a specially designed statistical technique that compares the model's historical runs (1950 to 2005) with the GMFD dataset.

On the other hand, the dynamically downscaled simulations employed in our study have been generated by the ETA regional climate model, provided by The Brazilian Center for Weather Forecasts and Climate Studies – CPTEC and Brazilian National Institute for Space Research – INPE, available at <https://projeta.cptec.inpe.br> (Chou et al. 2014a, b; MCTI 2016; Lyra et al. 2018).

The ETA simulations are based on 4 ESMs that have been downscaled to a 20-km resolution (Table 2.2). The model domain covers South America and most of Central America, available from 1960 to 2005. Regarding to Chou et al. (2014a) and Lyra et al. (2018), the ETA model largely improves the seasonal cycles and precipitation frequency distributions when compared to the driving ESM. However, they retain some of the distortions of trends in extreme indices present in the ESM simulations, such as the cooling trend in maximum and minimum temperatures in Eta-MIROC5, and different spatial patterns of extreme precipitation trends among the models (Chou et al. 2014a). More information on the simulations, including a detailed comparison between their results for some extreme indices, can be found in Chou et al. (2014a) and Lyra et al. (2018). For intercomparison purposes, the ETA 20 km grid here was interpolated to a common $0.25^\circ \times 0.25^\circ$ grid, using a first-order conservative remapping technique (Jones 1999), as proposed in the literature (Giorgi 2006; Cheng and Knutson 2008; Sillmann et al. 2013a; Torres and Marengo 2014).

Besides analyzing each model separately, we test whether using Multi-Model Ensembles (MMEs) can improve the representation of climate extremes. Taking the mean of a model ensemble is a common technique for avoiding the large spread found in individual model results (Knutti et al. 2010; Sillmann et al. 2013a; Nguyen et al. 2017). For that end, the mean of each index among the statistical (MME-Sta) and dynamical (MME-Dyn) models was calculated, and we treated those as separate results.

2.2.4. Evaluation metrics and trend calculation

The metrics used for evaluating the simulated indices include Percent Bias (*PBIAS*), *RMSE*-observations standard deviation ratio (*RSR*), refined index of agreement (d_r) (Willmott et al. (2012) and the Pearson correlation coefficient (*CORR*). These statistical parameters are calculated as follows:

$$PBIAS = \frac{\sum_{i=1}^n (m_i - O_i) * 100}{\sum_{i=1}^n O_i} \quad (1)$$

$$RSR = \frac{RMSE}{STDEV_{Obs}} = \frac{\sqrt{(m_i - O_i)^2}}{\sqrt{(O_i - \bar{O})^2}} \quad (2)$$

$$d_r = \begin{cases} 1 - \frac{\sum_{i=1}^n |m_i - O_i|}{2 * \sum_{i=1}^n |O_i - \bar{O}|}, & \text{when } \sum_{i=1}^n |m_i - O_i| \leq 2 * \sum_{i=1}^n |O_i - \bar{O}| \\ \frac{2 * \sum_{i=1}^n |O_i - \bar{O}|}{\sum_{i=1}^n |m_i - O_i|} - 1, & \text{when } \sum_{i=1}^n |m_i - O_i| > 2 * \sum_{i=1}^n |O_i - \bar{O}| \end{cases} \quad (3)$$

$$CORR = \frac{\sum_{i=1}^n (m_i - \bar{m}_i) (O_i - \bar{O})}{\sqrt{\sum_{i=1}^n (O_i - \bar{O})^2} \sqrt{\sum_{i=1}^n (m_i - \bar{m}_i)^2}} \quad (4)$$

where O_i is the observed value, \bar{O} is the mean of observed data, m_i is the simulated value, \bar{m}_i is the mean of simulated data, and n is the total observation number.

PBIAS indicates the average tendency of the simulation to be larger or smaller than the observed data (Gupta et al. 1999); values close to 0 indicate an optimal performance in a given model; positive and negative values indicate a bias toward overestimation or underestimation, respectively. *RSR* is calculated as the ratio of the *RMSE* and standard deviation of observed data (Moriassi et al. 2007); values closer to 0 mean better performing simulations. The refined index of agreement (d_r) developed by Willmott et al. (2012) varies between -1 and 1 . A d_r of 1 indicates a perfect agreement and $d_r = -1$ indicates either a lack of agreement between observed and simulated values or a lack of variability in the observed data (Willmott et al. 2015). Finally, *CORR* is used to describe the temporal association between observed data and model simulations. *CORR* is between -1 and 1 . A *CORR* of 1 (-1) shows complete positive (negative) linear relation. If the *CORR* is 0 , there is a lack of any linear relationship between observed (O_i) and simulated (m_i) data.

Individual extreme climate index scores allow us to rank models based on the performance metrics (*PBIAS*, *RSR*, d_r , and *CORR*). To summarize all the ranking possibilities, the comprehensive model rank (M_R) has also been calculated (Jiang et al. 2015; You et al. 2017; Zhang et al. 2018). M_R is a measure of how consistently each model is classified among all the ranking possibilities (indices and metrics):

$$M_R = 1 - \frac{1}{n \times m} \sum_{i=1}^n (\text{Rank}_{i_{PBIAS}} + \text{Rank}_{i_{RSR}} + \text{Rank}_{i_{d_r}} + \text{Rank}_{i_{CORR}}) \quad (5)$$

where n is the total number of indices, m is the number of models and the Rank_i indicates downscaled model's order on each index in a given performance metric. Note that we also rank all the downscaled ESMs along with the two MMEs (Table 2.2). Therefore, the maximum value of M_R is 1 , indicating that the model is the best in all indices and metrics (Jiang et al. 2015; You et al. 2017).

The linear trends of extreme climate indices from downscaled ESMs are estimated and compared to two observed datasets using the Theil-Sen slope estimator (Sen 1968). The trend significance of the slope was evaluated through Mann-Kendall (Mann 1945; Kendall 1975) trend significance test at the 95% confidence level. These tests have been broadly used in hydrometeorological studies for detecting trends because of their non-parametric approach (Yue et al. 2002; Wang et al. 2012; Liu et al. 2013; Wang and Li 2015; Avila et al. 2019).

The performance metrics and trends were evaluated for each grid point and averaged across each of the eight major hydrological basins (Fig. 2.1) used by the Brazilian National Water Agency (ANA). The basin acronyms in Fig. 2.1 refer to Amazon River (AMZ), Tocantins River (TOC), North Atlantic Region (NAR), São Francisco River (SFR), Central Atlantic Region (CAR), Parana River (PAR), Uruguay river (URU), and South Atlantic Region (SAR). The analysis in hydrological basins was done because the performance of each ESMs

within a given hydrological basin is expected to be consistently representative throughout that specific region (Nguyen et al. 2017; Xu et al. 2019).

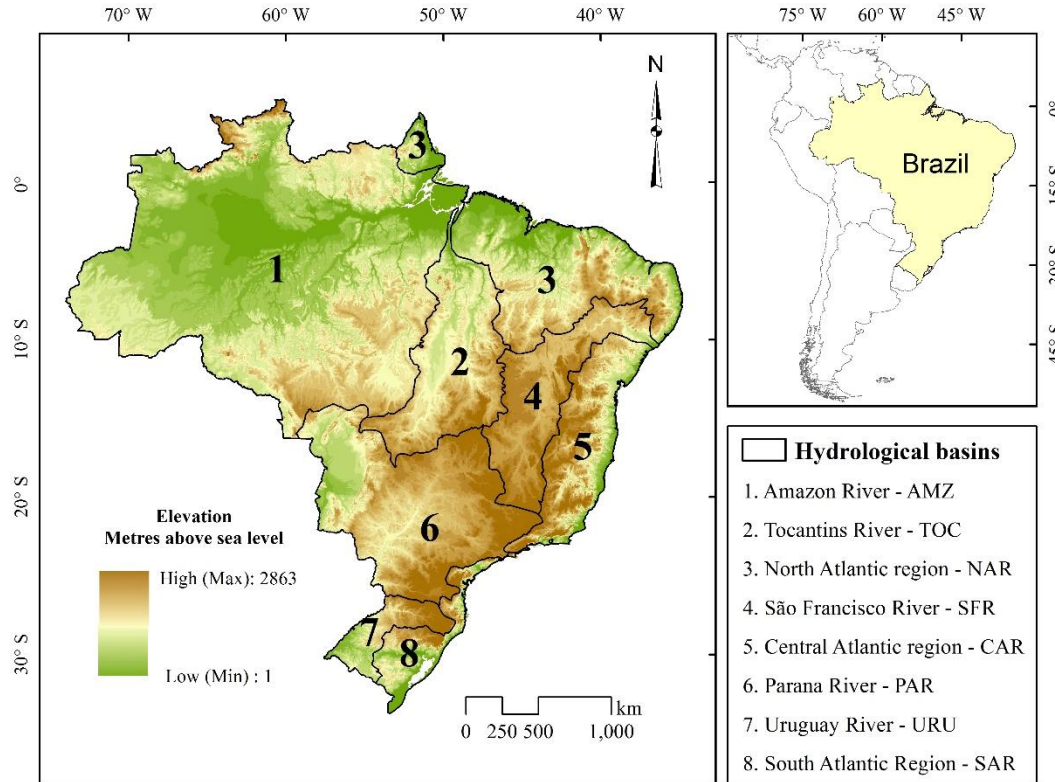


Figure 2.1 Geographical location of the eight hydrological basins in Brazil according to the Brazilian National Water Authority (ANA) classification-

2.3. Results and discussion

For sake of brevity, we discuss the results of climatology bias and spatial trend analysis for two indices, which represent extremes events of temperature (hottest days –TXx) and precipitation (annual total wet-day precipitation– PRCPTOT) as illustrative figures in the main text. Results for the other ETCCDI indices can be found in the supplementary material.

2.3.1. Temperature indices

2.3.1.1. Evaluation metrics

Figure 2.2 presents the climatology bias of the hottest day index (TXx). Almost all downscaled ESMs and the reanalysis (GMDF) captured the spatial pattern of the TXx relatively well. Furthermore, the evaluation metrics (*PBIAS*, *RSR*, *d_r*, and *CORR*) were calculated for each climate index, model, MMEs, and GMFD dataset in each hydrological basin and compared to observations during 1980-2005. These evaluation metrics are summarized in the portrait diagrams shown for annual and seasonal results in Figs. 3 and 4, respectively.

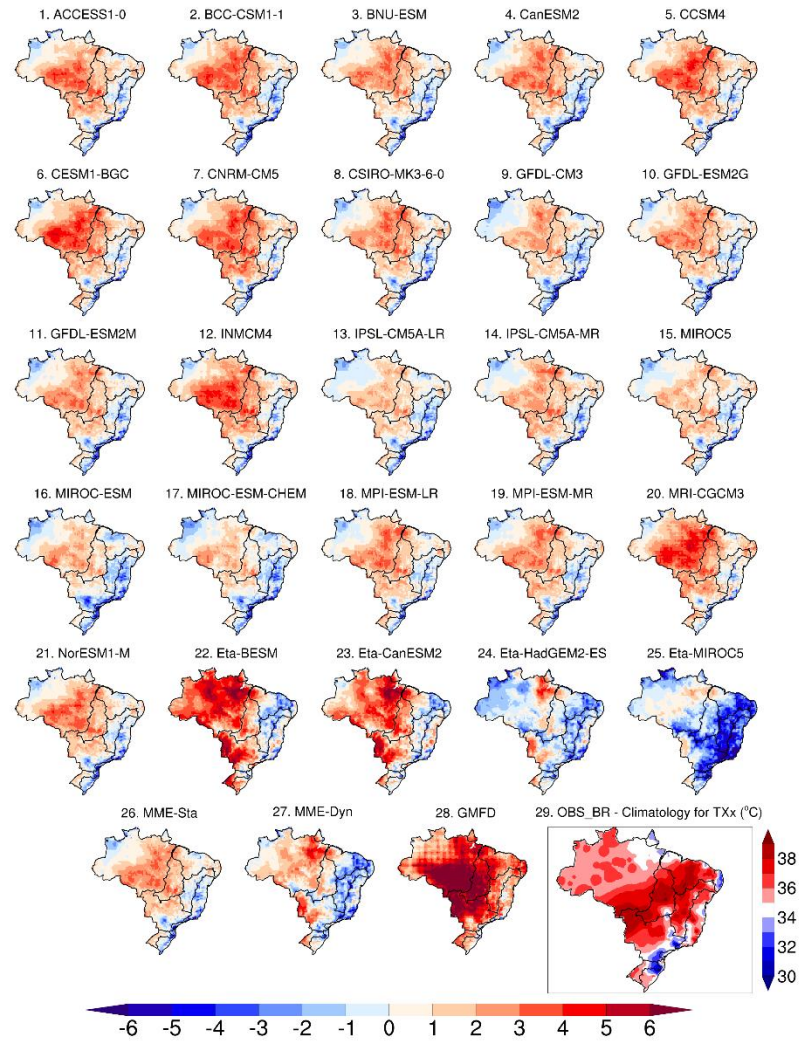


Figure 2.2 Climatology bias for the annual maximum of daily maximum temperature - TXx (°C) for 21 statically (NEX-GDDP; models 1-21) and 4 dynamically (Eta-INPE; models 22-25) downscaled models, MME-Sta (26), MME-Dyn (27), and GMFD (28) from 1980 to 2005. Climatology for TXx in the observations dataset (OBS-BR; gray rectangle dataset 29) for 1980-2005

In general, the statistical downscaling approach captures well the general spatial patterns of the temperature indices at the annual scale. However, the statistically downscaled ESMs more frequently overestimate TXx above 2 °C over the Amazon basin (Fig. 2.2). Also, there are generally low values of *PBIAS* for almost all temperature indices of GMFD (Fig. 2.3a) except for TXx, coldest night (TNn), and warm spell duration indicator (WSDI). The greatest *PBIAS* values for TXx are found over the Amazon, Tocantins, and Parana basins with values larger than 12%. GMFD underestimated observed values for TNn except for the São Francisco River and Central Atlantic basins (overestimated by slightly more than 1%). The worst values of *PBIAS* for TNn are identified over the Parana and Uruguay basins with -4 and -13%, respectively.

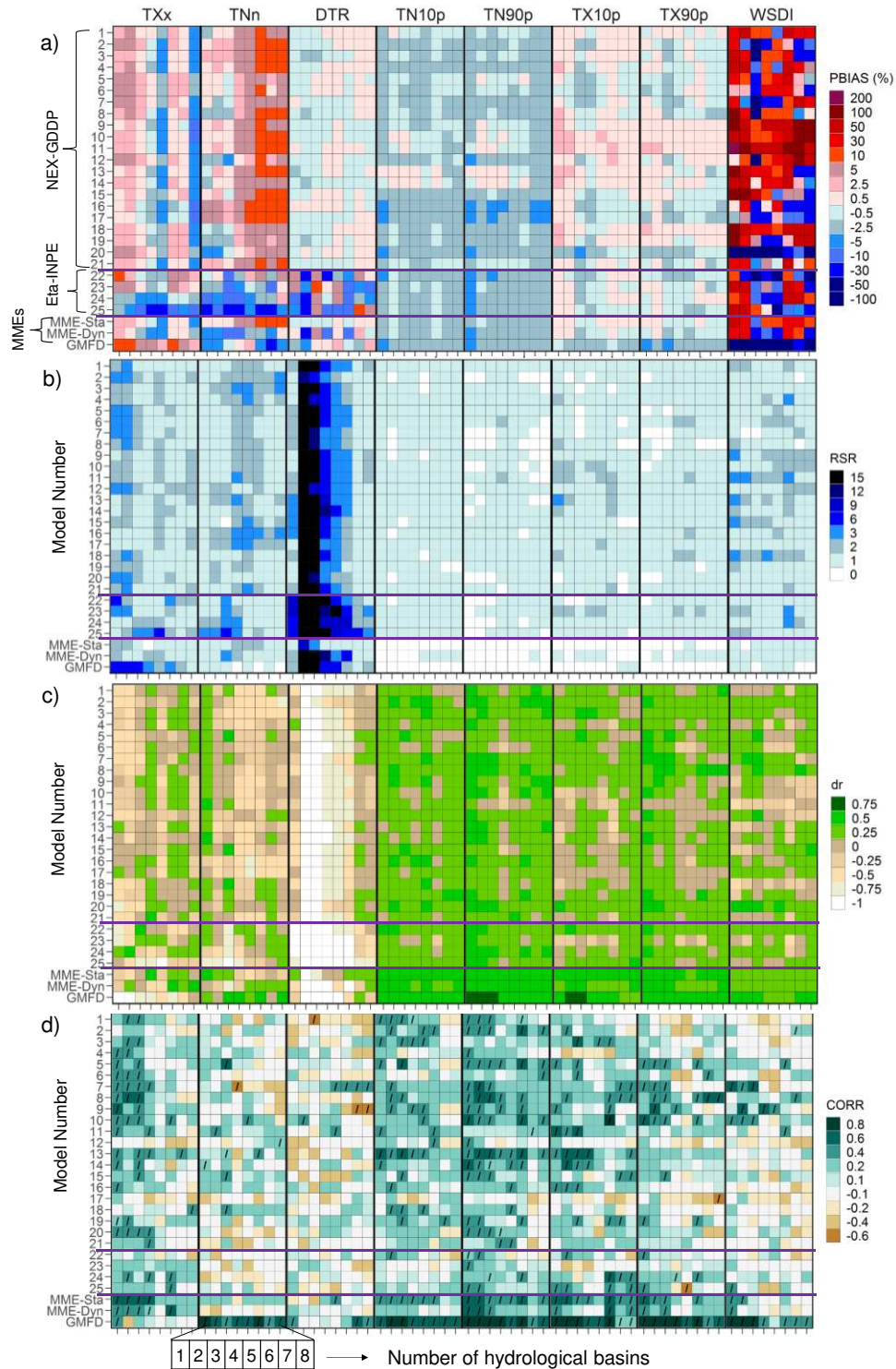


Figure 2.3 Statistics of performance obtained for annual temperature indices for statically (NEX-GDDP) and dynamically (Eta-INPE) downscaled models, MME-Sta, MME-Dyn, and GMFD from 1980 to 2005 over eight hydrological basins (Fig. 2.1). (a) Percent Bias (PBIAS); (b) RMSE-observations standard deviation ratio (RSR); (c) a refined index of model performance (d_r); (d) Correlation coefficients (CORR; the diagonal lines indicate significant correlations at 95% level). The horizontal purple lines refer to Eta-INPE datasets. For PBIAS and RSR, dark colors indicate models that perform worse than others, on average, and light colors indicate models that perform better than others, on average. Furthermore, for d_r and CORR, dark (light) colors show models that have better (worse) statistical metrics than others, on average

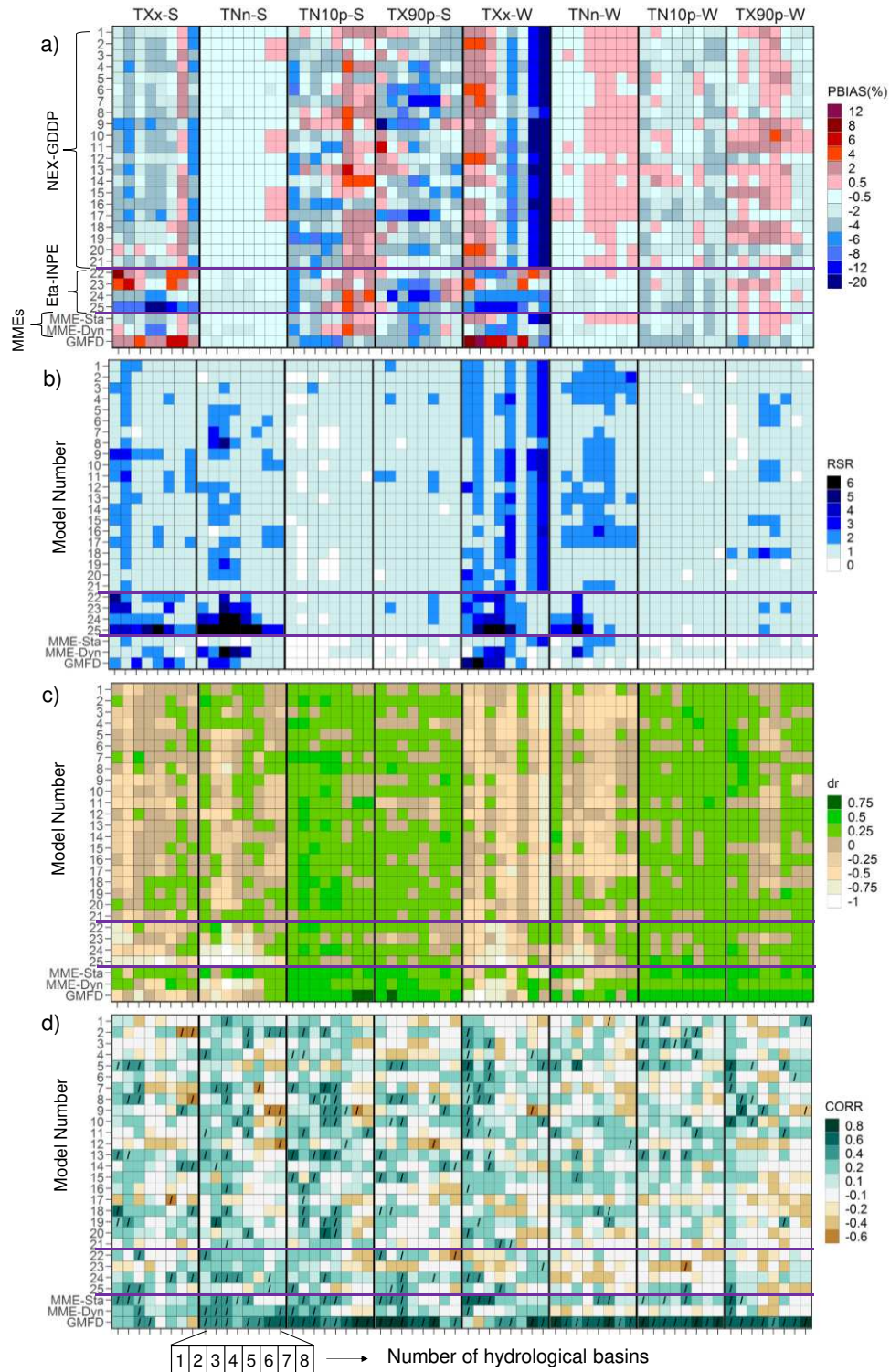


Figure 2.4 As in Fig. 2.2, but for extreme temperature indices in summer (DJF) and winter (JJA). The nomenclature of the ETCCDI indices was adapted to Index-“S” for summer and Index-“W” for winter

The *PBIAS* of TNn (Fig. 2.3a; second column) shows that some downscaled models are too cold (e.g., Eta-HadGEM2-ES (24) and Eta-MIROC5 (25)) or simulate higher values of minimum temperatures (e.g., MIROC-ESM (16) and MIROC-ESM-CHEM (17)) over Brazil. Furthermore, models 2, 3, 16, and 17 did not perform well for the TNn index over the Parana River, Uruguay River, and South Atlantic basins with values above 19% (Fig.

2.3a). In terms of the RSR , d_r , and correlation, higher limitations have been found for the majority of the 25 downscaled ESMs for TXx and DTR, especially for basins located in the North and Northeast of Brazil. It is important to note that TXx and TNn indices are generally underestimated in the Eta simulations over Brazil (e.g., models 24 and 25), in agreement with the results of Chou et al. (2014a).

Figure 2.4 displays the performance obtained for temperature indices in summer and winter. In general, the downscaled models underestimate the observations of the TXx and TNn indices in summer in almost all basins except for the Uruguay basin, which shows a warm bias only for TXx. Two of the ETA-INPE models (BESM and CanESM2) have the reverse behavior, tending to overestimate Txx in the summer in most basins, which offsets the strong underestimating bias of ETA MIROC5 in MME-Dyn. The results for winter show that the downscaled ESMs overestimate the TXx over Amazon, Tocantins, and North Atlantic basins, but strongly underestimate ($PBIAS > 30\%$) over Uruguay, Parana, and South Atlantic basins. The TNn index, for the winter, shows $PBIAS$ values lesser than 2%; however, poor performance in RSR , d_r , and $CORR$. The TXx index (TNn) shows that GMFD has a warm (cold) bias in both seasons (bottom of Fig. 2.4a). For the rest of the metrics (RSR , d_r , and $CORR$), GMFD shows better performance to reproduce TNn than the TXx index over the majority of basins.

The discrepancy of the majority of downscaled models is more evident for WSDI, which simulates higher values than the observations, especially over the Amazon, Tocantins, and Parana basins (Fig 2.3b). The WSDI underestimates the observed values by more than 25% and 30% for the Uruguay River and South Atlantic basins, respectively, and for the other basins by more than 66%. Moreover, eight temperature indices have values of RSR close to zero (Fig 2.3b), except for the TXx index. Additionally, the redefined index values ($d_r < 0.5$; Fig 2.3c) and correlation coefficients ($CORR < 0.5$; Fig 2.2d) show the poor performance of the downscaled models to reproduce the TXx and DTR (diurnal temperature range), especially over the Amazon and Tocantins basins

Evaluation metrics of the GMFD dataset demonstrate reasonable skill in the representation of the temperature-based percentile indices at the annual scale (e.g., TN10p, TX10p, TN90p, and TX90p) across all hydrological basins in Brazil (Fig. 2.3). For these four extreme climate indices in almost all basins, $PBIAS$ is within $\pm 3\%$, $RSR < 1$, $d_r \geq 0.50$, and $CORR \geq 0.54$. However, it has been found that TX10p has particularly poor performance over the Uruguay River and South Atlantic basins. Similar to the annual scale, GMFD performs well in reproducing the summer and winter patterns (Fig. 2.4a-d) of the selected percentile indices (TN10p, TX90p).

The evaluation metrics display good performance of the downscaled models to reproduce TN10p, TX10p, TN90p, and TX90p at the annual scale (see four to seven columns of Fig. 2.3). For these indices, the $PBIAS$ varies between -5 to 4%, and the RSR values are close to zero. According to d_r and correlation, models CSIRO-MK3-6-0 (8), CNRM-CM5 (7), and MRI-CGCM3 (20) show consistent performance over all eight basins shown in Fig. 2.1. The seasonal patterns of TN10p and TX90p are reproduced reasonably well by downscaled models (Fig. 2.4a-d). For TN10p and TX90p, the $PBIAS$ varies between -8 to 6%, and the RSR and d_r show good accuracy with values close to 0-1 over the majority of basins.

The low bias found in percentile indices is similar to previous studies that used raw ESMs (Marengo et al. 2010b; Rusticucci et al. 2010; Sillmann et al. 2013a) and regional climate model results over South America (Marengo et al. 2009; Dereczynski et al. 2013). The good performance for percentile indices is likely a

consequence of their construction, which includes exceedance rates (in percentage) of temperatures colder than the 10th percentile or warmer than the 90th percentile with respect to a base period, potentially minimizing model characteristics (Zhang et al. 2011). Moreover, the percentile indices have less extreme features of climate variability than absolute indices (e.g., TXx and TNn) (Sillmann et al. 2013a). Finally, the *PBIAS* magnitudes of WSDI are within $\pm 200\%$. The worst performance (based on *RSR*, *d_r*, and *CORR*) across almost all the 25 downscaled ESMs is found in the basins located over the North, Northeast, and Central-West regions of Brazil (see Figures. S2.2 S2.3, and S2.4).

In general, both MMEs over or underestimate the majority of temperature indices by less than 10%, except the WSDI, with *PBIAS* varying between -11 to 71% and -32 to 53% for MME-Sta and MME-Dyn, respectively. The MME-Sta display lower *PBIAS* and *RSR* and higher correlations and *d_r* than MME-Dyn for nearly all temperature indices. Our results suggest that MMEs-Sta can better reproduce the interannual variability of temperature extremes in Brazil than MME-Dyn. Some of the downscaled models show better DTR (models 2, 8, 7, 20, and MME-Sta) and WSDI (models 6 and 16) than the raw models analyzed by Sillmann et al. (2013a). This may be related to the quantile mapping applied to the statistical downscaling, which makes the probability distribution of the downscaled data more narrowed. As discussed by Tang et al. (2016), statistical downscaling is based on linear regression with fewer degrees of freedom with respect to the dynamical counterpart (Wilby and Dawson 2013). In terms of precipitation, the complexity in the latter approach is even higher due to the non-linear interaction between clouds, atmospheric circulation, meso-scale processes, and land-atmosphere interaction.

2.3.1.2. Trend analysis in temperature indices

Trends are calculated for the OBS-BR and GMFD observations and for each downscaled ESMs for temperature indices at the annual scale for 1980-2005 (Figs. 2.5, 2.6). The OBS-BR dataset shows warming trends for most of the temperature indices in all hydrological basins of Brazil, most of which are significant at the 95% confidence level. The interested reader is referred to Fig 2.S8 to follow the seasonal results for warm extremes (TXx, TX90P) and cold extremes (TNn, TN10P), that also shows warming trends. The warming is generally larger in indices related to the warmest days (TXx) than in the coldest days (TNn) (Fig. 2.5 and see the spatial trends of TXx in Fig. 2.6).

The trend signal of percentile indices (TN10p, T90p, TX10p, and TX90p) is in line with observational analyses from Vincent et al. (2005), Skansi et al. (2013) and Donat et al. (2013a), indicating warmer conditions over Brazil at annual (Fig. 2.5) and seasonal scales. Furthermore, the positive trends in TXx (Figs. 5a, 6) and a narrowing tendency of DTR (Fig. 2.5c) over southern Brazil by the OBS-BR are consistent with the results observed by Marengo and Camargo (2008) and Rosso et al. (2015) during 1960-2002 and 1961-2011 periods, respectively. However, they found positive trends for the TNn index, but our results indicate negative trends in southern Brazil. These authors employed different periods and more years than the ones used in this study, with low-frequency features of the time series potentially changing the evaluated trends in TNn.

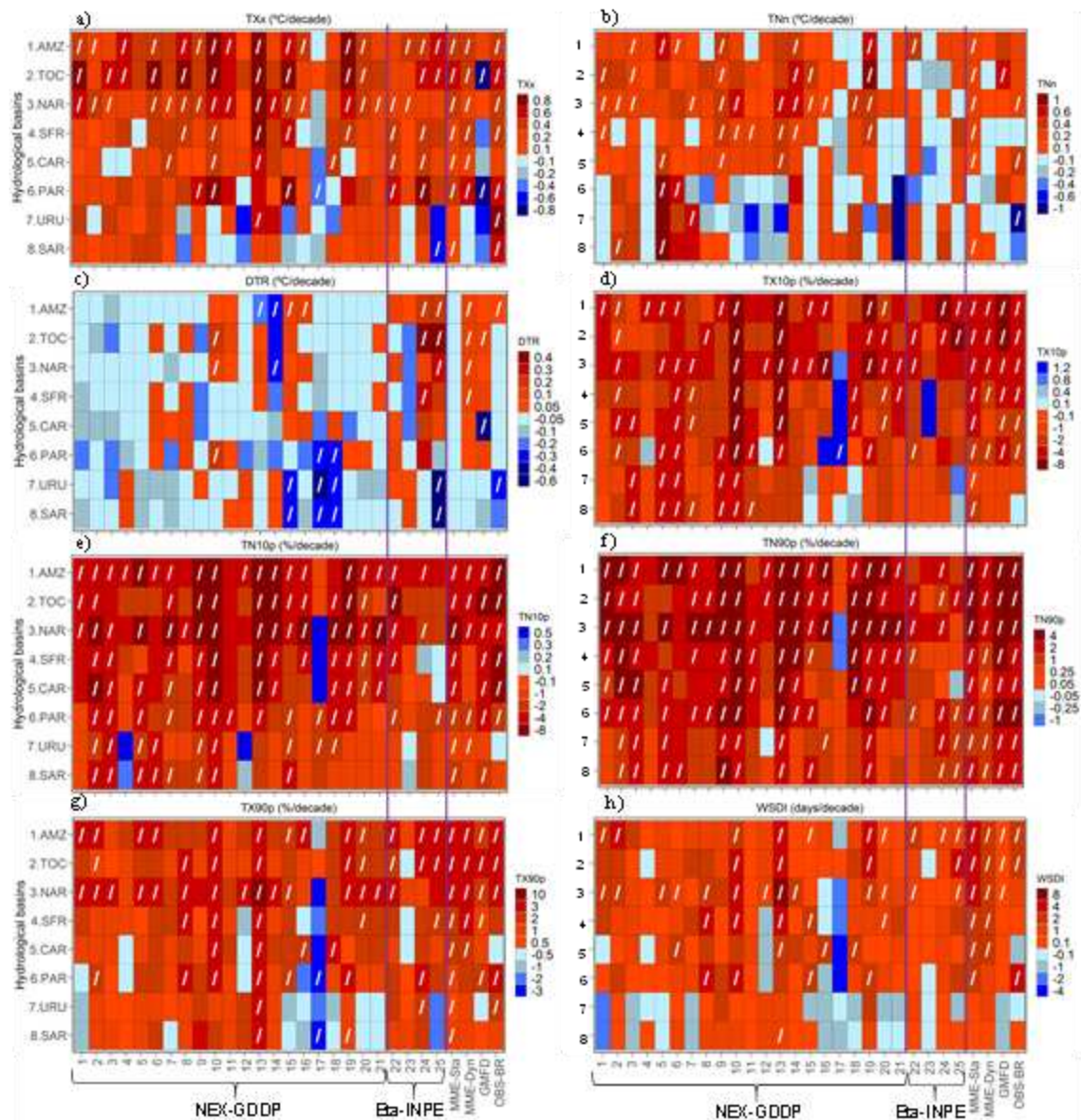


Figure 2.5 Trends per decade from 1980 to 2005 for temperature indices at the annual scale (a-h) for 21 NEX-GDDP climate models (1-21), 4 Eta-INPE climate models (22-25), MME-Sta (26), MME-Dyn (27), GMFD (28) and OBS-BR over eight hydrological regions in Brazil (Fig. 2.1). Diagonal lines indicate significant trends at 95% level. The vertical purple lines refer to ESMs from Eta-INPE datasets.

The magnitude of warming trends in cold nights, warm nights, cold days, warm days, and warm spell duration indices is relatively coherent across all the downscaled ESMs datasets and model ensembles (Fig. 2.5). Also, seasonal trend patterns in summer and winter for percentile indices (e.g., TN10p and TN90p) are well captured in almost all downscaled models. The upward trends found for most indices are a common feature delivered on the models evaluated except for MIROC-ESM-CHEM (17). This model shows negative (cooling) trends in several indices at annual and seasonal scales that are positive (warming) according to the observations. MIROC family of models generally has contradictory trends in many indices (e.g., TXx, DTR, and TX90p) compared to observations, particularly MIROC-ESM-CHEM.

Few downscaled models capture even moderately well the diurnal temperature range (DTR; Fig. 2.5c models 1, 2, 3, and 5) trends in most hydrological basins. In the case of the Eta-INPE models, none are able to replicate even the sign of the trend in all basins. In fact, the GMFD dataset also shows DTR trends slightly different from OBS-BR. This is possibly because DTR is highly affected by land surface characteristics, which are both transient in time and very heterogeneous inside the grid cells of climate models for both the GCMs (> 100 km of horizontal resolution) and Eta (20 km). This affects both the Eta-INPE models, which contain raw GCM output, and the NEX-GDDP models, for which the downscaling procedure explicitly attempts to conserve the GCM modeled trends (Thrasher et al. 2012). Maximum and minimum temperatures in GMFD are affected by both the underlying NCEP-NCAR reanalysis model and the monthly average DTR of the CRU dataset, which uses fewer meteorological stations in the region than OBS-BR. Finally, our results suggest that the better alternative for estimating the sign and magnitude of the temperature indices at the annual and seasonal scales is the use of the downscaled model ensembles (MME-Sta and MME-Dyn).

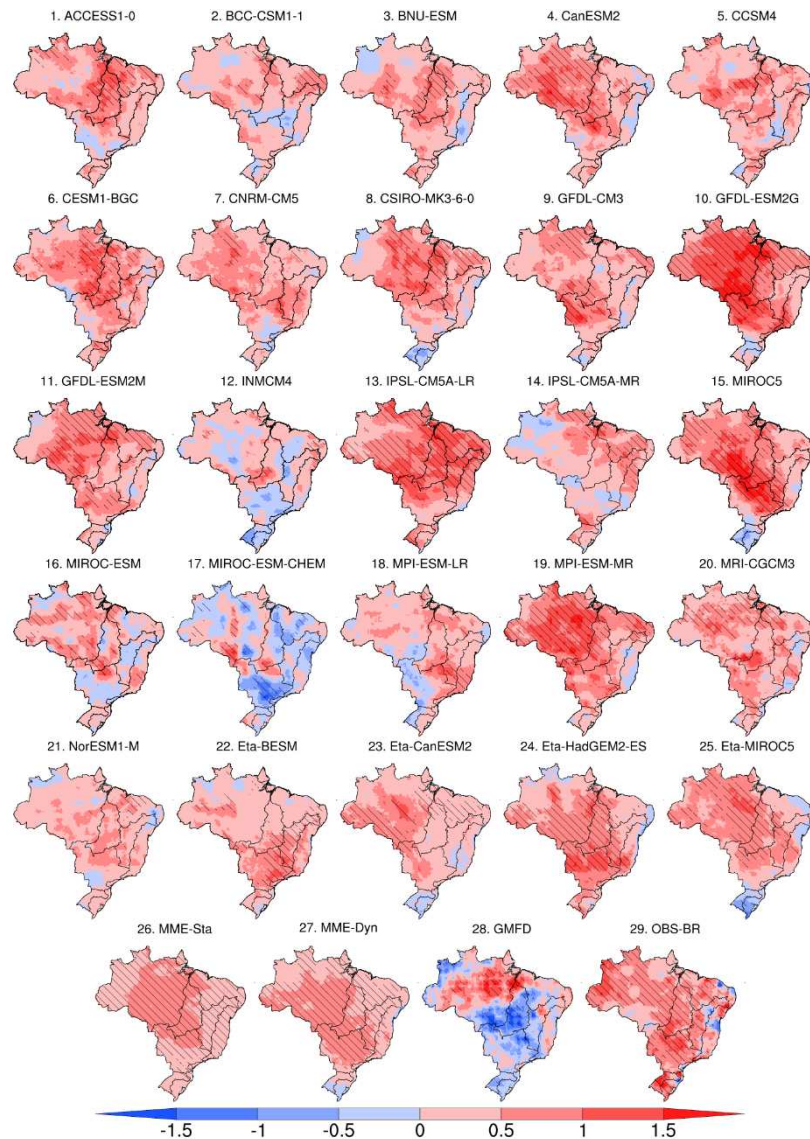


Figure 2.6 Trends ($^{\circ}\text{C}/\text{decade}$) in hottest days (TXx) for 21 NEX-GDDP climate models (1-21), 4 Eta-INPE Models (22-25), MME-Sta (26), MME-Dyn (27), GMFD (28) and OBS-BR (29; gray rectangle) from 1980 to 2005. Hatching indicates where trends are significant at the 95% level

2.3.2. Precipitation indices

2.3.2.1. Evaluation metrics

For the annual total wet-day precipitation index (PRCPTOT; Fig. 2.7), all statistically downscaled models show low bias (close to zero), especially for ACCESS1-0 (1), CESM1-BGC (6), and NorESM1-M (21). The dynamically downscaled models show less precipitation in the North region and slightly higher in the South region respect to OBS-BR (Fig. 2.8a; first column).

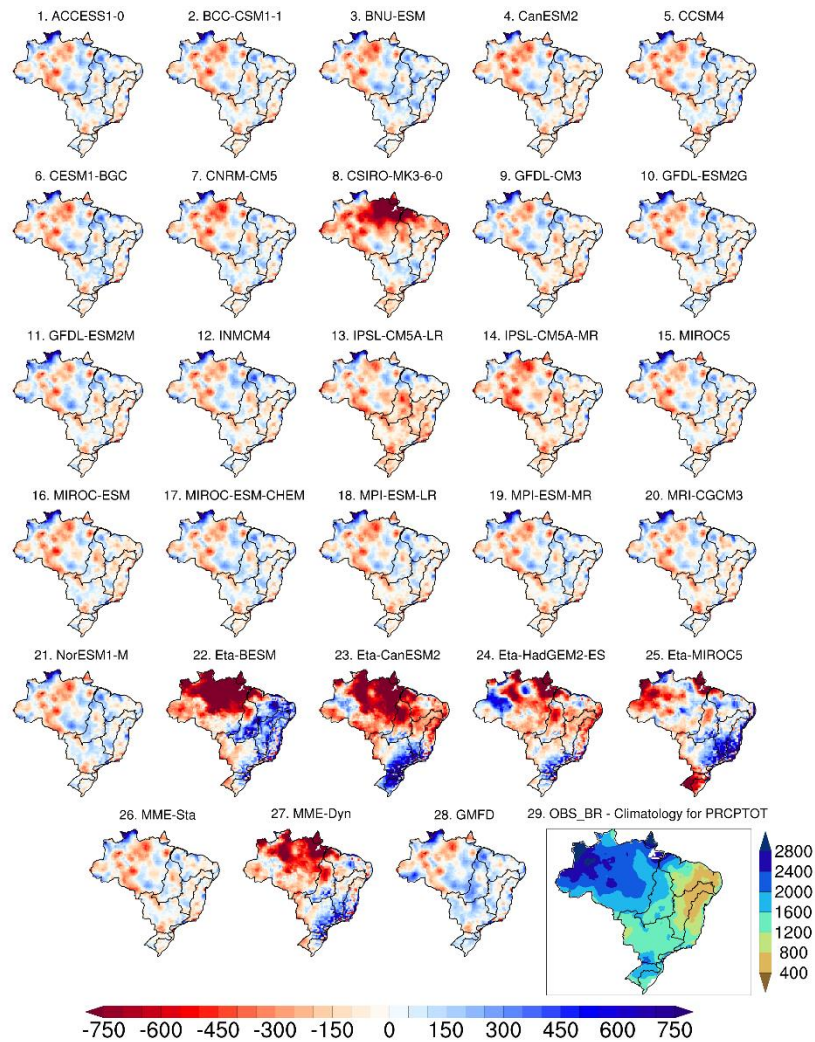


Figure 2.7 Climatology bias for the annual total wet-day precipitation - PRCPTOT (mm) for 21 statically (NEX-GDDP; models 1-21) and 4 dynamically (Eta-INPE; models 22-25) downscaled models, MME-Sta (26), MME-Dyn (27), and GMFD (28) from 1980 to 2005. Climatology for PRCPTOT in the observations dataset (OBS-BR; gray rectangle dataset 29) for 1980-2005.

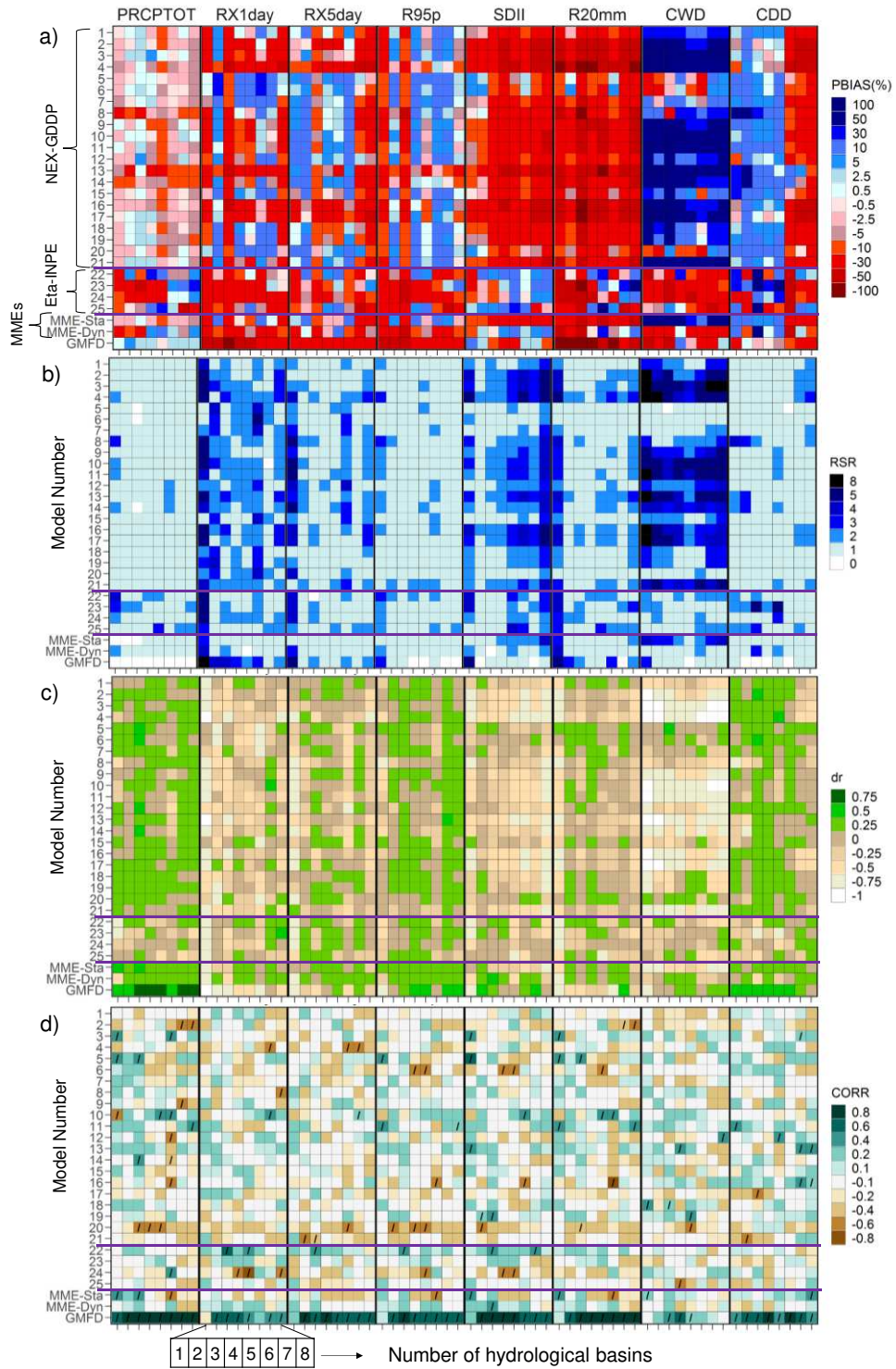


Figure 2.8 Statistics of performance obtained for annual precipitation indices for statically (NEX-GDDP) and dynamically (Eta-INPE) downscaled models, MME-Sta, MME-Dyn, and GMFD from 1980 to 2005 over eight hydrological basins (Fig. 2.1). (a) Percent Bias (PBIAS); (b) RMSE-observations standard deviation ratio (RSR); (c) a refined index of model performance (dr); (d) Correlation coefficients (CORR; the diagonal lines indicate significant correlations at 95% level). The horizontal purple lines refer to Eta-INPE datasets. For PBIAS and RSR, dark colors indicate models that perform worse than others, on average, and light colors indicate models that perform better than others, on average. Furthermore, for dr and CORR, dark (light) colors show models that have better (worse) statistical metrics than others, on average

Most of the downscaled models underestimate the observed values for intensity indices such as the annual maximum 1-day (RX1day) and the maximum 5-day precipitation amount (RX5day), especially in the North Atlantic basin (Fig. 2.8a; second and third column). Besides, models from statistically downscaled models (NEX-GDDP) overestimate the OBS-BR values, especially for the Tocantins River basin. Moreover, basins located in the South and Southern regions of Brazil show good performance according to *RSR* and *d_r*. Additionally, for the very wet days (R95p) index, all evaluation metrics show poor performance for all models over the Amazon River basin (Fig. 2.8; fourth column). On the other hand, the dynamically downscaled models from the Eta-INPE dataset tend to underestimate the R95p index for almost all basins. We note that summer and winter indices (e.g., PRCPTOT, RX1day, and RX5day) are generally underestimated across all Brazil for almost all downscaled models except for Eta-INPE models (models 22, 23, 24, and 25) that show wet bias in winter over most of the watersheds (Fig. 2.9a-d). Similar to the annual scale (Fig. 2.8a), the weak performance of downscaled ESMs is more evident for the Amazon basin.

In almost all basins, the statistically downscaled ESMs models underestimate the simple daily intensity index (SDII) and the number of very heavy precipitation day (R20mm) indices (see fifth and sixth columns of Fig. 2.8). For these indices, the performance of the Eta-INPE dataset is better than NEX-GDDP. The *PBIAS* shows that the simulations underestimate the observed values for the Amazon River and overestimate in Uruguay River and South Atlantic basins. In general, for all downscaled ESMs, the poorest performance (*RSR*, *d_r*, and *CORR*) is found over the Amazon River basin.

For the duration indices like consecutive dry days (CDD) and consecutive wet days (CWD) (see last two columns of Fig. 2.8), some models show the largest disagreement when compared with the observed dataset, and thus indicate considerable uncertainty. For instance, models 8, 13, 14, and 23 are generally too dry while others too wet (models 2, 3, 4, 11, 13, 16, and 17) over the North and Northeast of Brazil. The statistically downscaled ESMs show worse performance over the Amazon River, Tocantins Rivers, and the North Atlantic basin (Fig. 2.8). On the other hand, some models such as CCSM4 (5) and CESM1-BGC (6) have relatively good performance in the Central-West, Southeast, and South of Brazil. Downscaled NEX-GDDP models show better skill in simulating the CDD index at seasonal scale than ETA-INPE models. Noteworthy, statistically downscaled ESMs have better scores (Fig. 2.9) in simulating CDD index in winter than summer (see models 8, 10, 13, 14 in Fig. 2.9).

Comparison between observations (OBS-BR) and the reanalyses shows that the GMFD dataset underestimates approximately all precipitation indices at the annual scale (see dataset 28 of Fig. 2.7), except for PRCPTOT as the *PBIAS* varies between 0 and 6% (see bottom of Fig. 2.8a-d). However, in general, the RX1day, RX5day, and R95p indices are overestimated for all basins (Fig. 2.8a). The results do not indicate a dominant positive or negative pattern of *PBIAS* for SDII, R20mm, CDD, and CWD. It should be noted that the worst performance is found over the Amazon River, Tocantins Rivers, and North Atlantic basins (Fig. 2.8). In this sense, the main discrepancies between OBS-BR and GMFD are found for several indices such as RX1day, RX5day, R20mm, and CWD (Fig. 8). Fig. 2.9a shows a consistently dry bias in PRCPTOT, RX1day, RX5day, and CDD indices during the summer and low skill in reproducing intensity indices (RX1day, RX5day). GMFD also shows a better winter precipitation indices estimation over most parts of Brazil, according to *RSR*, *d_r*, and *CORR* (Fig.

2.9b-d). Furthermore, the Amazon River basin is poorly represented in GMFD for the annual, summer, and winter for almost all precipitation indices, except for PRCPTOT and CDD (see Figs. 8, 9).

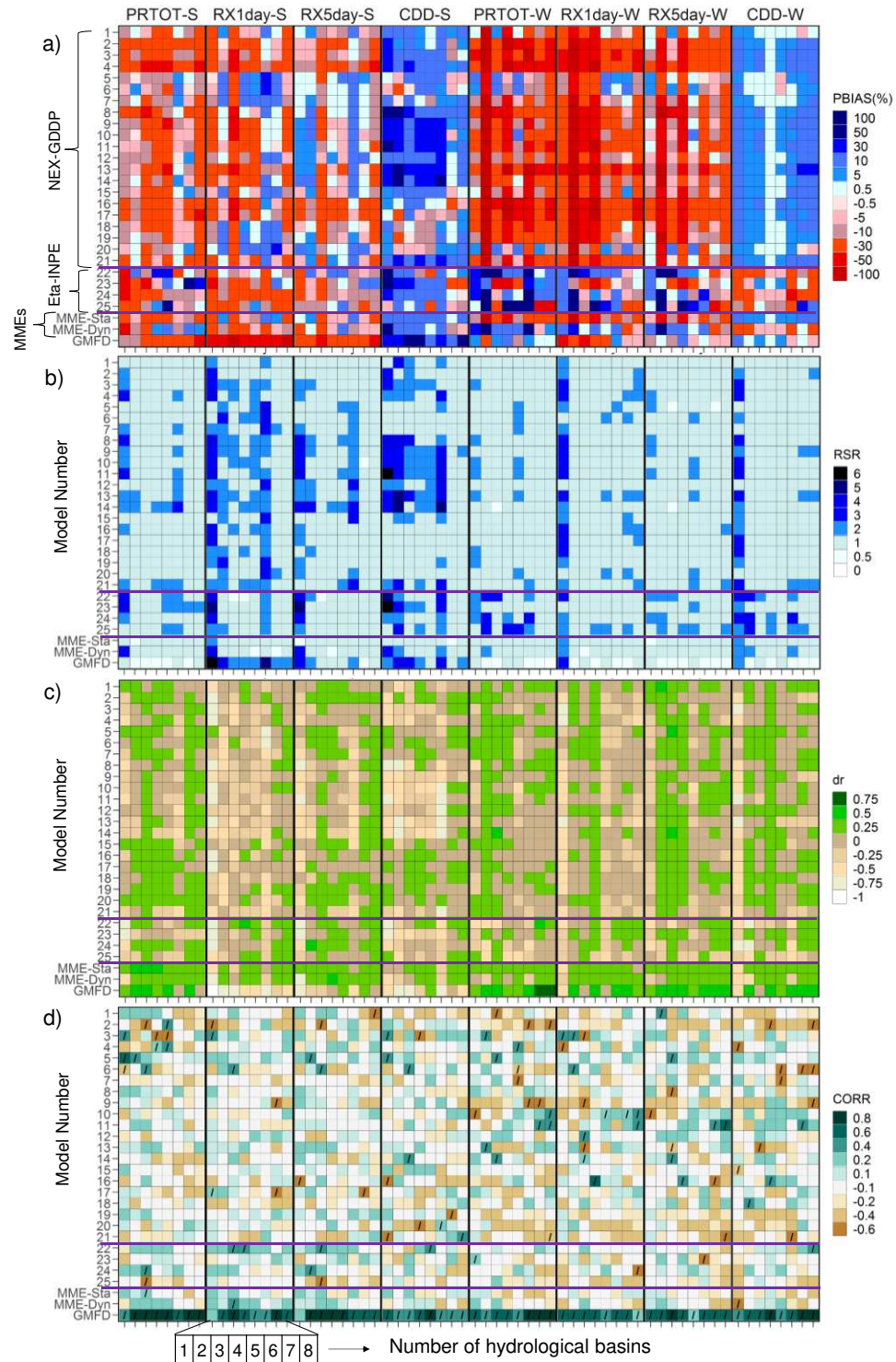


Figure 2.9 As in Fig. 2.8, but for extreme precipitation indices in summer (DJF) and winter (JJA). The nomenclature of the ETCCDI indices was adapted to Index-“S” for summer and Index-“W” for winter

The overall performance assessment (see bottom of Fig. 2.8) shows that the models from NEX-GDDP and Eta-INPE underestimate precipitation intensity (RX1day and R95p) and frequency (R20mm) over the Amazon River basin. However, the statistically downscaled models perform better for the PRCPTOT and CDD indices on the both annual and seasonal scale (Figs. 8, 9). The relative errors could be because PRCPTOT and CDD are less dependent on fine scale phenomena than the indices that represent extreme precipitation events (e.g., RX1day and RX5day). Besides, the coarse resolution of the underlying ESMs makes them have special difficulties in representing the spatial and temporal heterogeneity of precipitation over tropical regions (Marengo et al. 2010b; Rusticucci et al. 2010; Sillmann et al. 2013a).

Of particular importance is the fact that for several models and regions, the sign of the bias in CDD is different in the annual and seasonal scales. For example, most models show a negative *PBIAS* (fewer dry days) at the annual scale, but a positive (more dry days) *PBIAS* in both summer and winter seasons in regions more to the south (e.g., models 6, 7 and 8). Transition seasons (spring, autumn) have a larger influence on the overall annual number of precipitation days across these higher-latitude regions of Brazil (Rao et al. 2016). The opposite is true for some statistically downscaled models in other regions, and the sign of the CDD bias is also reversed between summer and winter in the dynamically downscaled models. Since some activities such as agricultural production are particularly sensitive to dry spells in specific seasons (e.g., da Silva et al. (2013)) special care should be taken when selecting downscaled models for this kind of application.

The MMEs have weakest representation of intensity indices principally over the Amazon basin at the annual and seasonal levels. Multi-model ensembles generally have a better performance than most individual models, but not all. Our results show that MME-Sta might be a better approach in precipitation indices (e.g., PRCPTOT and RX5day) over the Amazon River, where most models show poor performance (Figs. 8, 9). On the other hand, the SDII, R20mm, and CWD values from MMEs-Dyn generally agree more with the observations than MME-Sta over most hydrological basins. The MMEs-Sta and MME-Dyn overestimate and underestimate CWD and CDD, respectively, particularly over the Amazon, Tocantins, and North Atlantic basin. It should be highlighted that the bias is significantly smaller in the Eta simulations.

In general, the dynamically downscaled models simulate less total precipitation than OBS-BR, even for the NCEP-NCAR reanalysis used in GMFD. This underestimation by the Eta-simulations discussed here is consistent with the results obtained by Chou et al. (2014a) and Valverde and Marengo (2014), especially in northern Brazil. The agreement is generally much better for the statistically downscaled models, although the sign of the errors has a similar spatial pattern, with modest underestimation of total precipitation in northern Brazil. All downscaled models capture the main spatial features of extreme precipitation indices climatology, but significant biases were found, particularly in the Amazon River basin (Figs. 8 and 9). The systematic rainfall underestimation by the models can be related to many factors, such as the poor representation of cumulus convection, the biosphere-atmosphere interactions in the rainforest, soil moisture, and land surface processes (Torres and Marengo 2013; Yin et al. 2013). For example, representation of aerosol-related processes is a major source of uncertainty on climate models (Seinfeld et al. 2016), and precipitation extremes are particularly affected by it (Lin et al. 2018). On the other hand, there is poor data observation coverage in some portions of South America, mainly in the Amazon

Basin, in which few meteorological stations are available. This influences the magnitude and location of the bias patterns, mainly for precipitation (Torres and Marengo 2013).

2.3.2.2. Trend analysis in precipitation indices

Most of the climate trend analysis in precipitation extremes in Brazil have focused on specific basins in southern (Donat et al. 2013a; Skansi et al. 2013; Carvalho et al. 2014; Avila et al. 2016; Murara et al. 2018) or northern and northeastern Brazil (Oliveira et al. 2014, 2017; Valverde and Marengo 2014; Bezerra et al. 2019). It is quite challenging to compare these studies with ours since they included small areas and many factors can influence trends (e.g., study period, weather stations, data quality control, homogeneity and trend estimation methods). However, our findings are in line with the results of the prevalence of regions with an upward trend in the annual (Fig. 2.10) and summer maximum daily rainfall. The interested reader should refer to Fig. 2.S16 to the trends for the selected indices (PRCPTOT, RX1day, RX5day, and CDD) at the seasonal scale. Also, the positive trends in consecutive dry days are generally in line with those of Valverde and Marengo (2014) for southern Amazon, Upper São Francisco, Tocantins, and northern Paraná basins (Fig. 2.10).

Brazil-wide trends in precipitation indices are generally not significant for OBS-BR and GMFD (Fig. 2.10). Some hydrological basins have the same patterns, mainly showing decreases in PRCPTOT and CWD and some increases in CDD (Figs. 10, 11), especially in northeastern, southeastern, and southern Brazil. Also, results for the CDD index in winter and summer indicate dry trends in many downscaled models across the southern watersheds (e.g., PAR, URU, and SAR). The extreme precipitation indices display mixed signal trends and show less agreement between the different datasets than the temperature indices in both annual and seasonal scales. The precipitation trends in GFDL-ESM2G (10) and Eta-HadGEM2-ES (24) are especially troublesome (see Figs. 10, 11) in annual and seasonal trends, suggesting a much stronger drying trend than OBS-BR and other downscaled ESMs. Moreover, MMEs appear to agree better with trends in OBS-BR than trends in GMFD precipitation indices.

In general, there is not a single model that is the most appropriate to represent the observed trends for each index over the basins in both annual and seasonal temporal scales for the period 1980–2005. Although trend patterns vary widely across datasets (21 NEX-GDDP climate models, 4 Eta-INPE models, MMEs, GMFD, and OBS-BR), especially for precipitation indices, the multi-model ensembles are a good alternative to better capture observed trends.

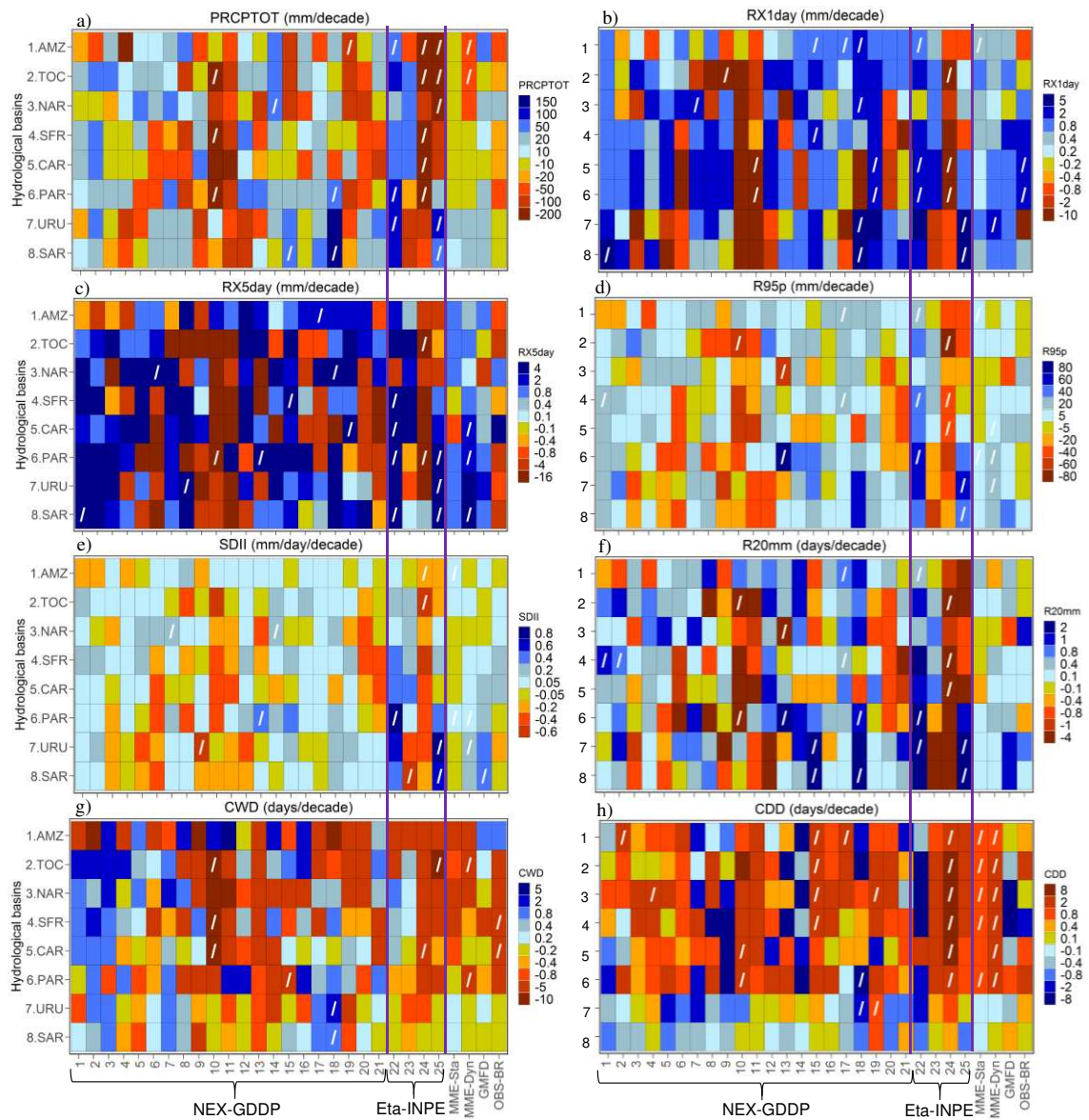


Figure 2.10 Trends per decade from 1980 to 2005 for precipitation indices at the annual scale (a-h) for 21 NEX-GDDP climate models (1-21), 4 Eta-INPE climate models (22-25), MME-Sta (26), MME-Dyn (27), GMFD (28) and OBS-BR over eight hydrological regions in Brazil (Fig. 2.1). Diagonal lines indicate significant trends at 95% level. The vertical purple lines refer to ESMs from Eta-INPE datasets.

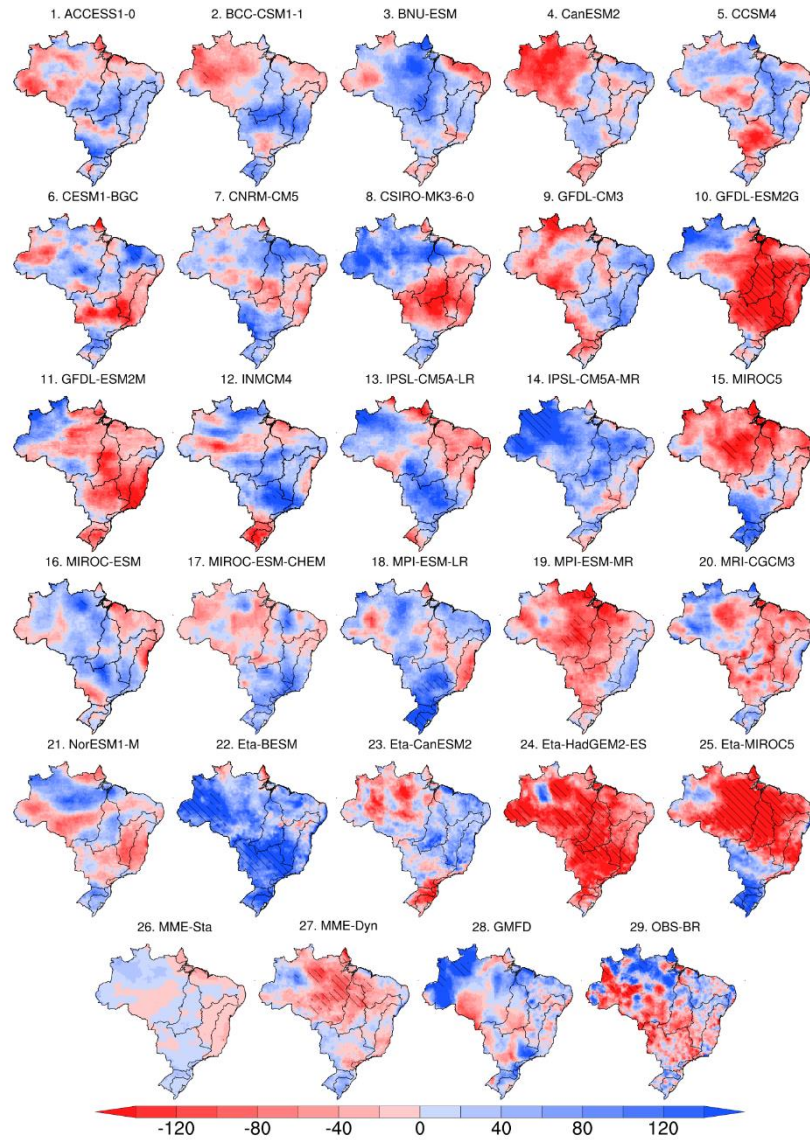


Figure 2.11 Trends (days/decade) in annual total wet-day precipitation - PRCPTOT (mm) for 21 NEX-GDDP climate models (1-21), 4 Eta-INPE climate models (22-25), MME-Sta (26), MME-Dyn (27), GMFD (28) and OBS-BR (29; gray rectangle) from 1980 to 2005. Hatching indicates where trends are significant at the 95% level.

2.3.3. The comprehensive model rank (M_R)

Table 2.3 provides the ranking for all models analyzed using 16 climate indices at the annual scale over eight hydrological basins throughout Brazil. In terms of temperature indices, the best models for the whole domain are, in order, CSIRO-MK3-6-0 (8) and CNRM-CM5 (7); these are the only models with $M_R \geq 0.85$. The models with the lowest M_R are Eta-CanESM2 (23) and GFDL-ESM2M (11). When considering the precipitation indices, the three four models are CCSM4 (5) followed by MRI-CGCM3 (20), and CNRM-CM5 (7), whereas models with the worst M_R are MIROC-ESM (16), IPSL-CM5A-LR (13) and CanESM2 (4). Considering all climate indices over all basins, the best individual models are CNRM-CM5 and CCSM4, followed by MRI-CGCM3, and the worst on the overall ranking are MIROC-ESM (16), GFDL-ESM2M (11) and CanESM (4). Furthermore, analyzing the country as a whole (Table 2.3), the multi-model ensemble of NEX-GDDP models (MME-Sta, $M_{R_{overall}} = 0.927$)

generally leads to better skill scores than individual models and ensemble of Eta-INPE models (MME-Dyn, $M_{\text{Roverall}} = 0.872$).

Table 2.3 Ranking of downscaled ESMs and MMEs for temperature and precipitation indices at the annual scale over Brazil. Downscaled models or MMEs in bold achieve a skill score ≥ 0.85 . The optimal value of M_R is 1.0

Overall Ranking (Average of $M_{\text{R-temperature}}$ and $M_{\text{R-precipitation}}$)			Temperature Indices		Precipitation Indices	
Models and MMEs (ID)	Rank	Skill score (M_R)	Rank	M_R	Rank	M_R
MME-Sta (26)	1	0.927	1	0.956	1	0.899
CNRM-CM5 (7)	2	0.877	3	0.883	4	0.870
MME-Dyn (27)	3	0.872	4	0.877	5	0.868
CCSM4 (5)	4	0.863	8	0.827	2	0.898
MRI-CGCM3 (20)	5	0.859	5	0.844	3	0.875
MPI-ESM-MR (19)	6	0.835	6	0.832	9	0.838
MIROC5 (15)	7	0.830	10	0.810	8	0.850
CESM1-BGC (6)	8	0.823	16	0.781	6	0.865
ACCESS1-0 (1)	9	0.822	13	0.790	7	0.853
CSIRO-MK3-6-0 (8)	10	0.819	2	0.887	21	0.751
BCC-CSM1-1 (2)	11	0.797	7	0.830	17	0.763
Eta-BESM (22)	12	0.791	19	0.771	12	0.810
Eta-HadGEM2-ES (24)	13	0.786	12	0.794	14	0.779
MPI-ESM-LR (18)	14	0.786	21	0.739	10	0.834
GFDL-ESM2G (10)	15	0.780	15	0.784	15	0.775
GFDL-CM3 (9)	16	0.779	11	0.796	18	0.761
INMCM4 (2)	17	0.778	21	0.739	11	0.818
BNU-ESM (3)	18	0.774	9	0.825	24	0.723
IPSL-CM5A-MR (14)	19	0.753	18	0.773	22	0.732
Eta-MIROC5 (25)	19	0.753	23	0.736	16	0.769
NorESM1-M (21)	21	0.750	17	0.776	23	0.724
IPSL-CM5A-LR (13)	22	0.744	14	0.789	26	0.699
MIROC-ESM-CHEM (17)	23	0.741	24	0.731	20	0.752
Eta-CanESM2 (23)	24	0.736	27	0.693	13	0.780
MIROC-ESM (16)	25	0.733	20	0.751	25	0.715
GFDL-ESM2M (11)	26	0.730	26	0.707	19	0.754
CanESM2 (4)	27	0.705	25	0.724	27	0.687

Furthermore, the ranking of the downscaled ESMs obtained at the seasonal scale is very similar to those presented at the annual scale. For instance, the best models are MRI-CGCM3, CNRM-CM5, and CCSM4, using the overall ranking of the selected temperature (TXx, TNn, TN10p, and TX90p) and precipitation (PRCPTOT, RX1day, RX5day, CDD) indices. Also, the MMEs-Sta performed better than MMEs-Dyn and individual downscaled ESMs in both summer and winter. Being aware of these results, we decided to emphasize the ranking discussion on an annual scale. Readers interested in the ranking for summer and winter can refer to Table 2.S1.

It is important to note that the top three models in Table 2.3 have a native horizontal resolution finer than $2^\circ \times 2^\circ$ – latitude/longitude (Table 2.1), which could indicate that a finer resolution allows the models to resolve better processes associated with climate extremes. Although models with coarser resolutions do tend to perform poorly, having a finer resolution is not necessarily a determining factor to choose the best performing model. For instance, the downscaled results of models with very fine native horizontal resolutions (e.g., CESM1-BGC: $0.924^\circ \times 1.250^\circ$) do not perform better in temperature indices than coarser resolution models such as BNU-ESM ($2.8^\circ \times 2.8^\circ$) or BCC-CSM1-1 ($2.8^\circ \times 2.8^\circ$). However, this association is stronger when considering precipitation

indices, as the top four models have native horizontal resolutions less than $1.5^\circ \times 1.5^\circ$ (Table 2.3), and the worst ones greater than $2^\circ \times 2^\circ$ such as CanESM2 ($2.8^\circ \times 2.8^\circ$) and MIROC-ESM ($2.791^\circ \times 2.813^\circ$). This is likely due to the higher spatial heterogeneity of the precipitation and has also been observed with raw ESM results over Australia (Alexander and Arblaster 2017) and East Asia (Kusunoki and Arakawa 2015). The number and extent of vertical layers in the model does not seem to be an important factor for either temperature or precipitation indices, as was previously observed over higher altitude regions such as the Equatorial Andes (Campozano et al. 2017).

Although the ensembles generally perform better in a larger number of basins than individual models, some models are better than both ensembles for some particular basins, especially for precipitation (Fig. 2.12). For example, although MME-Sta ranks better than most models for precipitation for the South Atlantic basin, individual models like CCSM4 (5), CESM1-BGC (6), and INMCM4 (12) rank considerably better than the ensemble. Although an improvement over most individual dynamically downscaled models for precipitation in most basins, MME-Dyn does not rank better than the best model in half of the basins and ranks especially poorly in the Amazon River basin. For temperature indices, using MMEs more consistently leads to better results than individual models, though not always. For example, individual models such as MPI-ESM-MR (19) show the highest values of M_R among models and ensembles for the Parana River basin. It is important to note that MME-Dyn is considerably worse than MME-Sta for most basins. However, MME-Dyn ranks better in the South Atlantic basin at both temperature and precipitation indices, and in the Tocantins, Parana, and South Atlantic basins for precipitation indices.

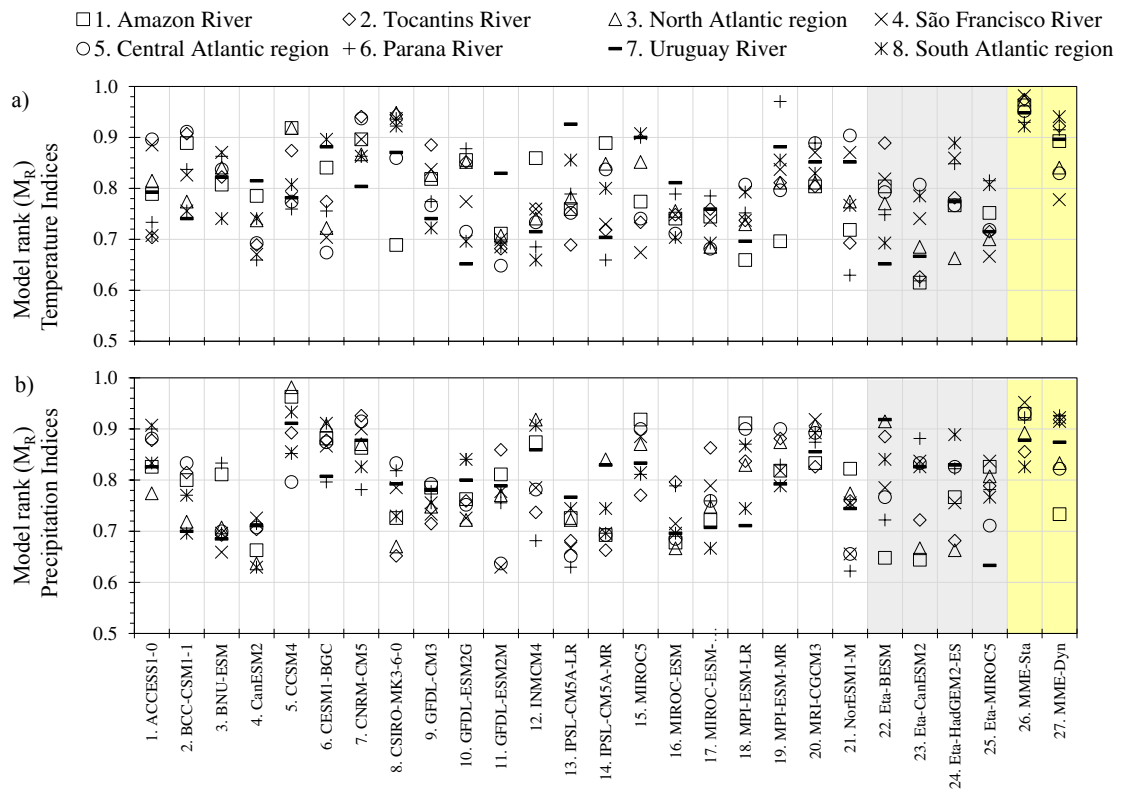


Figure 2.12 Model rank (MR) value for temperature (a) and precipitation indices (b) at the annual scale. Each symbol represents a given basin. White, gray and yellow areas refer to 21 NEX-GDDP climate models, four (4) Eta-INPE climate models and multi-model ensembles (MMEs), respectively

Noteworthy, the most successful downscaling simulations based on the Eta Regional Climate Model, are the ones forced by BESM (22) and HadGEM2-ES (24) (Table 2.3). The Eta-HadGEM2-ES appear to be better than Eta-BESM for temperature indices over hydrological basins located in the southern part of Brazil, and worse for precipitation indices over basins on the northeast of the country (Fig. 2.11).

The large difference in the number of models among different datasets used in the ensemble mean complicates a proper comparison between the dynamical and statistical downscaling techniques. Although none of the dynamically downscaled models are among the best in the overall ranking (Table 2.3), they perform very well in some aspects. Eta-BESM, for example, is ranked the best for precipitation indices in the Uruguay River basin, although it is ranked the worst for temperature indices in the same basin (Fig. 2.12). A more useful comparison can be made using the ESMs that were downscaled using both techniques, CanESM2 and MIROC5, but also show that one technique is not necessarily better than the other for evaluating climate extremes. Although the statistically downscaled CanESM2 is among the worst ranking models in all indices, the dynamically downscaled version performs reasonably well in all basins, except for the Amazon and Tocantins basins. On the other hand, the statistically downscaled MIROC5 is generally better than its dynamically downscaled counterpart, except for the Tocantins River basin.

2.4. Summary and conclusions

This paper provides an overview of the performance of 25 downscaled Earth System Models, generated by statistical (NEX-GDDP) and dynamical (Eta-INPE) downscaling techniques, to evaluate extreme climate indices during historical climate over eight hydrological basins across Brazil. Performance was evaluated for annual and seasonal indices (summer and winter) by contrasting simulations with an observational gridded dataset at high horizontal resolution.

The GMFD dataset used as reference for the statistical downscaling is problematic for precipitation over the Amazon River basin in both annual and seasonal scale, with little capacity to simulate the climatology and temporal variability of most precipitation indices, except for PRCPTOT and CDD. GMFD also tends to reproduce much higher TXx and lower WSDI than the observed values, and shows trends with the wrong sign (positive or negative) for several indices and basins. These discrepancies point to the possibility of improvement of statistically downscaled products for Brazil by using denser observational networks as reference.

Although the CNRM-CM5, CCSM4, and MRI-CGCM3 (NEX-GDDP models) statistically downscaled products have the best results among individual models in an overall comparison for Brazil for annual, summer and winter indices, the results varied widely among basins. Finer horizontal resolutions of the original ESMs appear to be somewhat related, but not determinant, to the performance of the downscaled product in representing extreme climate events, especially precipitation. The use of multi-model ensembles, although improving the overall representation, does not always lead to the best results depending on the region considered. The multi-model ensembles also show considerable discrepancies, especially across northern Brazil, in several extremes climate indices, particularly ones related to the persistence of climate events such as cumulative wet and dry days and warm spell duration. These conclusions are generally valid at both annual and seasonal scales. However, some models and regions present conflicting behaviors at the annual scale and in different seasons, especially for

consecutive dry days (CDD). Caution must be taken when selecting model products for applications that are particularly sensitive to extremes in specific seasons.

The downscaled ESMs appear to compare better with OBS-BR in terms of trend patterns than the GMFD dataset. Furthermore, downscaled product trends are much more spatially coherent in temperature than precipitation indices when compared with the observational dataset. In this sense, the trend pattern in most climate indices is generally better captured by multi-model ensembles than individual downscaled ESMs (especially for precipitation indices).

In conclusion, despite some models being generally better than others, no single downscaled product or ensemble is the best choice for every region. The results presented in this paper can guide researchers in choosing the best data for each particular application, as well as inform climate modelers about the shortcomings of models and downscaling approaches over Brazil.

2.5. Acknowledgments

The authors would like to thank the Universidade Federal de Viçosa. This work was supported by Minas Gerais Research Foundation (FAPEMIG) and to the Coordination for the Improvement of Higher Education Personnel (CAPES). The authors thank to the Byrd Polar and Climate Research Center. The authors are grateful to the climate simulations data generated by CPTEC/INPE and made available on the PROJETA platform, and we thank NEX-GDDP dataset, prepared by the Climate Analytics Group and NASA Ames Research Center using the NASA Earth Exchange, and distributed by the NASA Center for Climate Simulation (NCCS). The authors further thank Alexandre Xavier, Carey King, and Bridget Scanlon that provided a gridded observational dataset used in this work.

2.6. Supplementary material

Extreme Climate Indices in Brazil: Evaluation of Downscaled Earth System Models at High Horizontal Resolution

Alvaro Avila; Gabriel Abrahão; Flavio Justino; Roger Torres; Aaron Wilson. 2020.

Climate Dynamics. Manuscript number: CLDY-D-19-00584

Table S2.1 Ranking of downscaled ESMs and MMEs for temperature and precipitation indices at seasonal scale over Brazil. Downscaled models or MMEs in bold achieve a skill score ≥ 0.85 . The optimal value of M_R is 1.0.

Overall Ranking			Temperature Indices				Precipitation Indices			
			Summer		Winter		Summer		Winter	
Models and MMEs (ID)	Rank	Skill score (M_R)	Rank	M_R	Rank	M_R	Rank	M_R	Rank	M_R
MME-Dyn (26)	1	0.910	1	0.928	1	0.921	1	0.906	1	0.883
MME-Sta (27)	2	0.863	3	0.866	3	0.860	2	0.879	7	0.845
MRI-CGCM3 (20)	3	0.842	5	0.850	9	0.813	3	0.854	5	0.851
CCSM4 (5)	4	0.840	8	0.818	5	0.849	7	0.838	4	0.855
CNRM-CM5 (7)	5	0.832	7	0.826	3	0.860	16	0.792	6	0.849
ACCESS1-0 (1)	6	0.828	17	0.778	8	0.836	11	0.817	2	0.882
MPI-ESM-LR (18)	7	0.824	4	0.854	11	0.804	8	0.836	12	0.801
BCC-CSM1-1 (2)	8	0.820	2	0.898	17	0.778	6	0.843	18	0.762
MPI-ESM-MR (19)	9	0.820	13	0.798	6	0.842	4	0.850	14	0.788
CESM1-BGC (6)	10	0.813	19	0.772	10	0.813	5	0.844	9	0.824
MIROC5 (15)	11	0.806	10	0.816	14	0.800	10	0.817	13	0.790
Eta-BESM (22)	12	0.802	12	0.800	7	0.837	9	0.826	24	0.744
GFDL-ESM2G (10)	13	0.799	14	0.798	13	0.801	19	0.767	8	0.827
CSIRO-MK3-6-0 (8)	14	0.798	6	0.833	2	0.862	25	0.725	16	0.773
INMCM4 (12)	15	0.797	21	0.769	12	0.804	20	0.750	3	0.867
IPSL-CM5A-MR (14)	16	0.788	9	0.816	16	0.781	21	0.743	11	0.813
BNU-ESM (3)	17	0.779	16	0.785	15	0.788	15	0.795	23	0.747
Eta-HadGEM2-ES (24)	18	0.778	18	0.778	20	0.769	12	0.807	21	0.760
NorESM1-M (21)	19	0.768	11	0.806	23	0.735	18	0.768	17	0.763
GFDL-CM3 (9)	20	0.758	23	0.741	17	0.778	22	0.733	15	0.778
MIROC-ESM (16)	21	0.756	20	0.769	26	0.713	17	0.788	22	0.752
MIROC-ESM-CHEM (17)	22	0.752	24	0.741	27	0.702	13	0.806	19	0.761
Eta-CanESM2 (23)	23	0.752	26	0.694	19	0.770	23	0.731	10	0.813
GFDL-ESM2M (11)	24	0.746	25	0.736	21	0.761	24	0.725	20	0.761
IPSL-CM5A-LR (13)	25	0.735	15	0.788	24	0.735	26	0.716	27	0.702
CanESM2 (4)	26	0.734	22	0.760	22	0.740	27	0.700	25	0.737
Eta-MIROC5 (25)	27	0.733	27	0.673	25	0.731	14	0.800	26	0.729

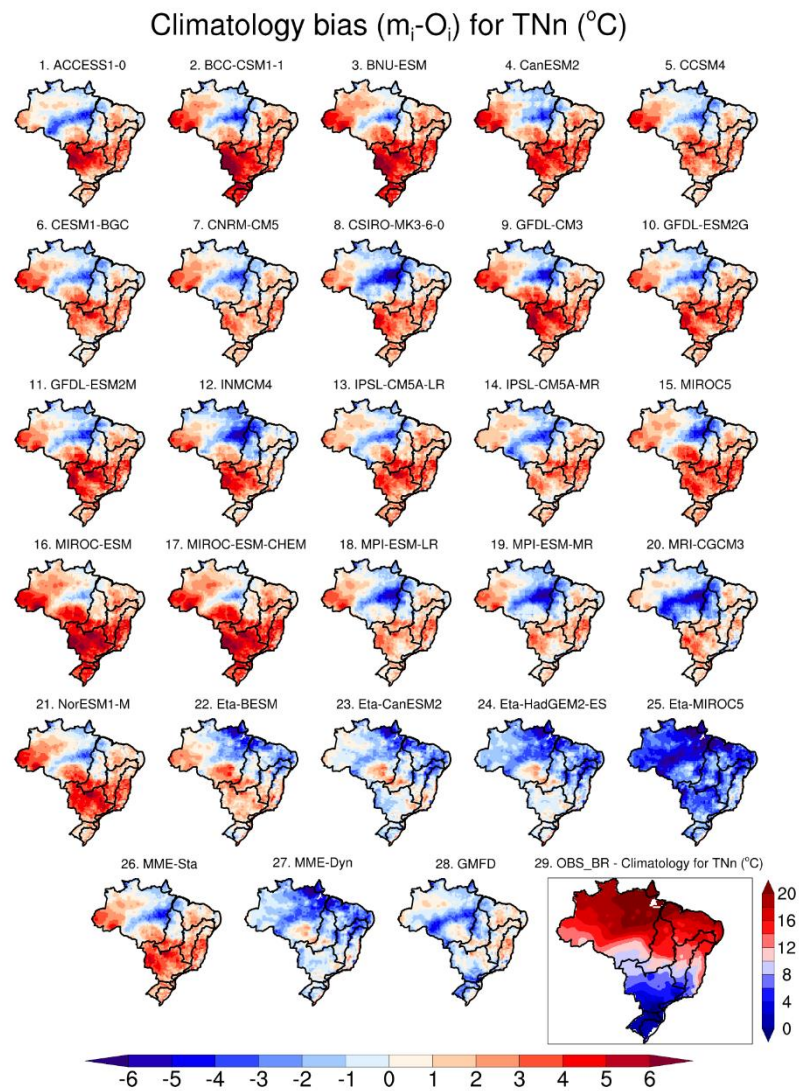


Figure S2.1 Climatology for the coldest night – T_{Nn} for 21 NEX-GDDP climate models (1-21), 4 Eta-INPE models (22-25), MME-Sta (26), MME-Dyn (27), GMFD (28) and OBS-BR (29; gray rectangle) from 1980 to 2005. (b) Climatology bias for 1980-2005

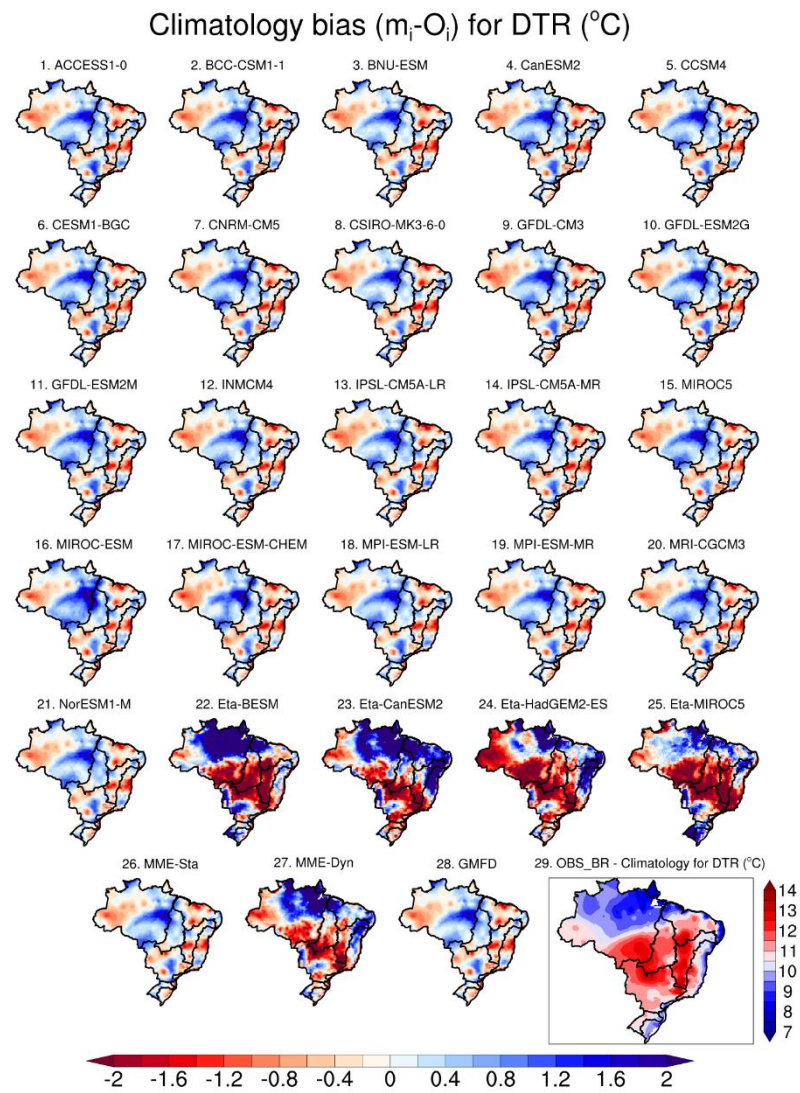


Figure S2.2 Climatology for diurnal temperature range – DTR for 21 NEX-GDDP climate models (1-21), 4 Eta-INPE models (22-25), MME-Sta (26), MME-Dyn (27), GMFD (28) and OBS-BR (29; gray rectangle) from 1980 to 2005. (b) Climatology bias for 1980-2005

Recourse: Authors

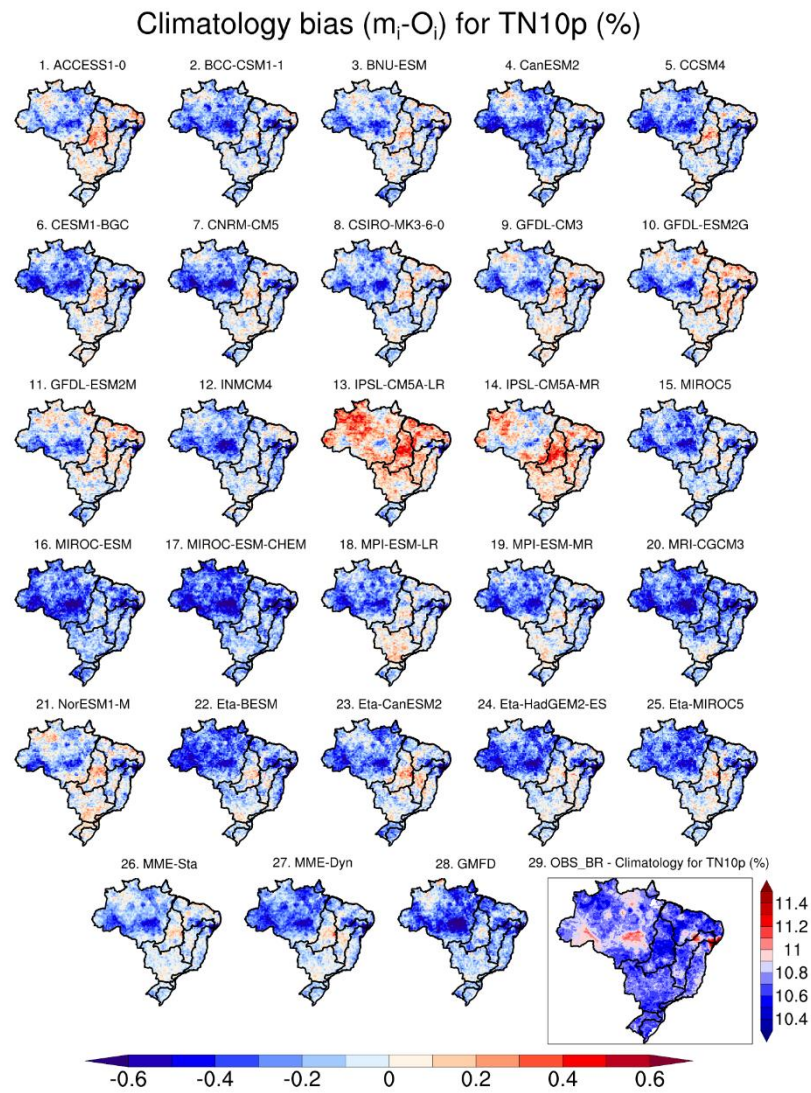


Figure S2.3 Climatology for cool nights – TN10p for 21 NEX-GDDP climate models (1-21), 4 Eta-INPE models (22-25), MME-Sta (26), MME-Dyn (27), GMFD (28) and OBS-BR (29; gray rectangle) from 1980 to 2005. (b) Climatology bias for 1980-2005

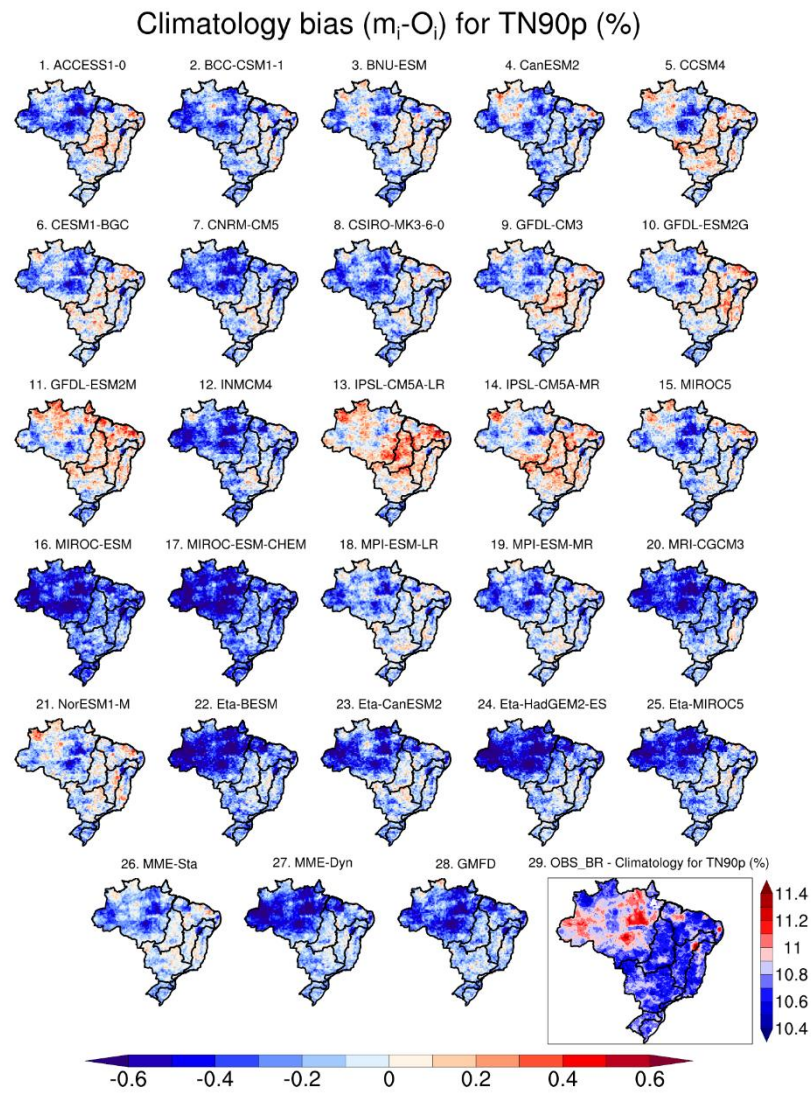


Figure S2.4 Climatology for warm nights – TN90p for 21 NEX-GDDP climate models (1-21), 4 Eta-INPE models (22-25), MME-Sta (26), MME-Dyn (27), GMFD (28) and OBS-BR (29; gray rectangle) from 1980 to 2005. (b) Climatology bias for 1980-2005

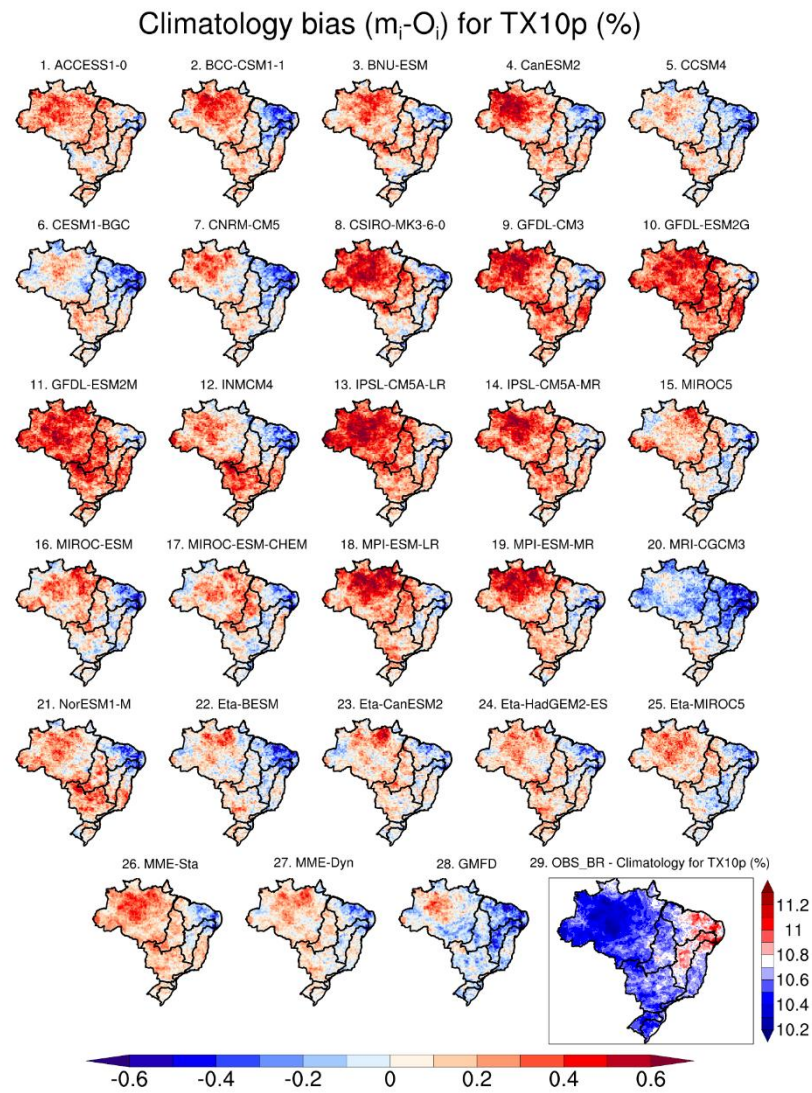


Figure S2.5 Climatology for cool days – TX10p for 21 NEX-GDDP climate models (1-21), 4 Eta-INPE models (22-25), MME-Sta (26), MME-Dyn (27), GMFD (28) and OBS-BR (29; gray rectangle) from 1980 to 2005. (b) Climatology bias for 1980-2005

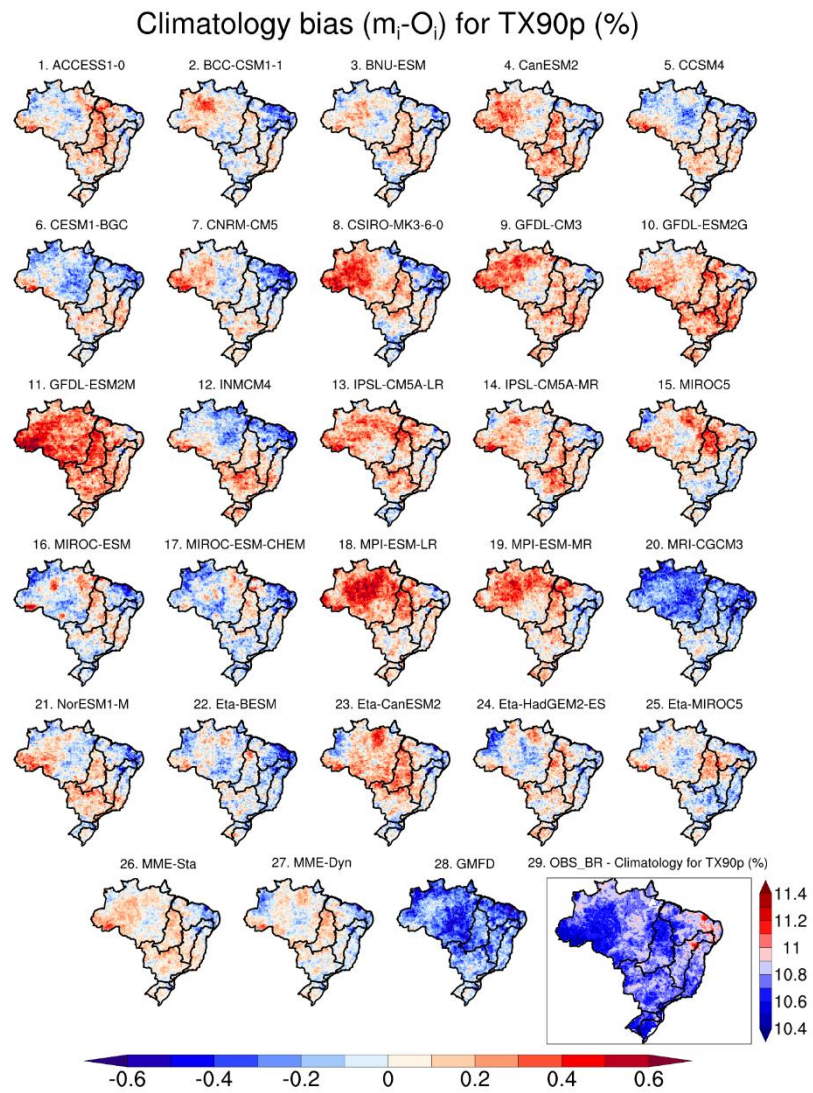


Figure S2.6 Climatology for warm days – TX90p for 21 NEX-GDDP climate models (1-21), 4 Eta-INPE models (22-25), MME-Sta (26), MME-Dyn (27), GMFD (28) and OBS-BR (29; gray rectangle) from 1980 to 2005. (b) Climatology bias for 1980-2005

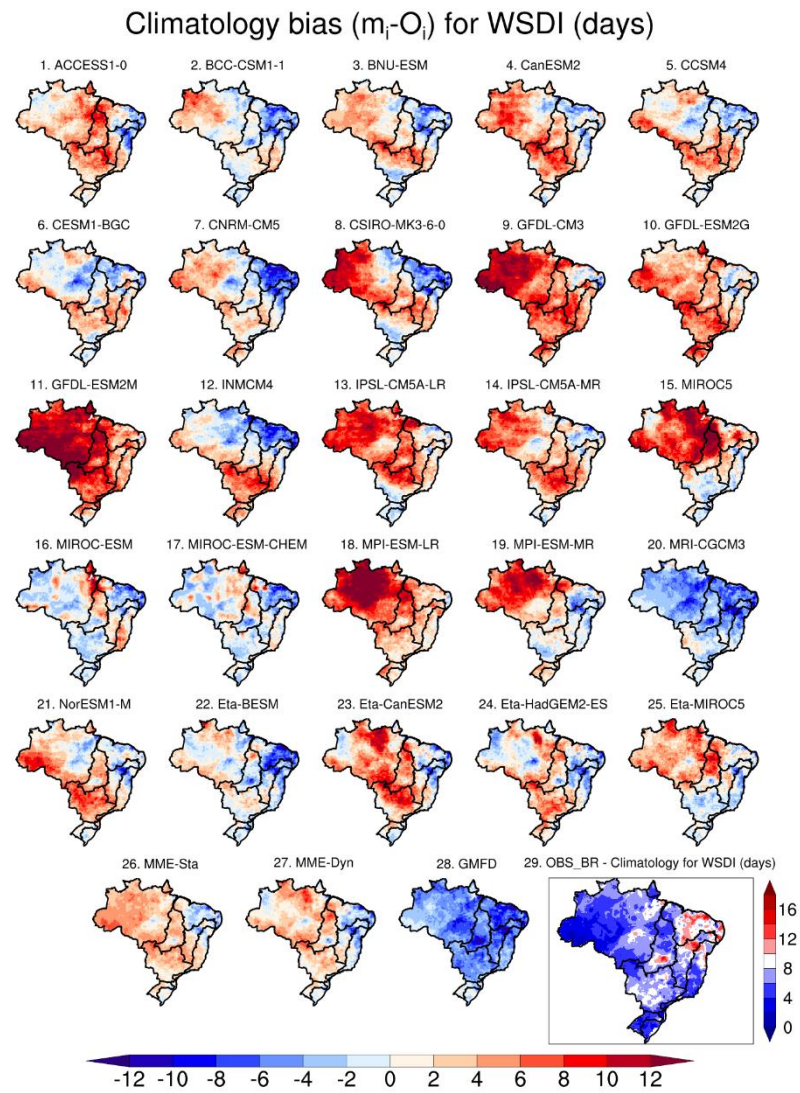


Figure S2.7 Climatology for warm spell duration indicator – WSDI for 21 NEX-GDDP climate models (1-21), 4 Eta-INPE models (22-25), MME-Sta (26), MME-Dyn (27), GMFD (28) and OBS-BR (29; gray rectangle) from 1980 to 2005. (b) Climatology bias for 1980-2005

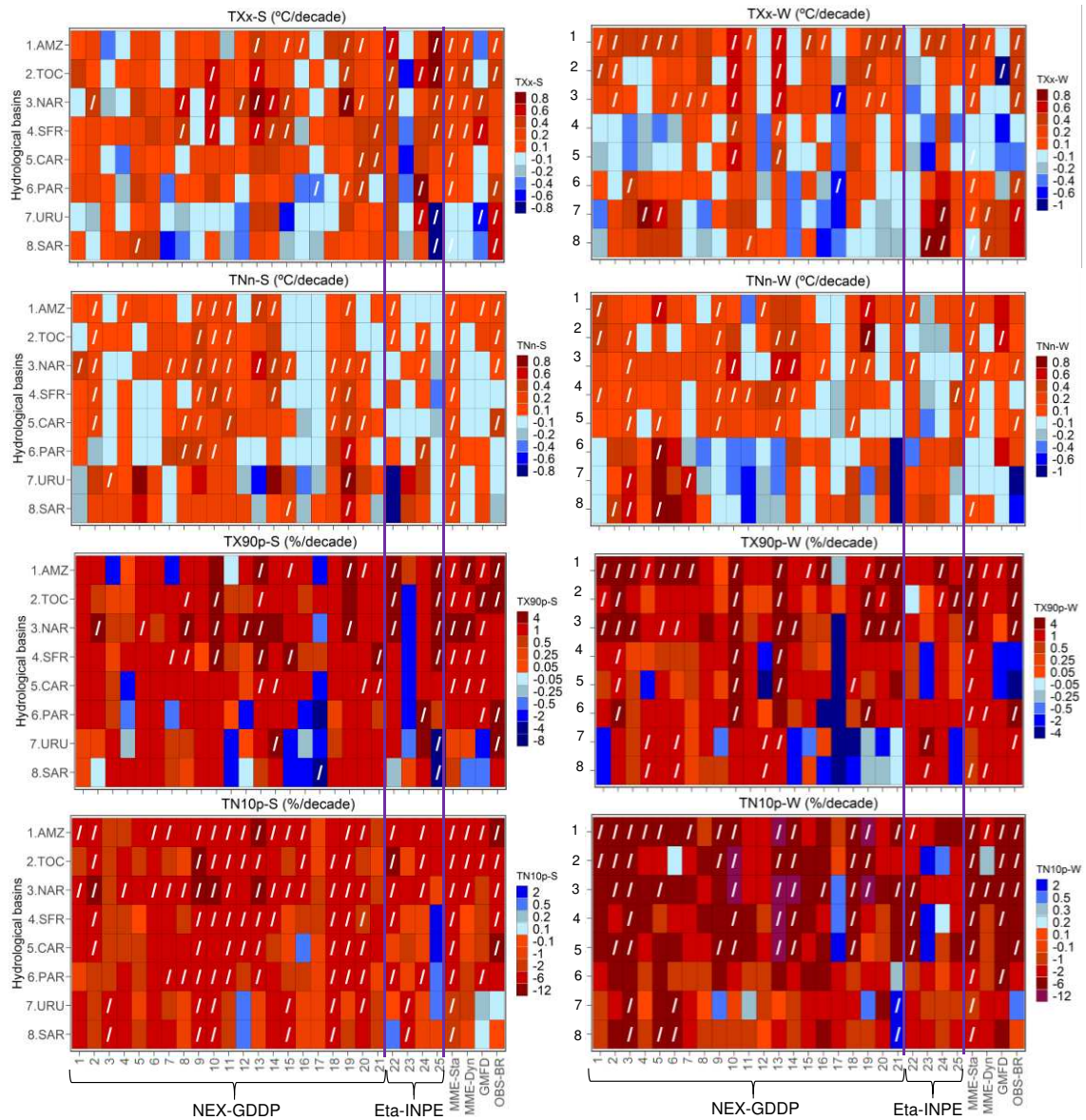


Figure S2.8 Trends per decade from 1980 to 2005 for temperature indices at the seasonal scale (a-h) for 21 NEX-GDDP models, 4 Eta-INPE models, MME-Sta, and MME-Dyn over eight hydrological basins in Brazil (Fig. 2.1). Diagonal lines indicate significant trends at 5% level. The vertical purple lines refer to ESMs from Eta-INPE datasets. The nomenclature of the ETCCDI indices was adapted to Index-“S” for summer and Index-“W” for winter

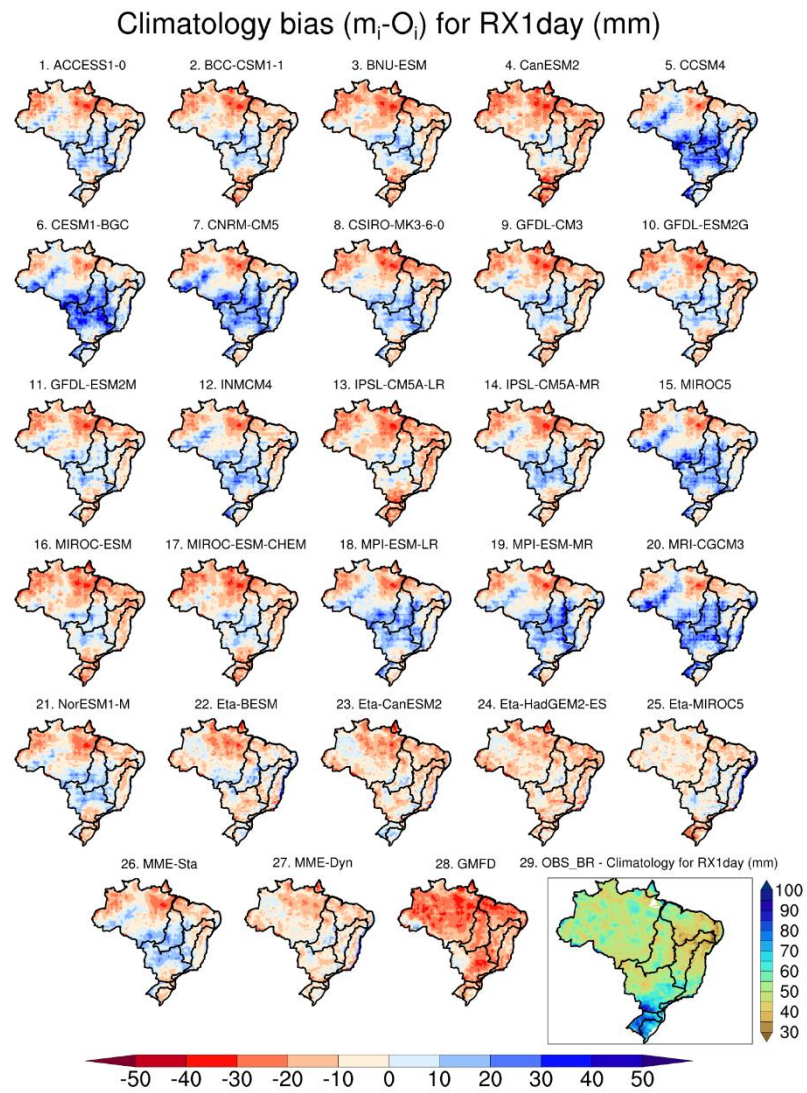


Figure S2.9 Climatology for max 1-day precipitation – RX1day for 21 NEX-GDDP climate models (1-21), 4 Eta-INPE models (22-25), MME-Sta (26), MME-Dyn (27), GMFD (28) and OBS-BR (29; gray rectangle) from 1980 to 2005. (b) Climatology bias for 1980-2005

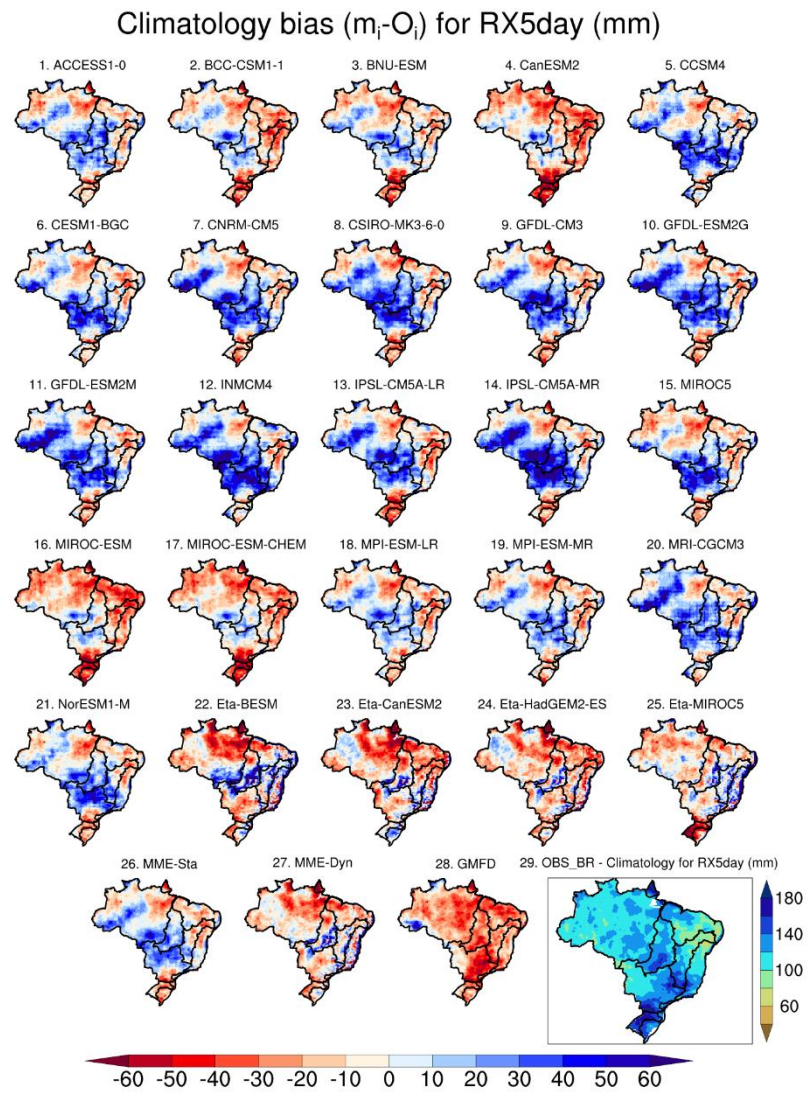


Figure S2.10 Climatology for max 5-day precipitation – RX5day for 21 NEX-GDDP climate models (1-21), 4 Eta-INPE models (22-25), MME-Sta (26), MME-Dyn (27), GMFD (28) and OBS-BR (29; gray rectangle) from 1980 to 2005. (b) Climatology bias for 1980-2005

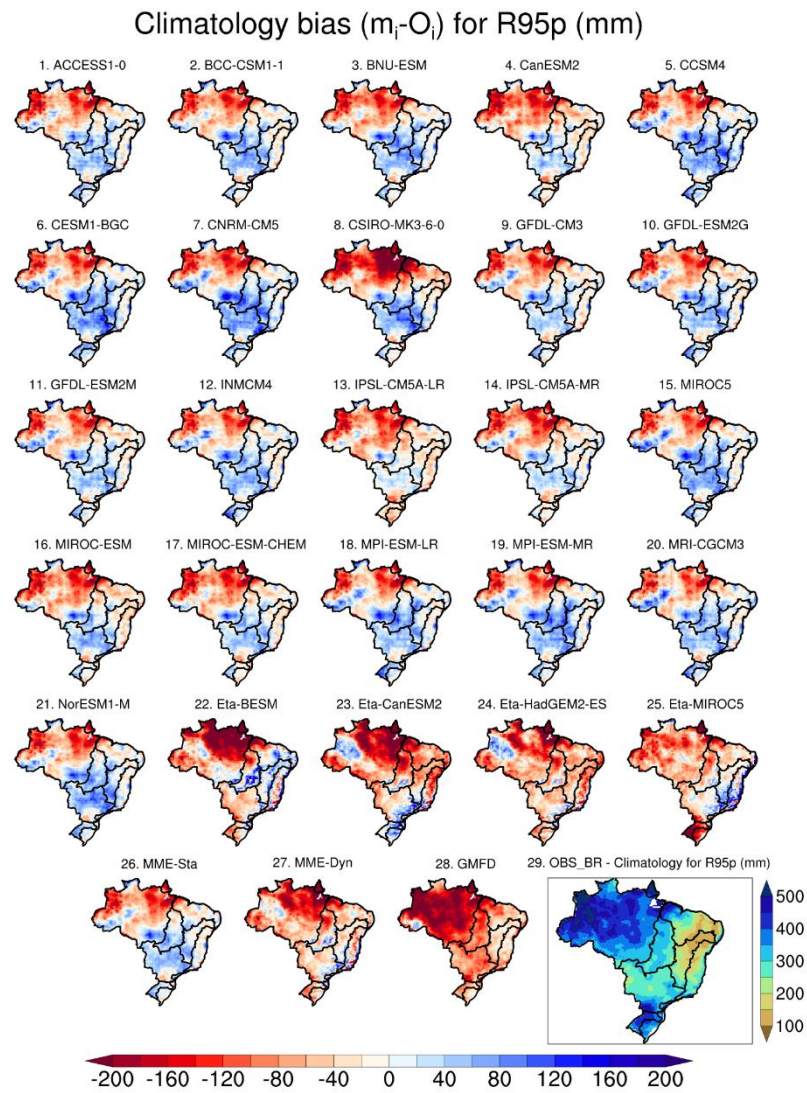


Figure S2.11 Climatology for very wet days – R95p for 21 NEX-GDDP climate models (1-21), 4 Eta-INPE models (22-25), MME-Sta (26), MME-Dyn (27), GMFD (28) and OBS-BR (29; gray rectangle) from 1980 to 2005. (b) Climatology bias for 1980-2005

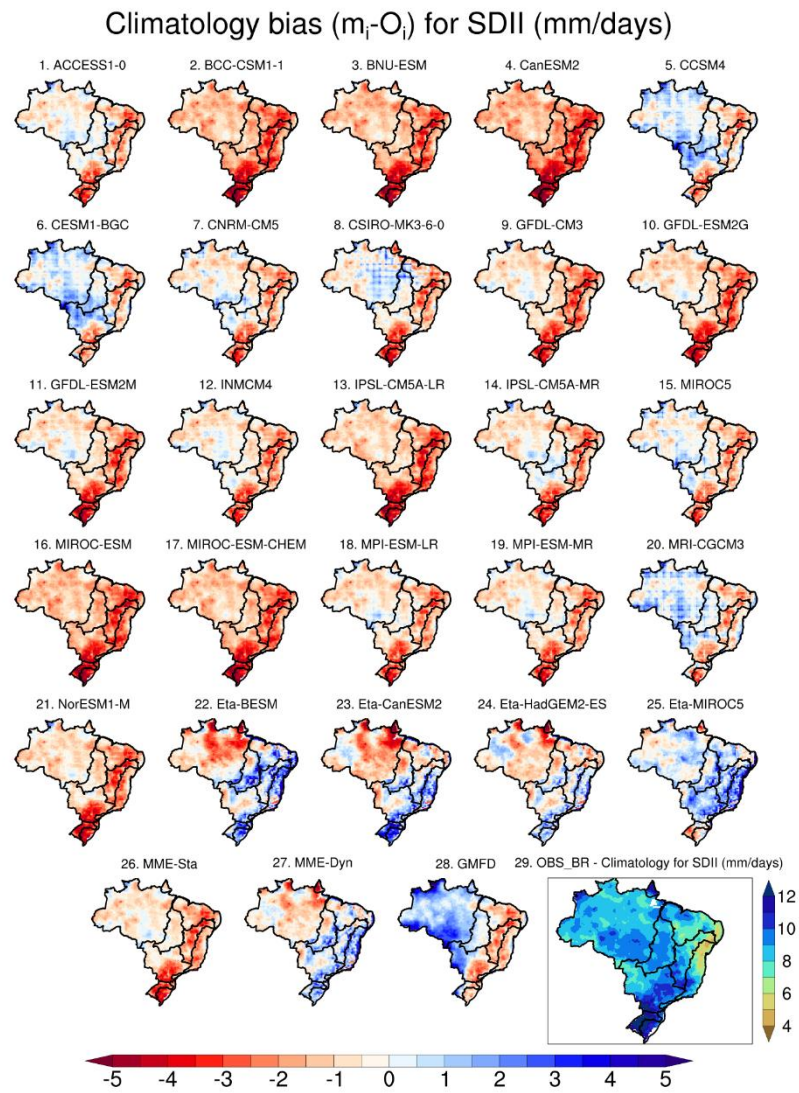


Figure S2.12 Climatology for simple daily intensity index – SDII for 21 NEX-GDDP climate models (1-21), 4 Eta-INPE models (22-25), MME-Sta (26), MME-Dyn (27), GMFD (28) and OBS-BR (29; gray rectangle) from 1980 to 2005. (b) Climatology bias for 1980-2005

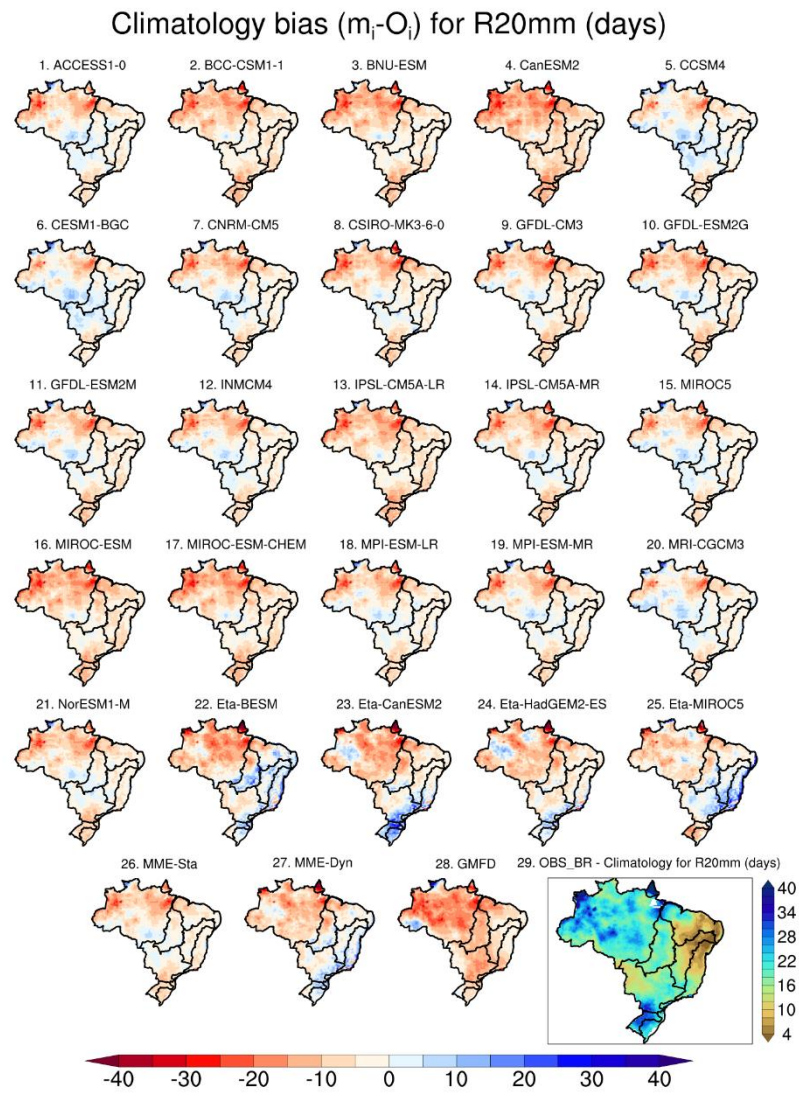


Figure S2.13 Climatology for number of very heavy precipitation days – R20mm for 21 NEX-GDDP climate models (1-21), 4 Eta-INPE models (22-25), MME-Sta (26), MME-Dyn (27), GMFD (28) and OBS-BR (29; gray rectangle) from 1980 to 2005. (b) Climatology bias for 1980-2005

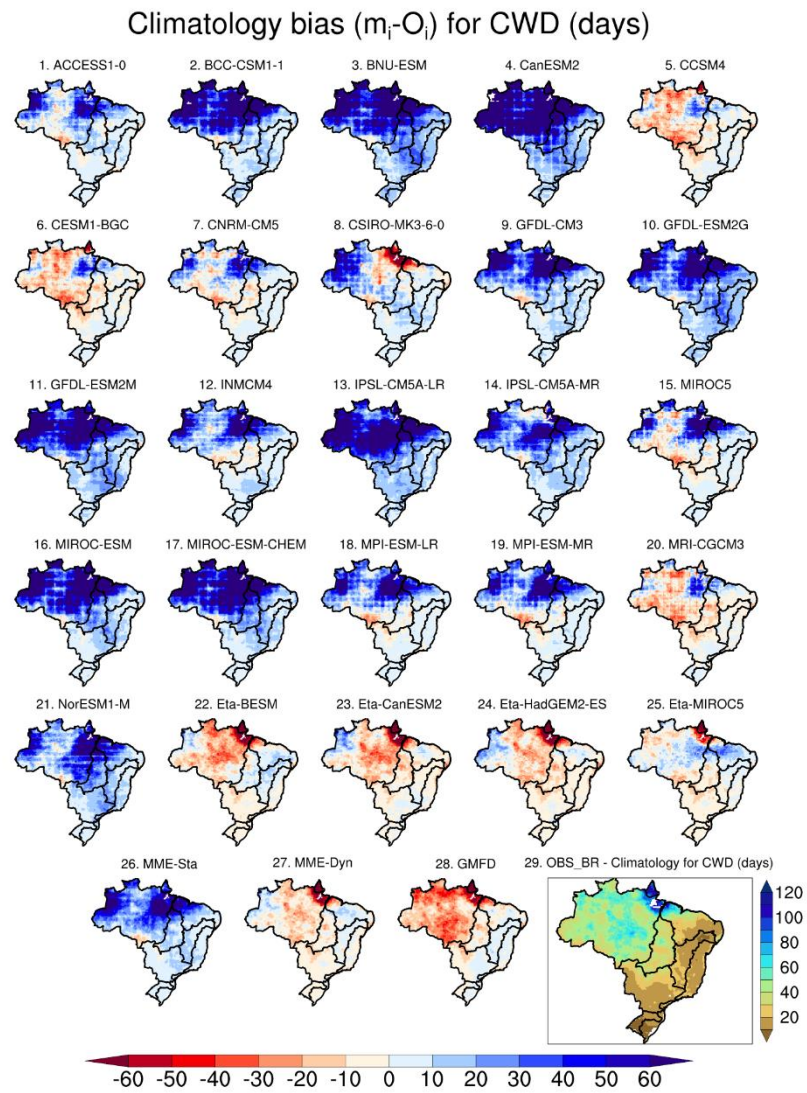


Figure S2.14 Climatology for consecutive wet days – CWD for 21 NEX-GDDP climate models (1-21), 4 Eta-INPE models (22-25), MME-Sta (26), MME-Dyn (27), GMFD (28) and OBS-BR (29; gray rectangle) from 1980 to 2005. (b) Climatology bias for 1980-2005

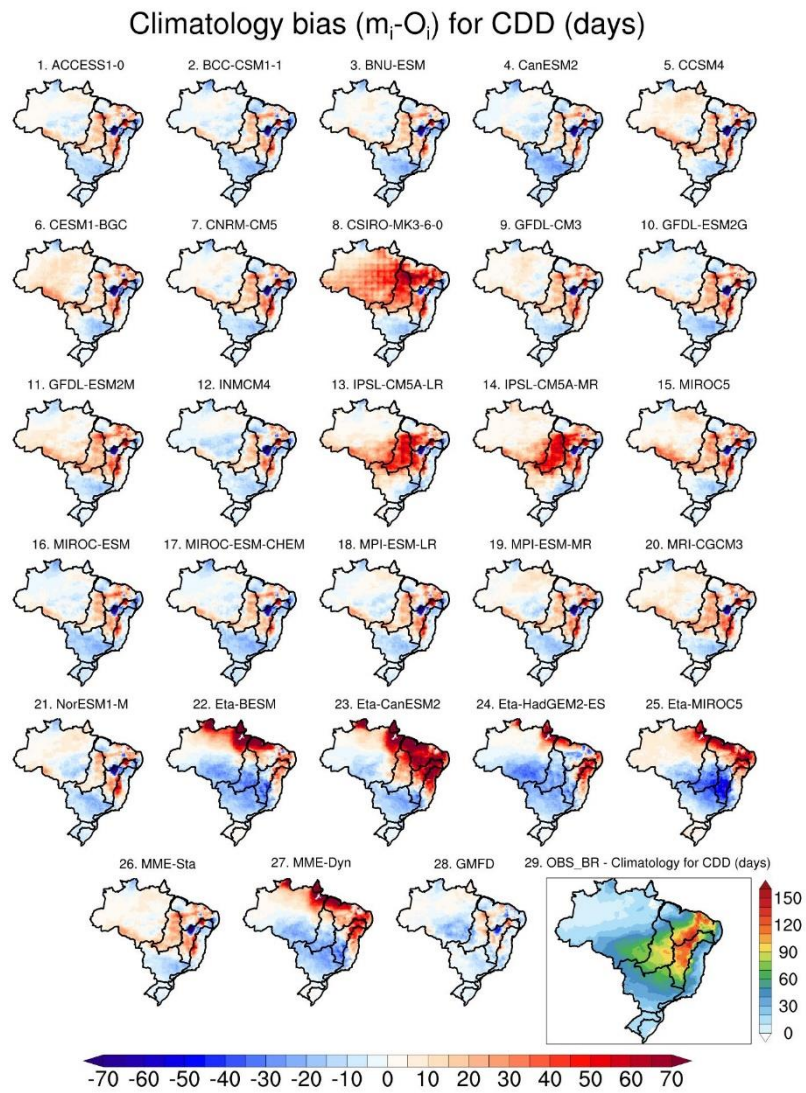


Figure S2.15 Climatology for consecutive dry days – CDD for 21 NEX-GDDP climate models (1-21), 4 Eta-INPE models (22-25), MME-Sta (26), MME-Dyn (27), GMFD (28) and OBS-BR (29; gray rectangle) from 1980 to 2005. (b) Climatology bias for 1980-2005

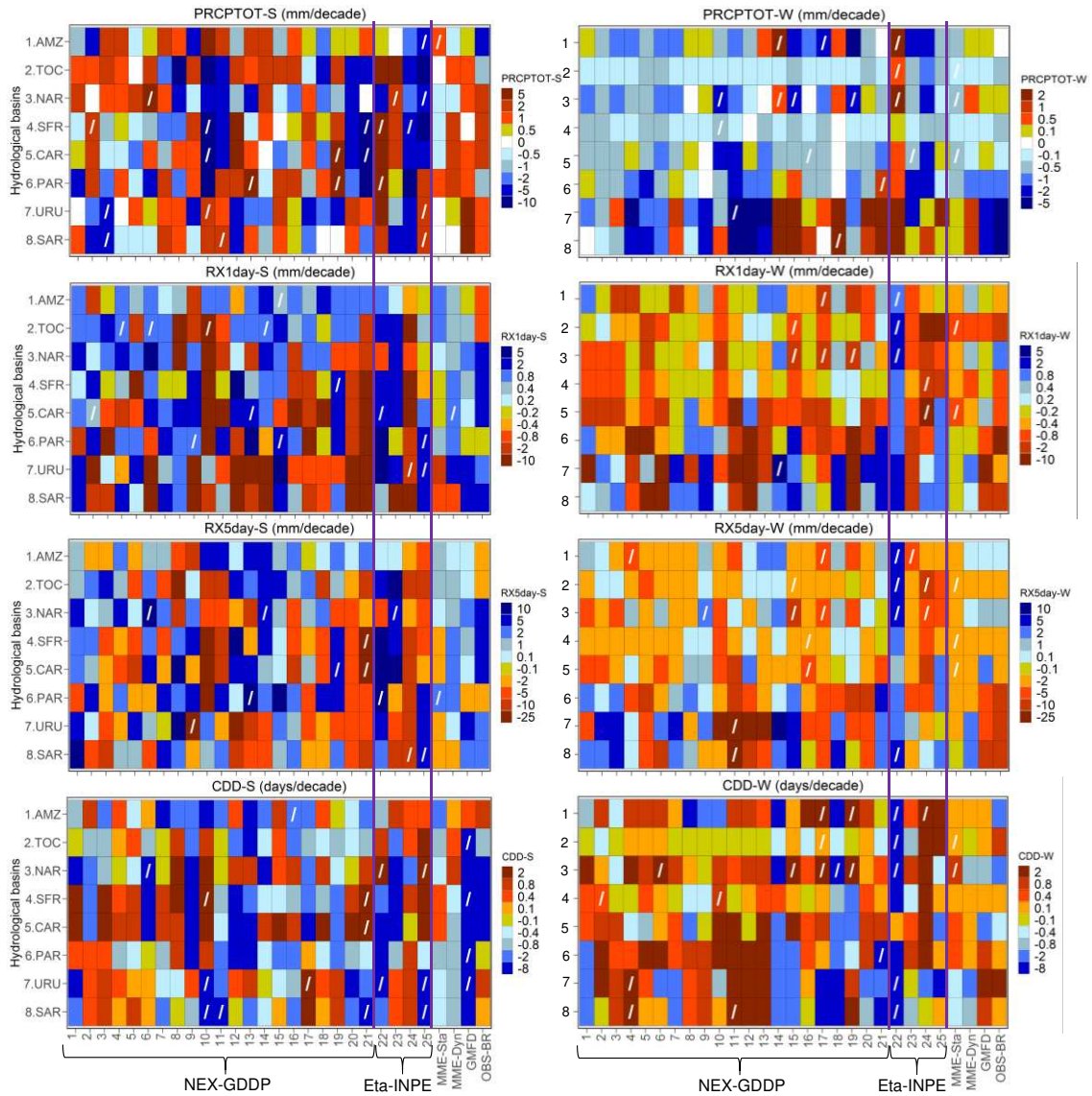


Figure S2.16 Trends per decade from 1980 to 2005 for precipitation indices at the seasonal scale (a-h) for 21 NEX-GDDP models, 4 Eta-INPE models, MME-Sta, and MME-Dyn over eight hydrological basins in Brazil (Fig. 2.1). Diagonal lines indicate significant trends at 5% level. The vertical purple lines refer to ESMs from Eta-INPE datasets. The nomenclature of the ETCCDI indices was adapted to Index-“S” for summer and Index-“W” for winter.

CHAPTER 3

3. Assessing Current and Future Trends of Climate Extremes Across Brazil Using Reanalyses and Earth System Model Projections

Alvaro Avila; Victor Benezoli; Flavio Justino; Roger Torres; Aaron Wilson.

Climate Dynamics. Manuscript number: CLDY-D-19-00921.

Abstract:

Brazil experiences extreme weather and climate events that cause numerous economic and social losses. Several extreme events have impacted the country in recent decades, and according to climate change projections, these events will increase in frequency by the end of this century. To understand the magnitude of these changes, this study analyzes the historical patterns and projected changes of temperature and precipitation extremes across Brazil through the World Climate Research Program's Expert Team on Climate Change Detection and Indices framework. Climate extreme events over the past four decades (1980-2016) are evaluated using multiple observed and reanalysis datasets. Future changes in climate extremes are analyzed from 20 downscaled Earth System Models at high horizontal resolution (0.25° of latitude/longitude), under two representative concentration pathway scenarios (RCP4.5 and RCP8.5). Projected changes in the extreme indices are analyzed over mid-21st century (2046-2065) and end-of-21st century (2081–2100) relative to the reference period 1986–2005. Results show consistent warming patterns with increasing trends in warm extremes and decreasing trends in cold extremes in the historical datasets. Furthermore, the frequency of warm days/nights have increased and cold days/nights have diminished, and an increase in the duration of heat waves over the 21st century is expected. A similar warm pattern is projected in the mid and end of the twenty-first century. For precipitation indices, observations show an increase in consecutive dry days and a reduction of consecutive wet days over almost all Brazil. The frequency and intensity of extremely wet days over Brazil are expected to increase according to future scenarios.

Key Words: Climate trends; CMIP5 models; Downscaling; ETCCDI; Hydrological basins; Performance

3.1. Introduction

Global temperatures have warmed, leading to changes in atmospheric patterns that intensify and increase the frequency of extreme precipitation and heat waves (Zhang et al. 2007; IPCC 2018; Giorgi et al. 2019). Earth System Models (ESMs) project a continued upward trend in extreme temperature and precipitation events over the majority of land regions throughout the twenty-first century (Sillmann et al. 2013b; Donat et al. 2016; Bador et al. 2018; Marelle et al. 2018; Mora et al. 2018).

Natural hazards such as floods, landslides, and droughts caused damage on the order of the R\$182.7 billion (about US \$ 56.0 billion) in Brazil between 1995 and 2014 (CEPED-UFSC 2016). Climate projections reveal increasing mean temperatures and decreasing precipitation that suggest more frequent/intense episodes of droughts

over northern and northeastern Brazil, with a large increase in the length of the most prolonged period of consecutive dry days (Sillmann et al. 2013b; Marengo et al. 2017; Betts et al. 2018). In addition, Debortoli et al. (2017) indicate that Brazil has many regions that are highly vulnerable to natural disasters including flash flooding and landslides. Moreover, Almagro et al. (2017) reveals future projections show an increase in rainfall-induced erosion potential across the southern regions, which can affect agricultural production in this area.

In Brazil, studies of climate extremes developed over the last few decades (e.g., the 1990s and 2000s) have encountered some limitations in their evaluations and model validations, mainly due to the lack of access to meteorological data (e.g., Marengo et al. 2009; Rusticucci et al. 2010). Presently, many researchers have used weather stations in specific areas to investigate climate extremes in present climate (Dufek and Ambrizzi 2008; Skansi et al. 2013; Silva Dias et al. 2013; Carvalho et al. 2014; Oliveira et al. 2014, 2017; Rosso et al. 2015; Avila et al. 2016; Zilli et al. 2017; Murara et al. 2018; Bezerra et al. 2019). Those studies found an increase of extreme temperature and precipitation events in the recent past, and climate models project additional increases in future climate extremes over South America, although ESMs with coarser resolutions (100 – 300 km) are not appropriate for climate change studies at local/regional scales (Marengo et al. 2009; Dereczynski et al. 2013; Sillmann et al. 2013b; Silva et al. 2014; Valverde and Marengo 2014; Nguyen et al. 2017). In addition, Lyra et al. (2017) used the highest resolution (5 km) climate projection and found that temperature extremes are projected to increase up to 9 °C in three metropolitan regions of southeast Brazil, where the annual precipitation could decrease by approximately 40-50 percent by the end of the century in the RCP8.5 scenario.

A more detailed study about historical and future climate extreme variability on a more local/regional scale using the recent high resolution climate datasets over Brazil has not yet been carried out. Hence, the following is a comprehensive evaluation using new sources (e.g., reanalysis and downscaled climate projections) that provide relevant information for climate processes and natural hazards monitoring. In order to expand previous work and improve our understanding of climate extremes events in Brazil, historical (1980-2016) and projected (2046-2100) changes in temperature and precipitation extremes indices are analyzed using the guidance defined by the Expert Team on Climate Change Detection and Indices (ETCCDI). To characterize the historical climate, datasets comprising observations, reanalysis, and other merged products, arranged in a regular grid of 0.25° latitude/longitude (~25 km x 25 km) from 1980 to 2016 are used. Observational uncertainty is also analyzed. Furthermore, the National Aeronautics Space Administration (NASA) Earth Exchange Global Daily Downscaled Projections (NEX-GDDP) were utilized for the period 2006-2100. The NEX-GDDP dataset is based on statistical downscaling of 20 ESMs from the Coupled Model Intercomparison Project Phase 5 (Taylor et al. 2012) under RCP4.5 and RCP8.5 scenarios. Section 2 describes the climate indices, data, and methods used in this investigation. Section 3 depicts observations and performance evaluations, historical trends, and future changes based on RCP4.5 and 8.5. Finally, Section 4 provides a summary of the main results and discussion concerning how these extreme climate impacts various aspects of the Brazilian population.

3.2. Data and Methodology

3.2.1. Extreme Climate Indices

Sixteen extreme climate indices defined by ETCCDI (Zhang and Yang 2004; Zhang et al. 2011; http://etccdi.pacificclimate.org/list_27_indices.shtml) were selected for this study, eight each related to air

temperature and rainfall (Table 3.1). These indices were calculated using daily maximum temperature (TX), minimum temperature (TN), and precipitation (PR).

Table 3.1 Extreme climate indices employed in this study as recommended by ETCCDI. The full list of indices and precise definitions are provided at http://etccdi.pacificclimate.org/list_27_indices.shtml. Abbreviations are as follows: TX (TN), daily maximum (maximum) temperature. A wet (dry) day is defined when precipitation ≥ 1 mm (PR<1mm).

Index – Indicator name	Description	Unit
1. TXx – Hottest day	Annual maximum value of daily maximum temperature	°C
2. TNn – Coldest night	Annual minimum value of daily minimum temperature	°C
3. DTR – Diurnal temperature range	Annual mean difference between daily max and min temperature	°C
4. TN10p – Cool nights	Percentage of days when TN<10th percentile	%
5. TN90p – Warm nights	Percentage of days when TN>90th percentile	%
6. TX10p – Cool days	Percentage of days when TX<10th percentile	%
7. TX90p – Warm days	Percentage of days when TX>90th percentile	%
8. WSDI – Warm spell duration indicator	Annual count of days with at least 6 consecutive days when TX>90th percentile	days
9. PRCPTOT ^a – Annual total wet-day precipitation	Annual total precipitation (PR) in wet days (PR \geq 1mm)	mm
10. RX1day – Max 1-day precipitation amount	Annual maximum 1-day precipitation	mm
11. RX5day – Max 5-day precipitation amount	Annual maximum consecutive 5-day precipitation	mm
12. R95p – Very wet days	Annual total precipitation from days > 95th percentile	mm
13. SDII – Simple daily intensity index	The ratio of annual total precipitation to the number of wet days (≥ 1 mm)	mm/day
14. R20mm – Number of very heavy precipitation days	Annual count of days when PR \geq 20mm	days
15. CWD – Consecutive wet days	Maximum number of consecutive days with daily PR \geq 1mm	days
16. CDD – Consecutive dry days	Maximum number of consecutive days with daily PR<1mm	days

Selected extreme temperature indices comprise absolute (associated with the maximum or minimum magnitudes within a year) and percentile-based indices (related to the frequency of hot or cold extreme events). Absolute indices include hottest day (TXx), coldest night (TNn), and diurnal temperature range (DTR); percentile-based indices include cold nights (TN10p), warm nights (TN90p), cold days (TX10p), and warm days (TX90p) indices. Additionally, warm spell duration index (WSDI) describing the annual count of days with at least 6 consecutive days when the maximum temperature is above the 90th percentile was calculated.

The eight precipitation-related extreme indices characterize intensity, frequency, and duration of rainfall events. The total wet-day precipitation (PRCPTOT), maximum 1-day precipitation (RX1day), maximum 5-day precipitation (RX5day), very wet days (R95p), and simple daily intensity (SDII) are used to characterize the intensity of rainfall events. The number of very heavy precipitation days (R20mm) expresses the frequency of extreme precipitation. Finally, consecutive dry days (CDD) and consecutive wet days (CWD) describe persistent drier and wetter conditions, respectively.

The selected climate indices have been calculated on an annual scale to improve knowledge and understanding of inter-annual extreme temperature and precipitation variability in Brazil. Furthermore, choices were based on their relevance to the study area and are comparable with others studies carried out in different parts

of the world (Sillmann et al. 2013b; Skansi et al. 2013; Alexander 2016; Alexander and Arblaster 2017; Giorgi et al. 2019). Several studies have used ETCCDI indices to evaluate the capabilities of reanalyses and ESMs in simulating the characteristics of the observed climate extremes (Dufek and Ambrizzi 2008; Zhou et al. 2014; Nguyen et al. 2017; Ongoma et al. 2018a; de Lima and Alcântara 2019; Dosio et al. 2019). Similar to Aerenson et al. (2018), we do not include a seasonal evaluation of ETCCDI extreme climate indices here as many of the indices are more meaningful on an annual scale.

3.2.2. Observation and reanalysis datasets

We selected four datasets to study the complexity of climate extremes at a high horizontal spatial resolution (Table 3.2) over the 1980-2016 period. We chose reanalyses and merged products that combine satellite precipitation, reanalysis estimates with in-situ records that offer prolonged periods of daily records of meteorological variables (e.g., TX, TN, and PR). Also, reanalyses and merged products have improved since the early 1980s as more climate datasets have become available, the understanding of the climate system has advanced, and numerical weather prediction techniques have improved (Sheffield et al. 2006; Dee et al. 2014; Beck et al. 2019b). The daily outputs were obtained from the following data projects:

Table 3.2 Characteristics of (a) gridded observations, (b) reanalyses, and (c) merged datasets. Variables are precipitation (PR), maximum temperature (TX) and minimum temperature (TN)

	Variables	Period	Resolution; Spatial Coverage
(a) Gridded observation			
OBS-BR https://utexas.app.box.com/v/Xavier-et-al-IJOC-DATA .	TX, TN, PR	1980-2016	0.25° (~28 km); Brazil
(b) Reanalysis product			
ECMWF ERA5 Reanalysis (ERA5) https://cds.climate.copernicus.eu/	TX, TN, PR	1979- 2018	0.25° (~28 km); Global
Global Meteorological Forcing Dataset for Land Surface Modeling (GMFD) http://hydrology.princeton.edu/data.pgf.php	TX, TN, PR	1948- 2016	0.25° (~28 km) Global
(c) Merging of different data sources (gauge, satellite, and reanalysis)			
Multi-Source Weighted-Ensemble Precipitation (MSWEP) Version 2.2 http://www.gloh2o.org/	PR	1979- 2017	0.1° (~10 km); Global

I. As a reference, we chose a gridded observational dataset (OBS-BR) produced by Xavier et al. (2015; 2017) available for Brazil with a horizontal resolution of 0.25° latitude/longitude (~25 km x 25 km) over the period 1980-2016. The temperature and precipitation fields are based on an interpolation of 735 and 9259 observations sites, respectively.

II. The fifth European Centre for Medium-Range Weather Forecasts (ECMWF) Reanalysis – ERA5 (Dee et al. 2011; Hersbach et al. 2018). ERA5 is a global high-resolution (0.25°) reanalysis, available for the period between 1979 and the near-present.

III. The Global Meteorological Forcing Dataset with a horizontal resolution of 0.25° covering the period from 1948 to 2016 was also used (GMFD; Sheffield et al. 2006). The GMFD dataset merges satellite, reanalysis data and surface observations.

IV. The Multi-Source Weighted-Ensemble Precipitation (MSWEP) Version 2, another merged product consisting of satellite data, reanalysis and rain gauges provides reliable precipitation estimates on a daily world scale (Beck et al. 2017b, 2019b), which is available on a horizontal resolution of 0.1° for the period from 1979 to 2017.

It is noteworthy to mention that OBS-BR, ERA5, GMFD, and MSWEP datasets have not been assessed regarding the temporal-spatial patterns of climate extremes. Dufek et al. (2008) evaluated the performance of the National Centers for Environmental Prediction/National Center for Atmospheric Research reanalysis - NCEP/NCAR in capturing the extreme temperature and precipitation indices over Brazil from 28 weather stations during the period 1961–1990. They found that NCEP/NCAR reanalyses have good agreement with observed climate extremes. We do not compare our results with Dufek et al. (2008) as their period and station network differ from the present study (1980–2016).

For intercomparison purposes, all datasets were regridded to a common 0.25° horizontal resolution grid using a bilinear interpolation algorithm, following analogous studies (Chaney et al. 2014; Zhou et al. 2014; Fotso-Nguemo et al. 2018; Beck et al. 2019b).

3.2.3. Climate change projections

The climate change projections used in this study were produced by the National Aeronautics Space Administration (NASA) Earth Exchange Global Daily Downscale Projection - NEX-GDDP (Thrasher et al. 2012). This product was derived from ESM experiments of the Coupled Model Intercomparison Project Phase 5 (CMIP5). We used 20 CMIP5 ESMs statistically downscaled to a horizontal resolution of 0.25° of latitude/longitude under two future emission scenarios, RCP 4.5 and RCP 8.5 (Table 3.S1). The NEX-GDDP dataset is prepared by the Climate Analytics Group and NASA Ames Research Center using the NASA Earth Exchange, and distributed by the NASA Center for Climate Simulation (NCCS), which is available at <https://cds.nccs.nasa.gov/nex-gddp/>. The NEX-GDDP produces three daily variables, TX, TN, and PR, over the periods 1950–2005 (historical) and 2006–2100 (projections under RCP 4.5 and RCP 8.5 scenarios). The Bias-Correction Spatial Disaggregation (BCSD) method was used to downscale each CMIP5 ESM output (Thrasher et al. 2012).

The Intergovernmental Panel on Climate Change (IPCC) Fifth Assessment Report (IPCC AR5) based their conclusions on projected changes in climate extreme events using the CMIP5 models for the time-slices 2046–2065 (mid-21st century) and 2081–2100 (end-21st century), relative to the reference period 1986–2005 (Collins et al. 2013; Hoegh-Guldberg et al. 2018). In this sense, we used the same intervals to facilitate a comparative analysis with other studies in other locations throughout the world (Fischer et al. 2013; Sillmann et al. 2013b; Alexander and Arblaster 2017; Ongoma et al. 2018b; Santos et al. 2018; Liao et al. 2019).

We used the methodology adapted from Tebaldi et al. (2011) to evaluate changes in the climate extremes index that applies the multi-model ensemble approach to ensure robust results (Parker 2013; Gulizia and Camilloni 2014). This methodology has been widely adopted in climate change and extreme weather events studies to address

the significance of the change between two periods and the signal agreement among the model (Sillmann et al. 2013b; Alexander and Arblaster 2017; Almazroui et al. 2017; Zhou et al. 2018; Dosio et al. 2019). For this purpose, we filled all grid cells with the mean multi-model relative change through a color pattern. To assess the significance of projected changes in annual climate extremes, we performed a Student's t-test between the historical (reference) and future (RCP4.5 and RCP8.5) scenarios. We stippled all grid cells where more than 66 percent of the models agreed on the change signal and more the 50 percent of the models showed a significant change (t-test, p-value < 0.05).

The relative change between the future and the historical periods in each climate extreme index (CEI) was calculated using equation (1) (adapted from Bador et al. 2018): In Eq. 1, \overline{CEI}_{future} and \overline{CEI}_{his} are 20-yr averages in a given CEI over the future (2046–2065 or 2081–2100) and historical (1986–2005) periods, respectively.

$$\text{Relative Change in CEI} = \frac{\overline{CEI}_{future} - \overline{CEI}_{his}}{\overline{CEI}_{his}} \quad (1)$$

3.2.4. Performance and trend analysis

This study employed four metrics to evaluate the performance of different datasets in reproducing the observed climate indices from 1980–2016 over the eight largest Brazilian hydrological basins (Fig. 3.1). The performance metrics include Percent Bias (PBIAS), RMSE-observations standard deviation ratio (RSR), refined index of agreement (d_r), and Pearson correlation coefficient (CORR). PBIAS indicates whether a given dataset overestimates or underestimates the observational information. The closer PBIAS and RSR are to 0, the better the model performs. Furthermore, the d_r varies between -1 and 1, 1 being the perfect agreement (Willmott et al. 2012). Finally, the value of CORR 1 (-1) indicates a stronger positive (negative) relationship between the two variables; meanwhile, 0 value indicates the absence of a relationship.

To detect trends in extreme climate indices, we used the Theil-Sen's slope estimator (Sen 1968). The significance of trends is calculated at the confidence level of 95 percent ($\alpha = 0.05$) using a Mann-Kendall test (Mann 1945; Kendall 1975). More details can be found in (Yue et al. 2002). These non-parametric tests are often used to detect trends in extreme climate indices, but also because this approach is less sensitive to outliers than parametric methods such as the ordinary least squares regression method (Cornes and Jones 2013; Donat et al. 2013b, 2016; Skansi et al. 2013).

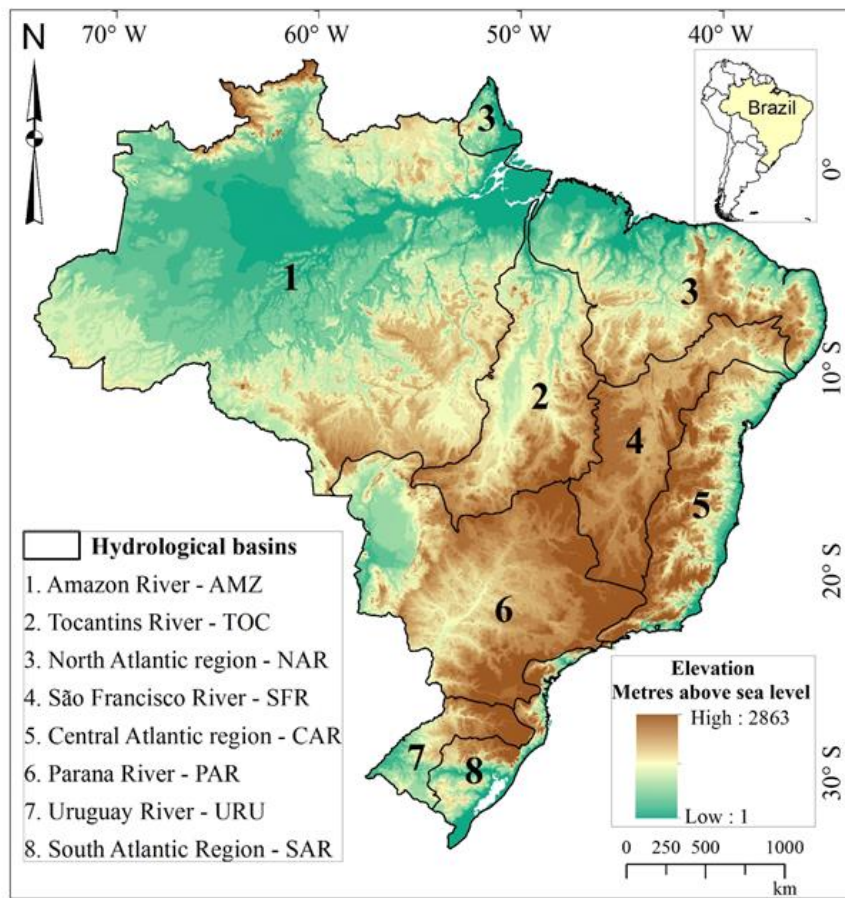


Figure 3.1 Hydrological basins in Brazil according to the Brazilian National Water Authority (ANA)

3.3. Results and analysis

To reduce the quantity of similar results (climatologies and spatial trends) for different extreme climate indices in each dataset, we present selected indices (two temperature and two precipitation) for each subsection. Additional figures can be found in the Supplementary Material.

3.3.1. Metrics analysis of datasets performance

3.3.1.1. Temperature indices

Climatologies of temperature indices from two climate datasets (ERA5 and GMFD) were compared to gridded observations (OBS-BR) over Brazil for 1980 to 2016 using different performance metrics (Figs. 2, 3). Observations and ERA5 climatologies are quite similar (Fig. 3.2). ERA5 presents better performance than GMFD in almost all indices, except for the diurnal temperature range (DTR; Figs. 2b, 2c). For the DTR index, GMFD has similar magnitudes as the gridded observational dataset with values of PBIAS close to zero (Fig. 3.2).

PBIAS in the warmest daily temperature index (TXx; Figs. 2, 3a-b) indicates cooler (warmer) than observed conditions in ERA5 (GMFD) for all hydrological basins. Overall, poorer performance is noted over the Amazon, Tocantins, and Parana basins, with PBIAS overestimated by up to 14 percent (3°C) compared to observations.

ERA5 overestimates the coldest daily minimum temperature (TNn; Figs. 2, 3c-d) for all basins, except for Uruguay and South Atlantic basins. GMFD reflects the worst PBIAS of TNn (-13 percent) over the Uruguay River.

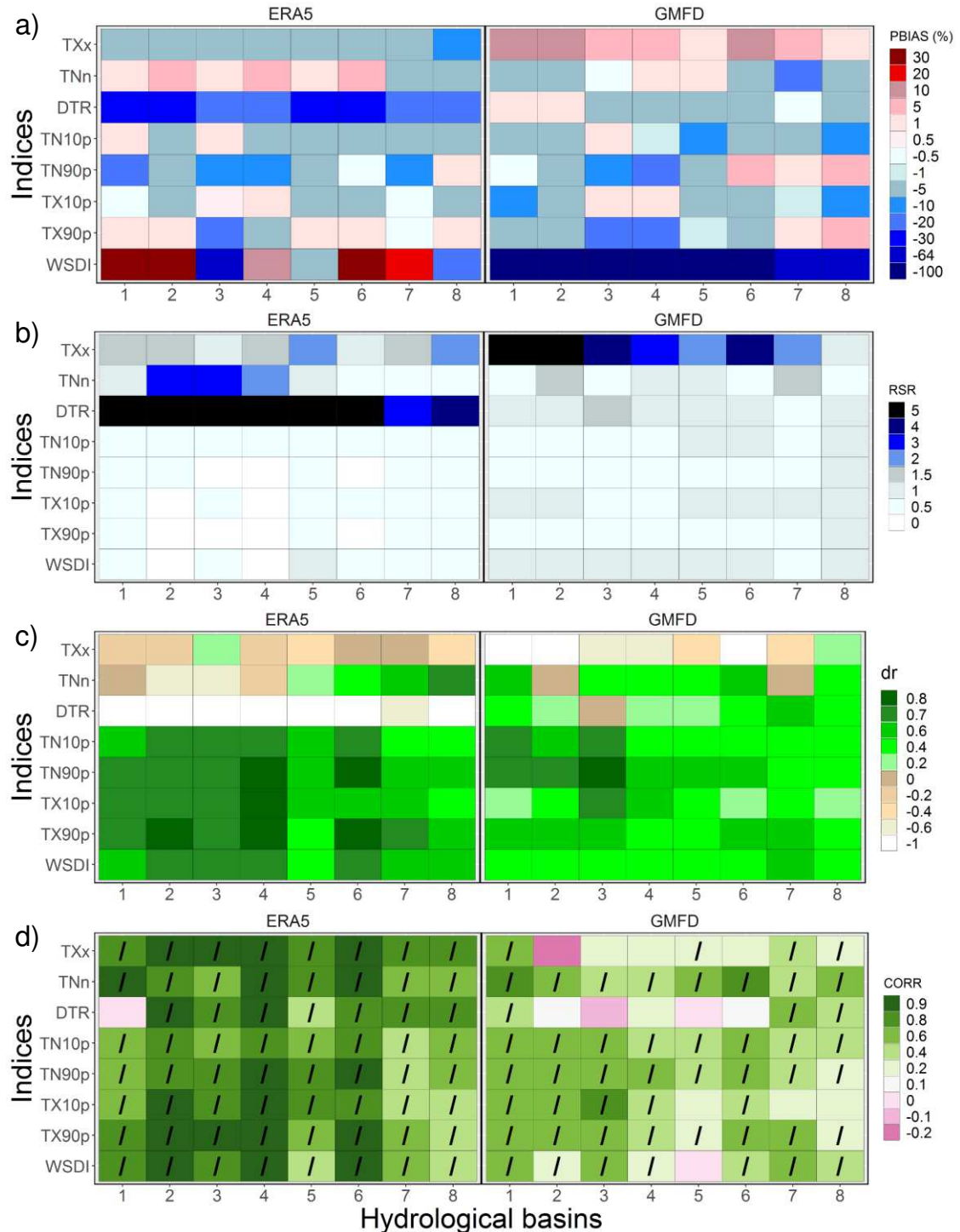


Figure 3.2 Evaluation metrics for temperature indices for ERA5 and GMFD with respect to the observational dataset (OBS-BR) from 1980 to 2016 over the eight hydrological basins in Brazil. (a) Bias in percentage (PBIAS) (b) RMSE-observations standard deviation ratio (RSR); (c) refined index of model performance (dr); (d) Pearson correlation coefficients (CORR); diagonal black lines indicate correlation values statistically significant correlations at 95% confidence level.

The best performance for percentile indices (TN10p, TN90p, TX10p, TX90p, and WSDI) are indicated by ERA5 results (Fig. 3.2). GMFD underestimates the warm spell duration index (WSDI) for all hydrological basins. The highest values of PBIAS (>80 percent) are found across north (Amazon basin) and northeast (Tocantins, North Atlantic, and São Francisco basins).

It is important to note that our analysis shows that the poorest performance in both ERA5 and GMFD occurs over the Amazon basin. Betts et al. (2009) indicate that cloud cover parameterization is a challenge in reanalysis models (ERA-40 and ERA-Interim), which implies a substantial underestimation of temperature indices (e.g., TXx, DTR, and TN90p) over the Amazon basin (Fig 3.1a).

3.3.1.2. Precipitation indices

Figs. 3.4 and 3.5 show the precipitation results for all datasets and hydrological basins. All datasets are consistent with observations for total precipitation of wet days index (PRCPTOT). PBIAS and RSR are low, and d_r and CORRs are close to 1. Intensity indices vary, however, with PBIAS quite large across all basins for RX1day, RX5day, and R95p, especially over the Amazon River basin (Fig. 3.4). RSR and d_r are generally lower for GMFD and MSWEP compared to ERA5 (Figs. 3.4 and 3.5).

The ERA5 and GMFD show good capabilities to estimate the number of consecutive dry days (CDD; Figs. 4a-b, 5c-d). However, the GMFD dataset exhibits the lowest performance for all intensity precipitation indices (e.g. RX1day and RX5day). It should be noted that the GMFD dataset is based on Climatic Research Unit (CRU) Time-Series (TS) Version 3.1 - CRU TS3.1 (monthly precipitation and temperature observations in a horizontal resolution of $0.5^\circ \times 0.5^\circ$), Global Precipitation Climatology Project - GPCC (daily precipitation in a $1^\circ \times 1^\circ$ resolution) and NCEP/NCAR reanalysis (3 hourly meteorological data in a $\sim 2^\circ \times 2^\circ$ resolution). In this way, the low performance in GMFD dataset over most of the indices can be explained, because CRU and GPCC products use a low density stations to reproduce the patterns of climate variability (Liebmann and Allured 2006; Rozante et al. 2010; Xavier et al. 2015), especially over the Amazon basin.

The analysis suggests that ERA5 can be useful as an alternative dataset to study daily temperature and precipitation indices over Brazil. In general, ERA5 outperforms GMFD for temperature-based extreme indices and ERA5 and MSWEP (only for precipitation-based extreme indices) capture spatial patterns of extreme climate indices when compared to observational values.

Noteworthy, MSWEP (a merged product) is dependent on the precipitation field of the ERA-Interim reanalysis. Donat et al. (2014) and Beck et al. (2017a) point out that the ECMWF reanalyses (ERA-40 and ERA-Interim) tend to show the best agreement with the observations. ERA5 has demonstrated many enhancements compared to its predecessor ERA-Interim, most notably increased horizontal and vertical resolution (~ 79 km/60 levels to ~ 31 km/137 levels; Hoffmann et al. 2019). As suggested by Beck et al. (2019b) and supported by our results, MSWEP can use ERA5 outputs to improve the accuracy of daily precipitation estimations. Therefore, caution is recommended when using reanalyses or merged products as reference datasets to evaluate changes or patterns for daily precipitation indices, especially in regions where station data are sparse (Rozante et al. 2010; Zhang et al. 2011).

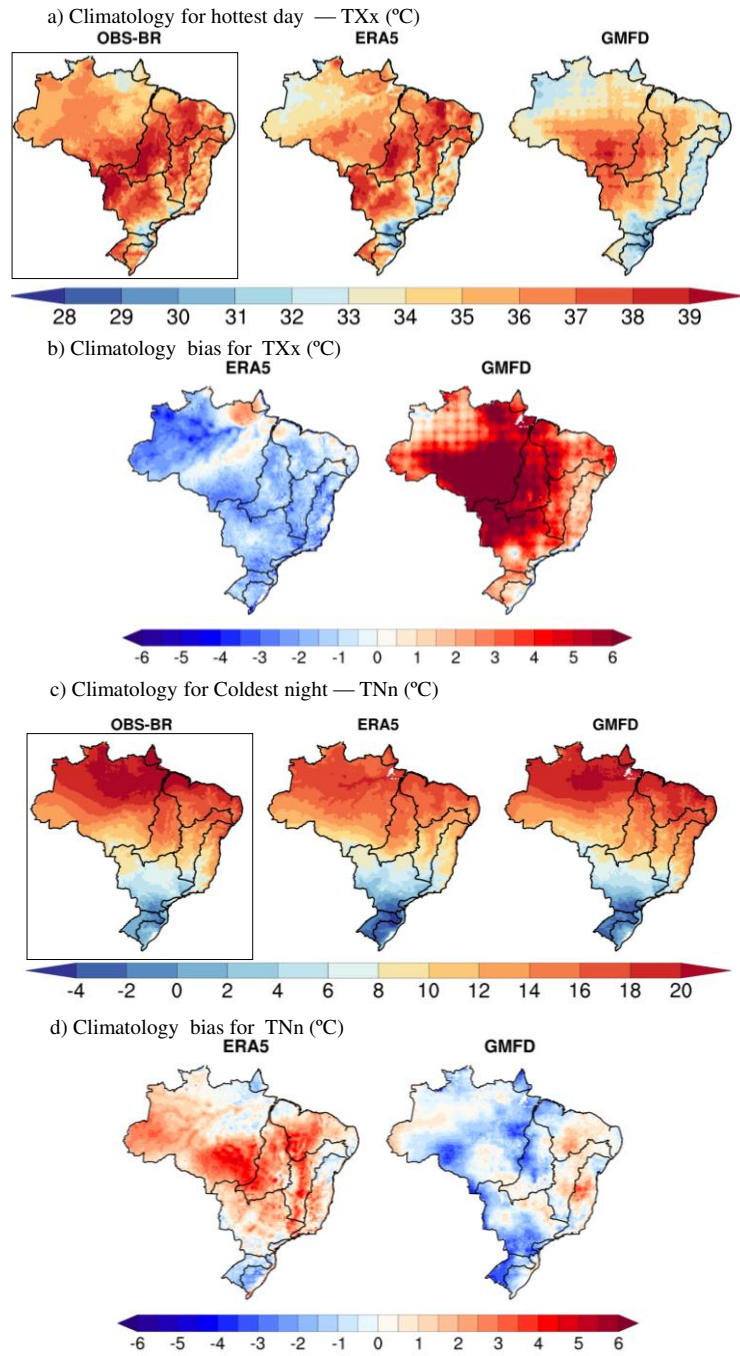


Figure 3.3 The 1980-2016 climatology and bias for TXx (a-b) and TNn (c-d) for OBS-BR (black rectangle; gridded observations), ERA5, and GMFD. Figures for additional temperature indices are in Supplementary Material

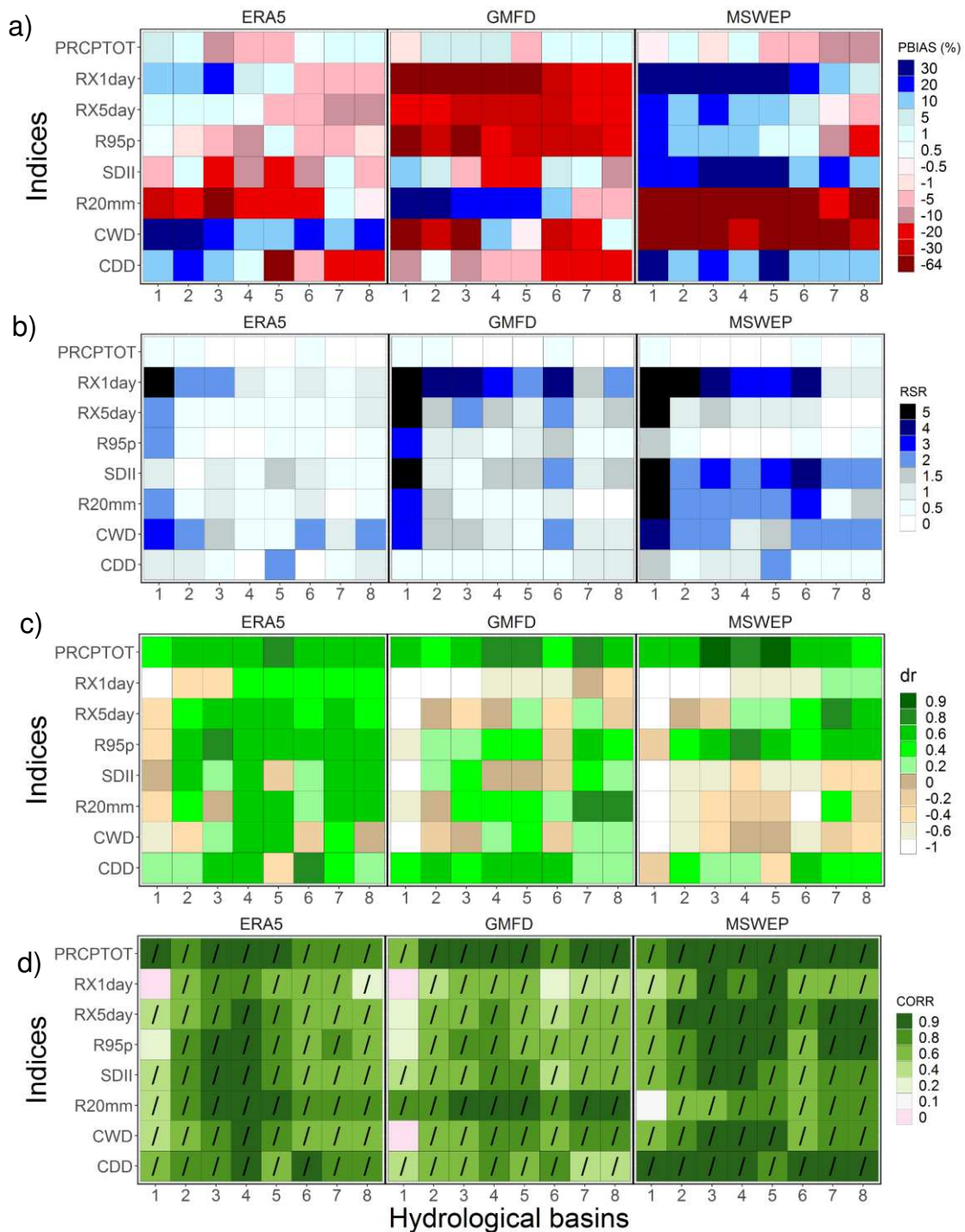


Figure 3.4 Evaluation metrics for precipitation indices for ERA5 and GMFD with respect to the observational dataset (OBS-BR) from 1980 to 2016 over the eight hydrological basins in Brazil. (a) Bias in percentage (PBIAS) (b) RMSE-observations standard deviation ratio (RSR); (c) refined index of model performance (dr); (d) Pearson correlation coefficients (CORR); diagonal black lines indicate correlation values statistically significant correlations at the 95% confidence level.

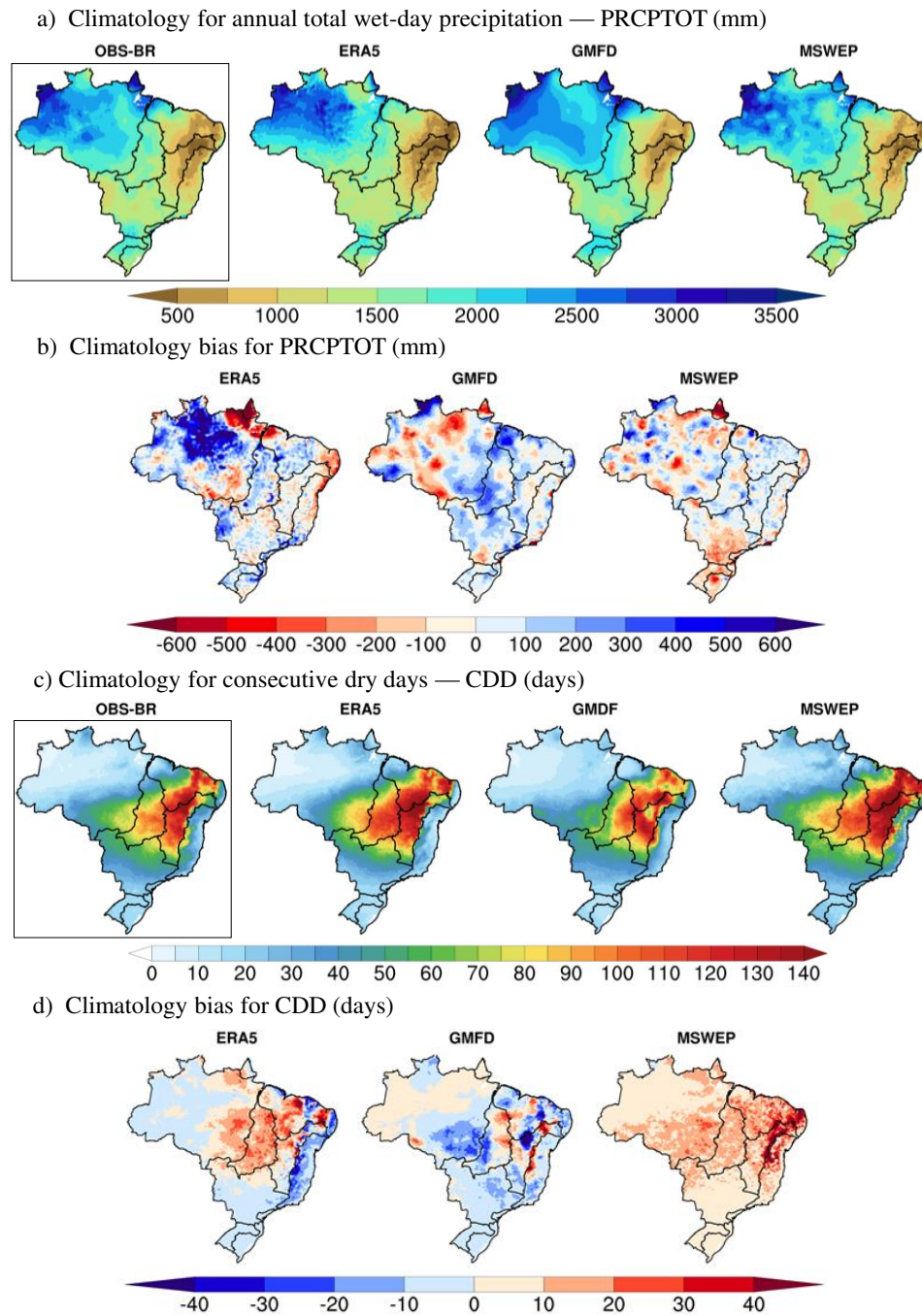


Figure 3.5 The 1980-2016 climatology and bias for PRCPTOT (a-b) and CDD (c-d) for OBS-BR (black rectangle; gridded observations), ERA5, and GMFD. Figures for additional precipitation indices are in Supplementary Material.

3.3.2. Historical changes in climate extremes

3.3.2.1. Observed trends in temperature indices

Table 3.3 and Fig. 3.6 depict the spatial trends and regional patterns in all three data sets across hydrological basins, respectively. Nearly all datasets show warming trends for cold (TNn, TN10p, TX10p) and warm climate extreme indices (TXx, TN90, TX90, and WSDI) across almost all of Brazil from 1980 to 2016. Note that

supplementary material displays more features of trends for all the set of climate indices mentioned in subsection 2.1 and Table 3.1.

Table 3.3 Decadal trends in temperature indices over the period 1980-2016. Values in bold indicate trends are significant at the 95% level. Colors signify cooling (blue), warming (red), or no trend (white)

Basin	Dataset	TXx	TNn	DTR	TN10p	TN90p	TX10p	TX90p	WSDI
		°C/decade			% / decade				days/decade
Amazon River	OBS-BR	0.54	0.53	-0.04	-5.61	6.20	-2.09	4.63	2.57
	ERA5	0.62	0.34	0.10	-2.23	2.94	-1.08	3.41	1.41
	GMFD	0.40	0.41	0.01	-3.39	5.01	-3.99	2.30	0.51
Tocantins River	OBS-BR	0.59	0.26	0.13	-3.22	4.62	-2.50	3.63	1.55
	ERA5	0.51	0.21	0.12	-3.32	2.79	-2.52	2.79	1.39
	GMFD	-0.21	0.54	0.00	-3.17	4.12	-3.41	1.93	0.53
North Atlantic	OBS-BR	0.64	0.21	0.13	-3.94	4.97	-3.23	4.31	1.89
	ERA5	0.34	0.11	0.04	-2.69	2.67	-1.69	2.60	1.07
	GMFD	0.07	0.14	0.00	-2.75	3.54	-2.20	1.77	0.87
São Francisco	OBS-BR	0.56	0.11	0.16	-2.27	3.47	-2.62	2.70	1.46
	ERA5	0.43	0.10	0.11	-2.33	2.60	-2.09	2.32	2.01
	GMFD	-0.04	0.17	0.00	-2.12	2.56	-1.68	1.02	0.42
Central Atlantic	OBS-BR	0.32	0.19	-0.12	-1.24	2.12	-0.58	-0.17	-0.20
	ERA5	0.59	0.06	0.18	-1.13	1.83	-1.87	2.56	1.37
	GMFD	0.12	0.21	0.00	-1.38	1.54	-1.15	0.52	0.03
Parana River	OBS-BR	0.64	0.07	0.15	-0.39	2.74	-0.79	3.25	2.89
	ERA5	0.59	0.39	0.13	-1.51	2.31	-1.60	2.87	3.13
	GMFD	-0.08	0.53	-0.01	-1.79	3.55	-2.16	1.90	0.74
Uruguay River	OBS-BR	0.53	-0.74	0.00	0.88	1.13	0.22	0.38	0.05
	ERA5	0.18	0.10	0.01	-0.70	0.58	-0.81	0.17	0.07
	GMFD	-0.12	0.10	-0.09	-0.96	1.97	-0.62	0.51	-0.03
South Atlantic	OBS-BR	0.26	-0.46	-0.10	1.02	-0.06	0.96	-0.55	-0.27
	ERA5	0.14	-0.02	0.00	-0.52	0.67	-0.82	0.32	0.26
	GMFD	0.03	0.08	-0.04	-1.34	1.77	-1.07	1.01	0.00

To illustrate, the annual maximum temperature (TXx) shows significantly increasing trends at rates of 0.07 to 0.64 °C/decade across much of the country (Table 3.3 and Fig. 3.6a). ERA5 and GMFD show weaker regional cooling in southern parts of the Uruguay River and South Atlantic basins; however, the trend signal is not statically significant. The frequency of the warm nights (TN90p; 0.58–6.2 percent of days/decade) has increased greater than the frequency of warm days (TX90p; 0.17–4.63 percent of days/decade) in almost all basins, except in the South Atlantic basin for OBS-BR (Table 3.3). The warm spell duration indicator index (WSDI) has increased consistently across the country, with regional increases between 0.03 and 3.13 days/decade. The largest positive trends are found throughout many areas of northwest Amazon and Parana River basins (Fig. 3.S3). Central Atlantic and South Atlantic basins show insignificant decreasing trends for WSDI. Our results are consistent with previous studies, with increasing trends across northern Brazil and smaller increases across southern portions of the country (Gloor et al. 2015; Geirinhas et al. 2018; Feron et al. 2019).

Cold extremes also show increasing trends. All data sets agree that the coldest night of the year (TNn) is warming, with trends of 0.07 to 0.54 °C/decade over the recent past in several parts the country (Fig. 3.5b). On the other hand, gridded observations for Uruguay and South Atlantic basins show statically significant cooling trends by -0.74 and -0.46 °C/decade, respectively. Finally, cold nights (TN10p; Fig. 3.5b) and cold days (TX90 Fig. 3.5d) display warming trends over Brazil, but decreasing trends are found over Uruguay and South Atlantic basins.

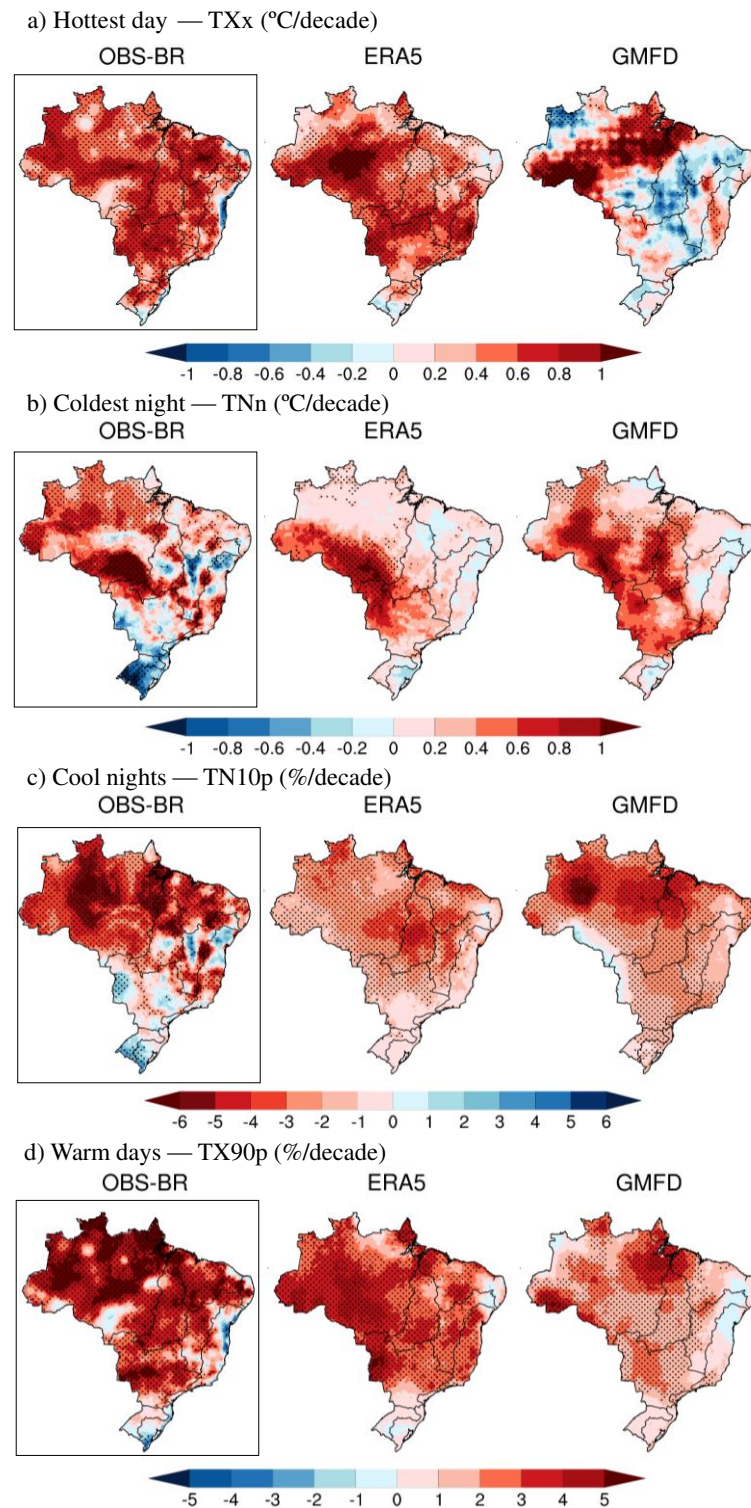


Figure 3.6 Decadal trends in TXx (a), TNn (b), TN10p (c), and TX90p (d) during the period 1980–2016 for OBS-BR (black rectangle; gridded observations), ERA5, and GMFD. Hatching indicates where trends are significant at the 95% level. Trends for additional temperature indices are in Supplementary Material.

Results of extreme temperature indices reveal significant warming trends and are broadly similar across all datasets, which are consistent with other global and regional studies (Donat et al. 2013a, b; Skansi et al. 2013; Rosso et al. 2015; Almeida et al. 2017; Soares et al. 2017; Marengo et al. 2018b; Silva et al. 2018). However, there are some differences in the Uruguay and South Atlantic basin. In these regions, ERA5 and GMFD displayed a

warming trend, and OBS-BR indicates a cooling trend. Also, over the same hydrological basins, the OBS-BR disagrees with GMFD for the diurnal temperature range (DTR; Fig. 3.S3). The interaction between complex topography and regional climate systems play an essential role in the regulation of inter-annual variability over the Uruguay River and South Atlantic basins (Fig. 3.1), which are not well represented by ERA5 and GMFD. In this sense, Gao et al. (2012) and Cornes and Jones (2013) indicated that the high-elevation terrain still poses a challenge for reanalysis, principally because the model topography used by reanalysis does not have sufficient resolution to resolve the climate interaction in small scale. To help solve the topography-dependent problems is necessary to do a topographic correction of reanalysis data to reduce the bias between the estimated and observations values (Gao et al. 2012; Luo et al. 2019).

3.3.2.2. Observed trends in precipitation indices

Extreme precipitation indices show less agreement among the observational trends (OBS-BR) and those estimated by ERA5, GMFD, and MSWEP (Table 3.4 and Fig. 3.7).

Table 3.4 Decadal trends in precipitation indices over the period 1980-2016. Values in bold indicate trends are significant at 95% level. Colors signify wetting (blue), drying (yellow), or no trend (white).

Basin	Dataset	PRCPTOT	RX1day	RX5day	R95p	SDII	R20mm	CWD	CDD
		mm/decade				mm.day ⁻¹ /10yr	days/decade		
Amazon River	OBS-BR	4.43	-0.05	0.64	2.38	-0.004	0.19	2.08	0.62
	ERA5	8.94	6.76	8.32	84.94	0.31	2.53	-5.17	3.67
	GMFD	14.55	0.08	-0.15	-3.18	0.15	-0.29	-0.16	1.26
	MSWEP	62.72	2.06	4.05	38.32	0.24	1.43	0.23	0.44
Tocantins River	OBS-BR	-34.32	-0.11	-1.83	-11.94	-0.08	-0.72	-1.64	4.13
	ERA5	-90.88	-1.13	-4.90	-2.49	-0.07	-0.20	-5.11	7.97
	GMFD	-4.99	2.25	2.88	16.02	0.18	0.50	-1.78	0.85
	MSWEP	17.63	2.03	0.98	25.01	0.35	0.74	-1.39	3.46
North Atlantic	OBS-BR	-19.60	1.34	0.33	5.27	0.06	0.07	-1.67	1.80
	ERA5	-39.83	2.75	1.27	16.41	-0.08	0.12	-4.49	1.30
	GMFD	21.76	0.69	-0.08	5.78	0.26	0.21	-1.27	-5.11
	MSWEP	-23.20	1.96	-1.37	3.83	0.13	-0.24	-1.21	2.98
São Francisco	OBS-BR	-39.52	0.75	-1.32	-5.17	0.06	-0.48	-1.33	2.80
	ERA5	-73.49	-0.62	-2.35	-14.73	-0.16	-0.82	-2.06	4.93
	GMFD	-24.90	1.28	-1.02	2.65	0.05	-0.06	-1.23	-2.91
	MSWEP	-32.75	1.86	0.57	2.24	0.29	-0.25	-1.10	4.16
Central Atlantic	OBS-BR	-35.26	1.73	3.14	7.07	0.14	-0.12	-1.19	1.22
	ERA5	-62.87	0.32	0.22	-12.69	-0.05	-0.71	-1.47	1.75
	GMFD	-37.05	0.08	-1.50	-8.11	-0.03	-0.29	-0.45	0.86
	MSWEP	-26.64	5.17	7.37	30.54	0.63	0.15	-0.82	4.67
Parana River	OBS-BR	-5.32	0.54	0.60	1.13	-0.02	-0.14	0.03	2.14
	ERA5	-51.13	0.57	0.71	1.13	0.00	-0.28	-1.31	4.26
	GMFD	29.29	1.09	3.09	23.25	0.47	0.93	-1.13	1.28
	MSWEP	32.27	2.53	4.24	32.19	0.44	1.07	-0.63	1.78
Uruguay River	OBS-BR	-7.05	0.45	3.50	15.96	-0.01	0.28	-0.13	0.48
	ERA5	-48.99	-0.15	-2.38	-6.90	-0.19	-1.10	-0.36	0.55
	GMFD	-1.30	2.74	-0.14	24.41	0.41	1.23	-0.27	0.31
	MSWEP	30.77	4.54	6.20	43.09	0.57	0.92	-0.33	0.20
South Atlantic	OBS-BR	12.94	1.02	2.97	16.19	0.01	0.29	0.02	-0.01
	ERA5	-25.78	-0.96	-1.89	-12.09	-0.15	-0.55	-0.16	0.33
	GMFD	14.68	2.79	4.32	40.85	0.39	1.23	-0.42	0.58
	MSWEP	21.65	3.17	4.64	29.23	0.43	0.86	-0.38	0.26

The spatial and regional precipitation trends vary considerably compared to the temperature trends across the different datasets. The PRCPTOT increases range from 4.43 to 12.94 mm/decade for the Amazon South Atlantic regions (Table 3.4). However, negative trends are found over the northwestern and southeastern Amazon basin in OBS-BR, ERA5, and MSWEP (Fig. 3.7a). Tocantins, North Atlantic, São Francisco, and Central Atlantic basins show a decrease (not statistically significant) for all four datasets. The dry patterns, especially over the southeastern Amazon and Tocantins basins, are consistent with Gloor et al. (2015).

Mixed trends are demonstrated in the intensity indices (Table 3.4). Similar to previous studies, RX1day, RX5day, and R95p indices show increased extreme rainfall events for the North Atlantic, Central Atlantic, Parana, Uruguay, and South Atlantic basins (Haylock et al. 2006; Skansi et al. 2013; Avila et al. 2016; Zilli et al. 2017; Murara et al. 2018). With regard to the frequency index R20mm, our results show a positive trend over parts of northern and southern Brazil (Amazon, Uruguay, and South Atlantic basins). However, the northeastern part of the country (São Francisco and Central Atlantic basins) exhibit dominantly drying trends.

Changes in duration indices (CDD and CWD; Table 3.4 and Fig. 3.7d) demonstrate mostly non-significant drying trends, with good agreement among the reanalyses and merged datasets (Table 3.4). Our results of CDD agree well with Valverde and Marengo (2014) who used historical rainfall stations in their assessment. The regionally-specific decadal trends of CWD show increasing tendencies for all basins and only disagree with the OBS-BR product for the Amazon basin (statistically significant rate of 2.08 mm/decade) and Parana and South Atlantic basins (trends not significant in these regions). Differences between these datasets in terms of the signal may arise from the longer observed daily rainfall stations for Amazon basins are scarce in both spatial and temporal coverage (Xavier et al. 2015).

In general, precipitation changes show statistically non-significant trends, although the ERA5, MSWEP and OBS-BR exhibit reasonable spatial coherency. Results show increasing trends in annual total wet-day precipitation in northern and southern basins and dry patterns in northern and central Basins. Northern and central hydrological regions such as the North Atlantic region, São Francisco, Central Atlantic, and Parana basins show increasing trends in the more extreme precipitation events (RX1day) during the last four decades. Southern basins (e.g., Parana, Uruguay, South Atlantic basins) reveal increasing trends in events related to intensity and frequency. Duration indices exhibit a reduction of CWD; meanwhile, the CDD index shows positive trends over the majority of Brazil.

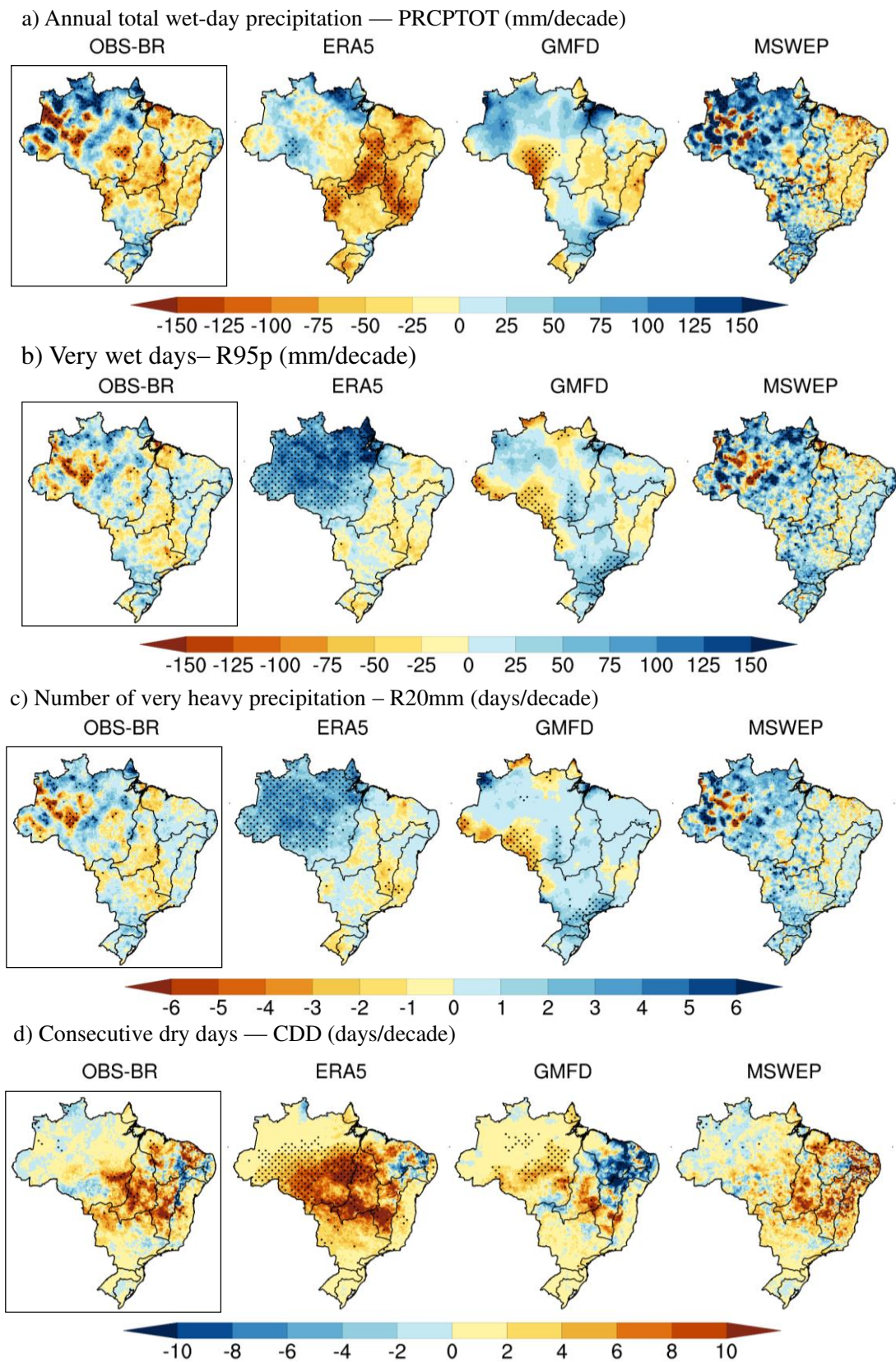


Figure 3.7 Decadal trends in PRCPTOT (a), R95p (b), R20mm (c), and CDD (d) during the period 1980–2016 for OBS-BR (black rectangle; gridded observations), ERA5, GMFD, and MSWEP. Stippling indicates where trends are significant at the 95% level. Trends for additional precipitation indices are in Supplementary Material.

3.2.3. Future projections in climate extremes

3.2.3.1. Changes in future temperature indices

Fig. 3.8 shows the spatial changes patterns of temperature indices for period 2046–2065 relative to the baseline period (1986–2005), under the representative concentration pathway (RCP) scenarios 4.5 and 8.5. Note: Fig. 3.9 displays the same regional projected changes were summarized in box-and-whisker plots and presented per hydrological basins. Mean projected changes for 2081–2100 period (end-21st century) are in Supplementary Figs. S6 and S7.

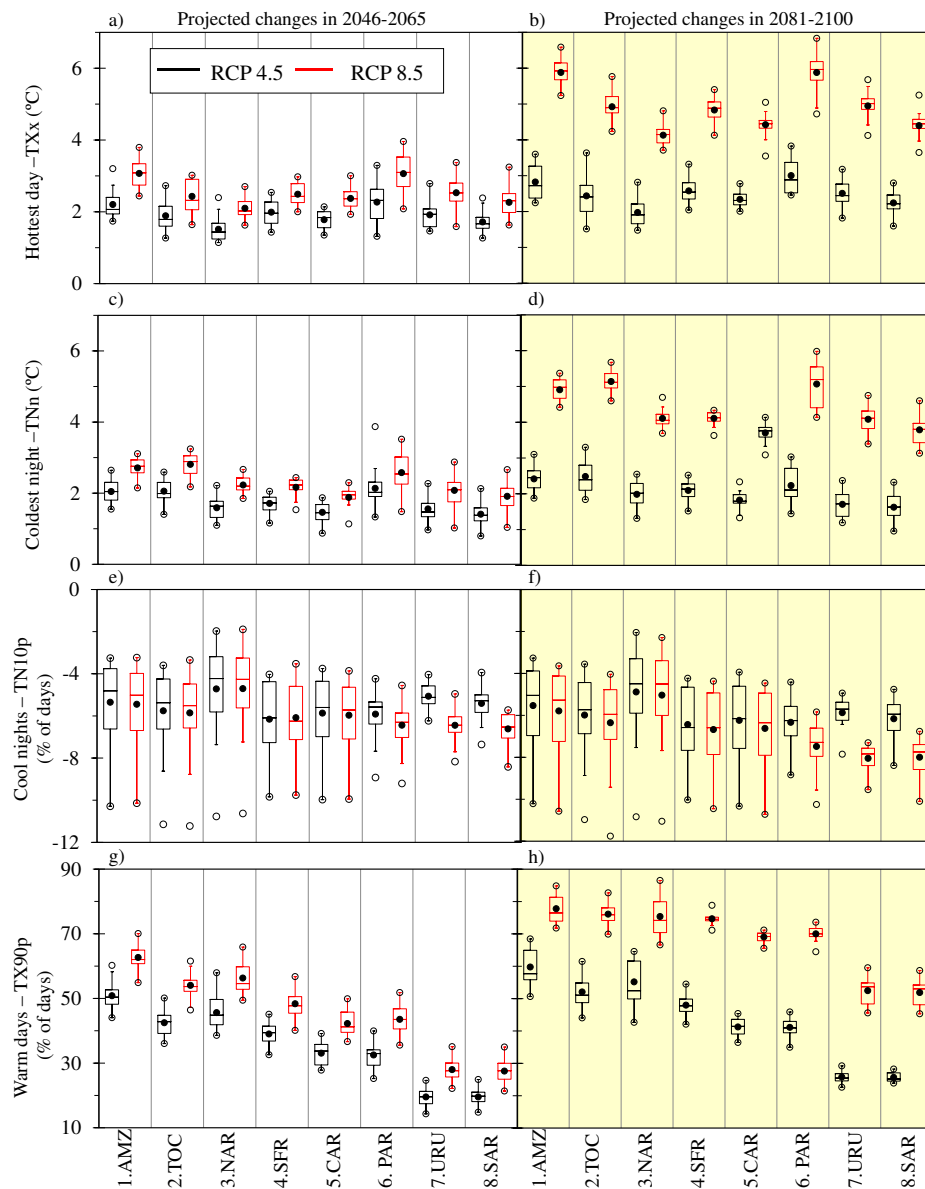


Figure 3.8 Projected changes in the hottest day–TXx (a-b), coldest night–TNn (c-d), cool nights – TN10p (e-f) and Warm days – TX90p (g-h) over the period 2046–2065 (white zone) and 2081–2100 (yellow zone) relative to the reference period (1986–2005) for RCP4.5 (black line) and RCP8.5 (red line). Regional mean changes are shown for each hydrological regions; the acronyms are defined in Fig. 3.1. The boxes indicate the variability of the ensemble of the downscaled models–MME (Table S3.1), which include the interquartile range (25th–75th percentiles), median (horizontal line), mean (black dots), maximum and minimum values (black circles).

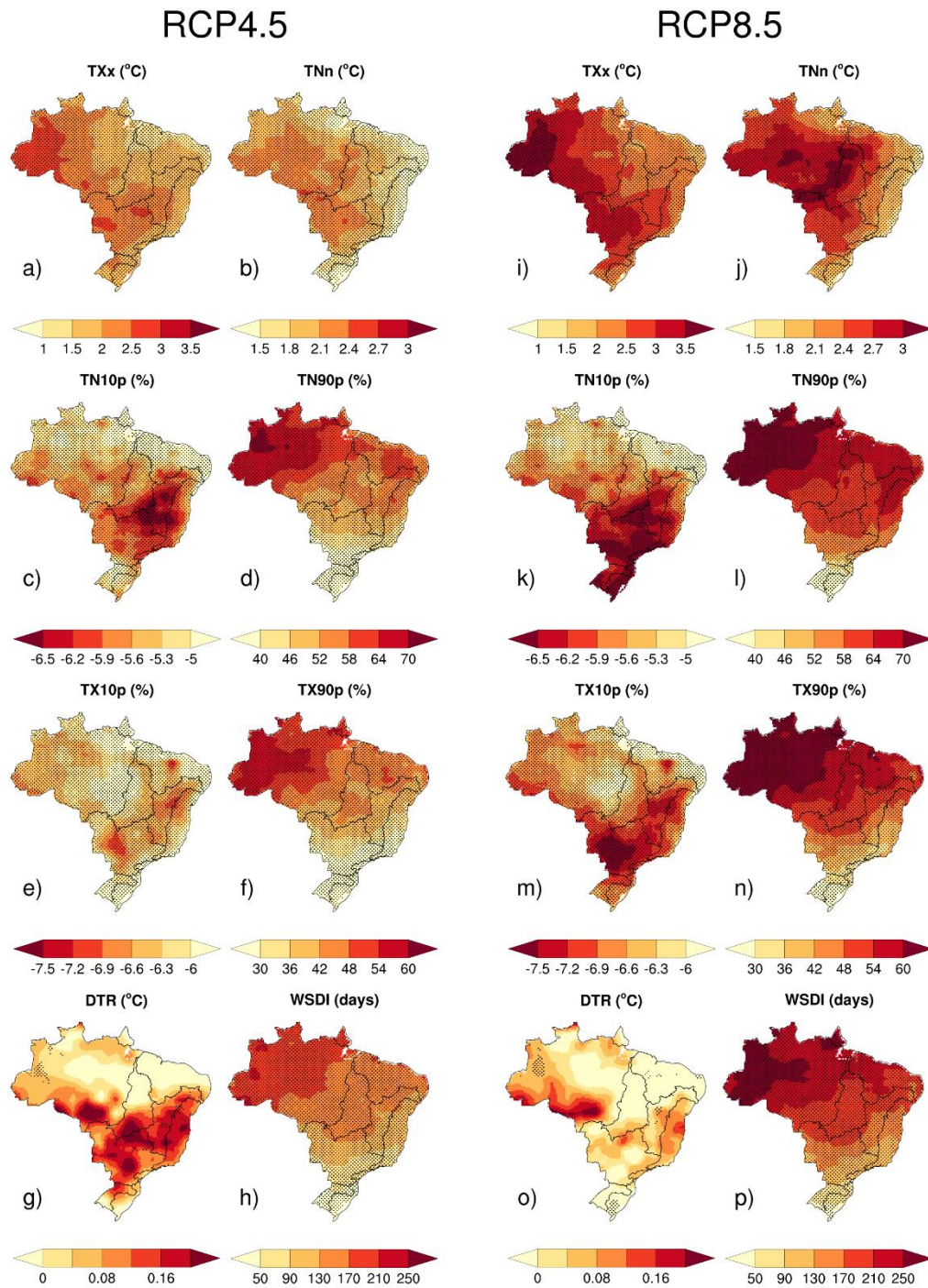


Figure 3.9 Future changes of multi-model ensemble in temperature extremes indices under the (a-h) RCP4.5 and (i-p) RCP8.5 scenarios for the period 2046-2065 relative to the reference period (1986-2005). Stippling indicates grid-points where more than 66 percent of the models agreed in change signal and in which more than 50 percent of the models show a significant change.

The multi-model ensemble (MME) mean projects significant warming in annual maximum temperature (TXx; Fig. 3.8a-b) and annual minimum temperature (TNn; Fig. 3.8c-d). These indices increase across the different basins by mid-21st century and vary between 1.4 to 2.3 °C in RCP4.5 and 1.9 to 3.1°C in RCP8.5. By the end of the 21st century, these indices increase 1.6 to 3.0 °C in RCP4.5 and 3.7 to 5.9 °C in RCP8.5. Figs. 8 and 9 show

that the maximum warming is found over the Amazon, Tocantins, and Parana Rivers basins. Similar results for the end of the 21st century are noted by Sillmann et al. (2013b) and López-Franca et al. (2016).

There are similar patterns of increasing frequency of warm extremes (TX90p and TN90p) and reduction of cold extremes (TN10p and TX10p) by the middle end of the 21st century over Brazil (Figs. 8, 9, S5). Projected changes in warm indices are more pronounced than those for cold indices. Under the scenario RCP4.5, increases in the occurrence of TX90p and TN90p vary between 20 and 63 percent in the mid-century projections and 28 to 69 percent in RCP8.5. Also, end of the 21st century mean changes are 6 to 15 percent higher compared to the projected increases for mid-century under both scenarios.

In addition to stronger warming, warm spell duration index (WSDI) increases significantly for 2046–2065 and 2081–2100 under the RCPs scenarios (Figs. 9, S6). The significant increase in WSDI is projected in all basins with mean changes greater than 39 (56) days by the middle and end of the 21st century under RCP4.5 (8.5). Consistent with the warming patterns, decreases in cold nights (TN10p) and cold days (TX10p) are projected. The TN10p (TX10p) index decreases from about 6.2 percent (6.6 percent) in 2046–2065 to 6.4 percent (7.1 percent) under RCP4.5 and 8.5, with slightly negative trends by the end of the century. The regional changes in percentile indices by middle and end of the century are consistent with previous studies over South America (Marengo et al. 2009; Sillmann et al. 2013b; López-Franca et al. 2016; Feron et al. 2019). These results are in agreement with other regions throughout the globe (Zhou et al. 2014; Lelieveld et al. 2016; Schoof and Robeson 2016; Alexander and Arblaster 2017).

In summary, the most significant increases (decreases) in warm (cold) extremes occur in the Amazon, Tocantins, and North Atlantic basins. However, the smallest changes of ensemble mean temperature extremes are projected in the Uruguay River and South Atlantic basins. The findings are in agreement with the results by Sillmann et al. (2013b) who used CMIP5 models to project extreme climate indices over South America.

3.2.3.2. Changes in future precipitation indices

Changes in precipitation indices relative to the 1986–2005 reference period are presented in Figs. 10 and 11. For comparison purposes with other studies (e.g., Sillmann et al. (2013)), relative changes (see equation 1) are expressed in percentage. Mean projected changes for 2081–2100 period (end-21st century) are in Supplementary Figs. S8 and S9.

The ensemble mean of PRCPTOT reflects a reduction over Amazon, Tocantins, North Atlantic, São Francisco, and Central Atlantic basins (Figs. 10a-b, 11a, 11i). At the same time, the CDD projections indicate an increase across most regions of Brazil for RCP4.5 (8.5), ranging from 1 to 18 percent (3 to 27 percent) by the mid-century and ranging from 1 to 22 percent (3 to 61 percent) by the end of 21st century (Fig. 3.10c-d). CWD shows a pattern opposite to that of CDD (Figs. 10h-g, 11g-h, o-p). Small trends in ensemble mean PRCPTOT, CDD, and CWD are projected over southern Brazil (URU and SAR). In general, future projections show a reduction in PRCPTOT and CWD and increases in CDD. This trend toward a drier future climate is consistent with previous authors (Amorim et al. 2014; Chou et al. 2014b; Marengo et al. 2017; Lyra et al. 2018)

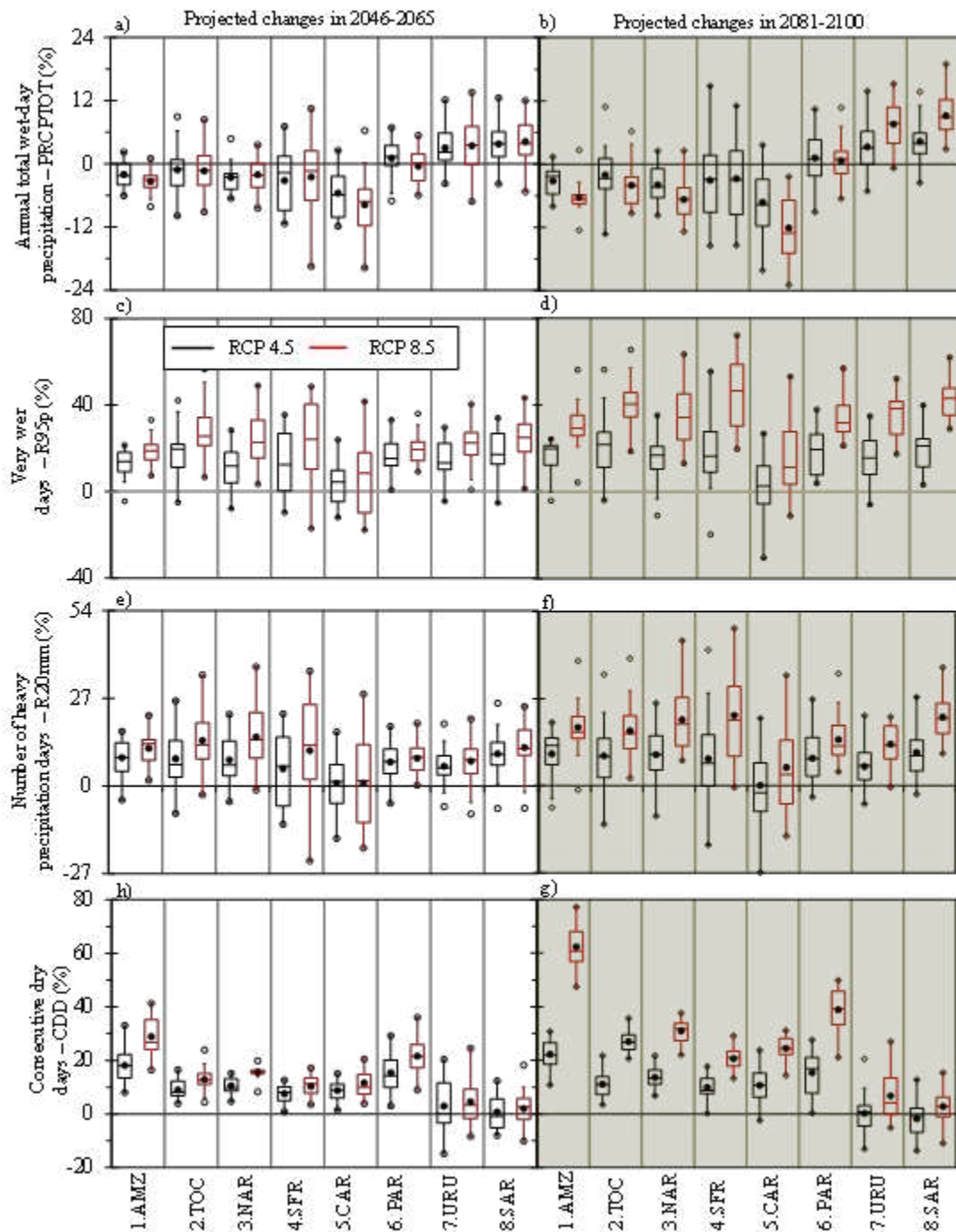


Figure 3.10 As Fig. 3.7 but for the annual total wet-day precipitation - PRCPTOT (a-b), very wet days-R95p (c-d), Number of heavy precipitation days-R20mm (e-f), and consecutive dry days-CDD (h-g)

For rainfall intensity extremes (RX1day, RX5day, R95p, and SDII), increasing trends are projected over most of Brazil under both scenarios, more pronounced by the end of the century (Figs. 10, 11). The largest increases of R95p index, on the order of 4 to 18 percent (6 to 29 percent), are expected for the mid-century in the RCP4.5 (8.5) scenario. By the end of the 21st century, the R95p mean increases most in the RCP8.5 scenario (16 to 45 percent). In general, projections of intensity indices indicate the weakest trends over the Central Atlantic basin, whereas the most significant changes are generally found in the Tocantins, São Francisco, and South Atlantic basins (Fig. 3.11). The signal of change in intensity indices such as RX1day is consistent with those obtained by

Valverde and Marengo (2014) and Bador et al. (2018), and projected increases in R20mm index over southern Brazil are evident over Uruguay and South Atlantic basins. These results are in agreement with that of Sillmann et al. (2013b) and Lyra et al. (2017), who reported the reduction in the number of heavy precipitation days.

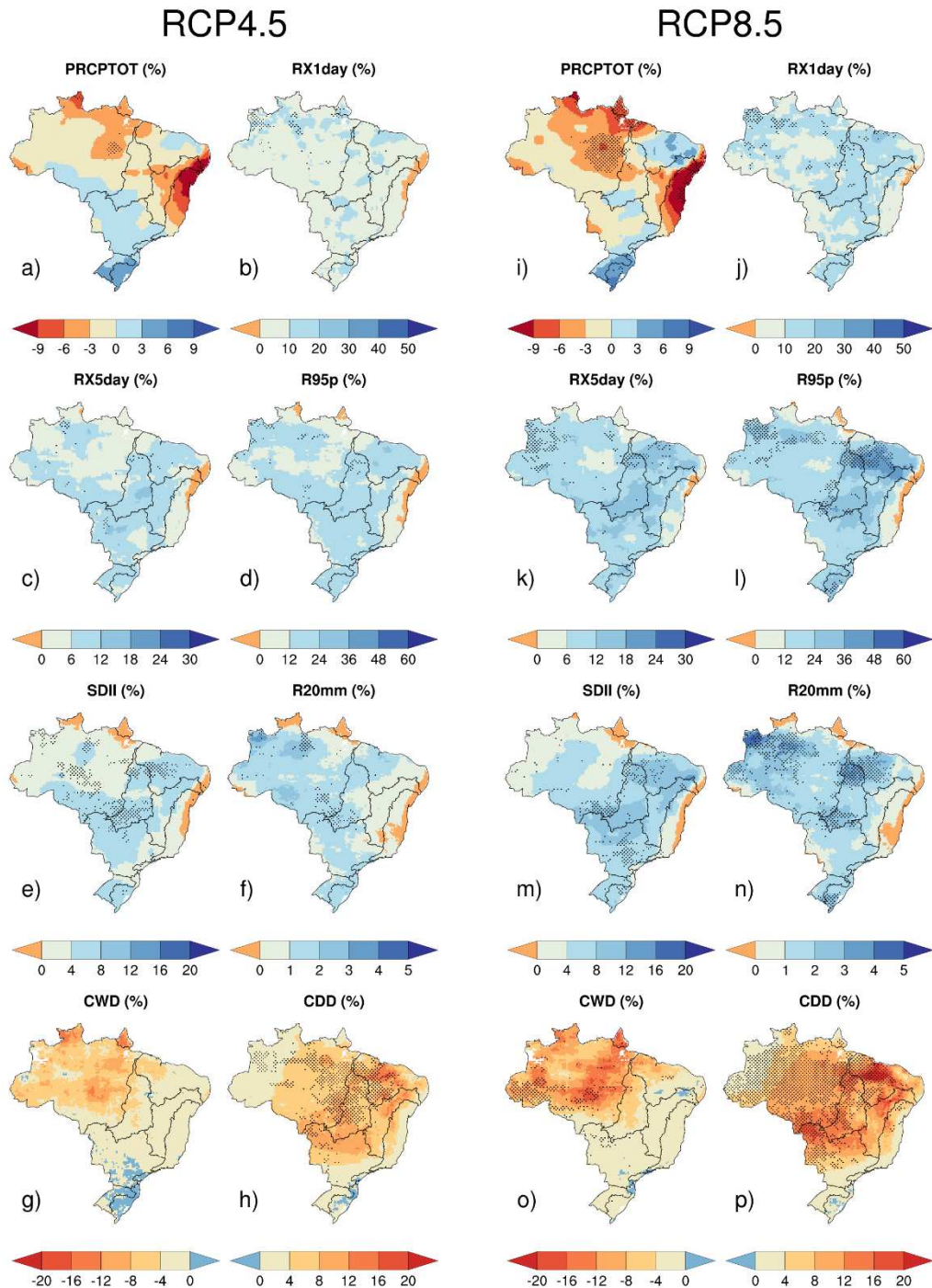


Figure 3.11 Future changes of multi-model ensemble in precipitation extremes indices under the (a-h) RCP4.5 and (i-p) RCP8.5 scenarios for the period 2046-2065 relative to the reference period (1986–2005). Stippling indicates grid-points where more than 66 percent of the models agreed in change signal and in which more than 50 percent of the models show a significant change

Caution must be given when interpreting the results of these precipitation indices. Unlike temperature indices, most models disagree with the direction of change, with fewer than half of the models showing a significant change. For example, our results point out the model agreement increase in both RCP4.5 and RCP8.5 scenarios compared to the historical (e.g., PRCPTOT, R95p, and CDD). This is in concert with previous studies showing similar lower confidence for precipitation indices over other parts of the world (e.g., Sillmann et al. (2013); Alexander and Arblaster (2017)). In this sense, Lin et al. (2018) indicated that the CMIP5 multimodel ensemble shows a significant sensitivity of precipitation extremes to aerosol forcing on the large-scale rainfall processes, which may be influencing the confidence in agreement of climate projections across most of Brazil. To resolve the low confidence in the long-term projections of MMEs, Guyennon et al. (2013) and Yhang et al. (2017) concluded that the combination of dynamical and statistical downscaling of ESMs produced a better representation of regional precipitation, which can be resulted in much improved in simulations and increased in the agreement of projection in the MMEs.

3.4. Discussion and Concluding remarks

We investigated the changes in temperature and precipitation extremes in historical observations from 1980–2016 in Brazil comparing multiple gridded datasets (ERA5, GMFD, and MSWEP) that using various techniques and station networks to calculate daily gridded fields. We analyzed changes in climate extremes indicated by an ensemble of 20 downscaled ESMs under RCP4.5 and RCP 8.5 scenarios over the periods of 2046–2065 and 2081–2100 relative to the reference period 1986–2005.

ERA5 performs better than GMFD and MSWEP capturing the spatio-temporal patterns of historical climate extremes. In general, the performance over 1980–2016 shows that all datasets have a greater ability to capture extreme temperatures compared to extreme precipitation indices. However, almost all precipitation indices have large uncertainties over the Amazon basin.

During the last four decades (1980–2016), observations, reanalysis and merged datasets show statistically significant warming patterns for both warm (TXx, TX90, TN90, and WSDI) and cold (TNn, TX10, and TN10) extreme indices over almost all areas in Brazil. Multi-model climate projections reveal that the observed historical warming patterns may be intensified with the increase in the radiative forcing under the representative concentration pathways for (RCP4.5 to RCP8.5). Mid-century (End-of-century) maximum and minimum temperatures over hydrological basins exceeds 1.4 °C (1.6 °C) in RCP 4.5 and 1.9 °C (3.2 °C) in RCP8.5. Simultaneously, the frequency of warm days/nights has increased (TX90p/TN90p) more than cold days/nights (TX10p/TN10p), and heat wave duration (greater than 56 days) over the 21st century is expected in all basins.

Historical gridded datasets indicate a reduction in consecutive wet days and an increase of dry consecutive drays days since the 1980s in almost all areas of the study domain. Analysis of annual total precipitation shows negative trends over the Tocantins, North Atlantic, São Francisco, and Central Atlantic basins. Trends in rainfall extremes indices are not statistically significant across the gridded precipitation products. Moreover, future changes show a reduction in the total amount precipitation, consecutive wet days, and the number of very heavy rainfall (R20mm) for most of the hydrological basins, except for Uruguay and South Atlantic basins. The extreme precipitation intensity indices (RX1day, RX5day, R95p, and SDII) are projected to increase for future scenarios

in the majority areas. These patterns could aggravate the impacts of flash floods and landslides, which are the most common hydrological hazards, principally over Southern Brazil (CEPED-UFSC 2013; Debortoli et al. 2017), which is the highest densely populated of the country. Noteworthy, the intensification of temperature warm extreme events (e.g., WSDI) could increase the incidence of respiratory and cardiovascular diseases (Son et al. 2016).

Brazilian Central-West region (parts of Paraguay and Tocantins basins), the most important agricultural region of Brazil, has experienced an increase in warm extremes, while the total annual precipitation has decreased since the 1980s. Future scenarios indicate that the maximum and minimum temperatures will become warmer, and the differences between the minimum and maximum temperatures increase. The amount of annual precipitation will also increase but will be concentrated in short and intense events. In other words, most of the observed and future trends could bring conflicts of water rights and irrigation for food production, negative impacts for water availability, greatly affecting the population that depends on hydroelectricity in northern and northeastern basins of Brazil (Marengo et al. 2017; Jong et al. 2018; Llopart et al. 2019).

Northeastern Brazil (parts of Central Atlantic, São Francisco, and North Atlantic basins) are getting drier and the frequency of extreme precipitation events has been increasing since the 1980s. The frequency of hot days has been decreasing near the coast. Annual precipitation amounts have been reducing in this region overall, as well as the extreme rainfall events frequency. However, the northeastern region is the driest and poorest region of Brazil, and projections point to the largest reduction of total precipitation there, threatening the survival of millions of people due to water scarcity (Darela-Filho et al. 2016; Marengo et al. 2017).

The southern part of Amazon and Tocantins basins have been experiencing a reduction in annual precipitation and an increase in consecutive dry days since the 1980s, and projections indicate that this trend will be continue throughout the 21st century. These drier conditions could fuel additional drought events, increasing the risk of forest fires (Aragão et al. 2007).

These important climate-change connections improve our current lack of understanding with regard to temperature and precipitation extremes in Brazil. This increased knowledge plays an important role in designing effective adaptation and mitigation measures related to climate change impacts. Still, the future climate projections should be interpreted with caution as climate extremes tend to increase the variability of extreme values and uncertainty among the downscaled ESMs, especially for rainfall extremes.

3.5.Acknowledgments

This work was possible thanks to the Minas Gerais Research Foundation (FAPEMIG) and the Coordination for the Improvement of Higher Education Personnel (CAPES) for supporting the study. We also thank different modeling groups for providing the NEX-GDDP, Reanalysis (ERA5) and merged (MSWEP and GMFD) products. The authors acknowledge to Alexandre Xavier, Carey King, and Bridget Scanlon who provided daily climate data over Brazil.

3.6. Supplementary material

Assessing Current and Future Trends of Climate Extremes Across Brazil Using Reanalyses and Earth System Model Projections.

Alvaro Avila; Victor Benezoli; Flavio Justino; Roger Torres; Aaron Wilson.

Climate Dynamics. Manuscript number: CLDY-D-19-00921.

Table S3.1 The downscaled Earth System Models (ESMs) with a statistical downscaling

No.	Modeling center	Model name	Resolution (°lon. × °lat.)
1 ^a	Beijing Climate Center, China Meteorological Administration (China)	BCC-CSM1-1	2.8 × 2.8
2	Beijing Normal University (China)	BNU-ESM	2.8 × 2.8
3	Canadian Centre for Climate Modeling and Analysis (Canada)	CanESM2	2.8 × 2.8
4	National Center for Atmospheric Research (NCAR-USA)	CCSM4	1.25 × 0.94
5	National Science Foundation, Department of Energy and NCAR (USA)	CESM1-BGC	1.25 × 0.94
6	Centre National de Recherches Météorologiques and Centre Européen de Recherche et Formation Avancée en Calcul Scientifique (France)	CNRM-CM5	1.4 × 1.4
7	Commonwealth Scientific and Industrial Research Organization (Australia)	CSIRO-MK3-6-0	1.875 × 1.875
8 ^c	NOAA Geophysical Fluid Dynamics Laboratory (USA)	GFDL-CM3	2.5 × 2.0
9	NOAA Geophysical Fluid Dynamics Laboratory (USA)	GFDL-ESM2G	2.5 × 2.0
10	NOAA Geophysical Fluid Dynamics Laboratory (USA)	GFDL-ESM2M	2.5 × 2.0
11	Institute for Numerical Mathematics (Russia)	INMCM4	2 × 1.5
12	Institut Pierre-Simon Laplace (France)	IPSL-CM5A-LR	3.75 × 1.895
13	Institut Pierre-Simon Laplace (France)	IPSL-CM5A-MR	2.5 × 1.27
14 ^c	Atmosphere and Ocean Research Institute (The University of Tokyo), National Institute for Environmental Studies, and Japan Agency for Marine-Earth Science and Technology (Japan)	MIROC5	1.41 × 1.41
15	Japan Agency for Marine-Earth Science and Technology, Atmosphere and Ocean Research Institute (The University of Tokyo), and National Institute for Environmental Studies	MIROC-ESM	2.8 × 2.8
16	Japan Agency for Marine-Earth Science and Technology, Atmosphere and Ocean Research Institute (The University of Tokyo), and National Institute for Environmental Studies	MIROC-ESM-CHEM	2.81 × 2.81
17	Max Planck Institute for Meteorology (Germany)	MPI-ESM-LR	1.875 × 1.875
18	Max Planck Institute for Meteorology (Germany)	MPI-ESM-MR	1.875 × 1.875
29	Meteorological Research Institute (Japan)	MRI-CGCM3	1.125 × 1.125
20	Norwegian Climate Centre (Norway)	NorESM1-M	2.5 × 1.9

^aAll two RCPs projections of temperature and precipitation data on BCC-CSM1-1 and MIROC5 were only available until year 2099. ^bThe RCP4.5 projections of precipitation data on GFDL-CM3 were available until year 2095.

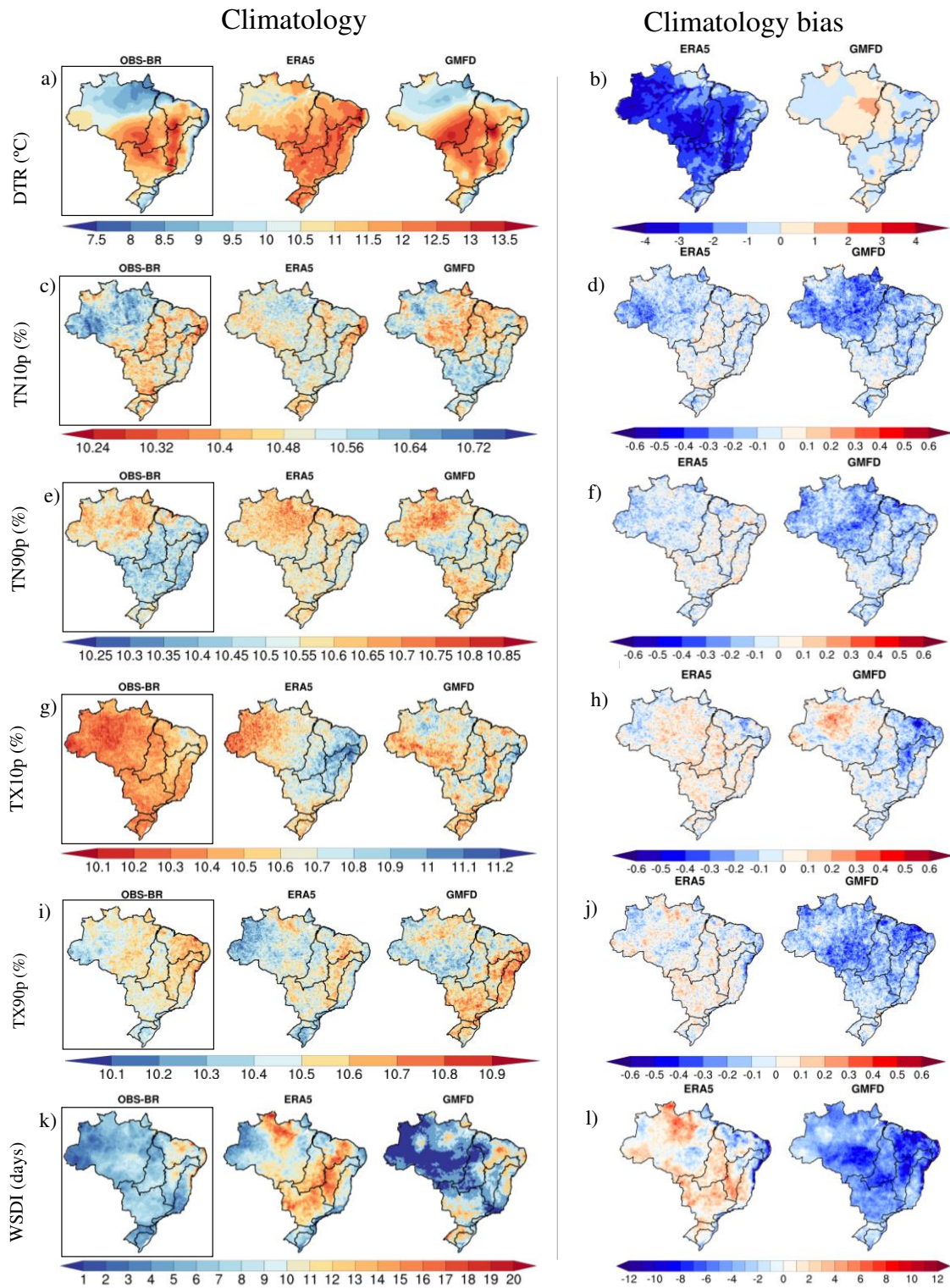


Figure S3.1 The 1980-2016 climatology and bias of the DTR (a-b), TN10p (c-d), TN90p (e-f), TX10p (g-h), TX90p (i-j) and WSDI (k-l) for OBS-BR (black rectangle; gridded observations), ERA5 and GMFD

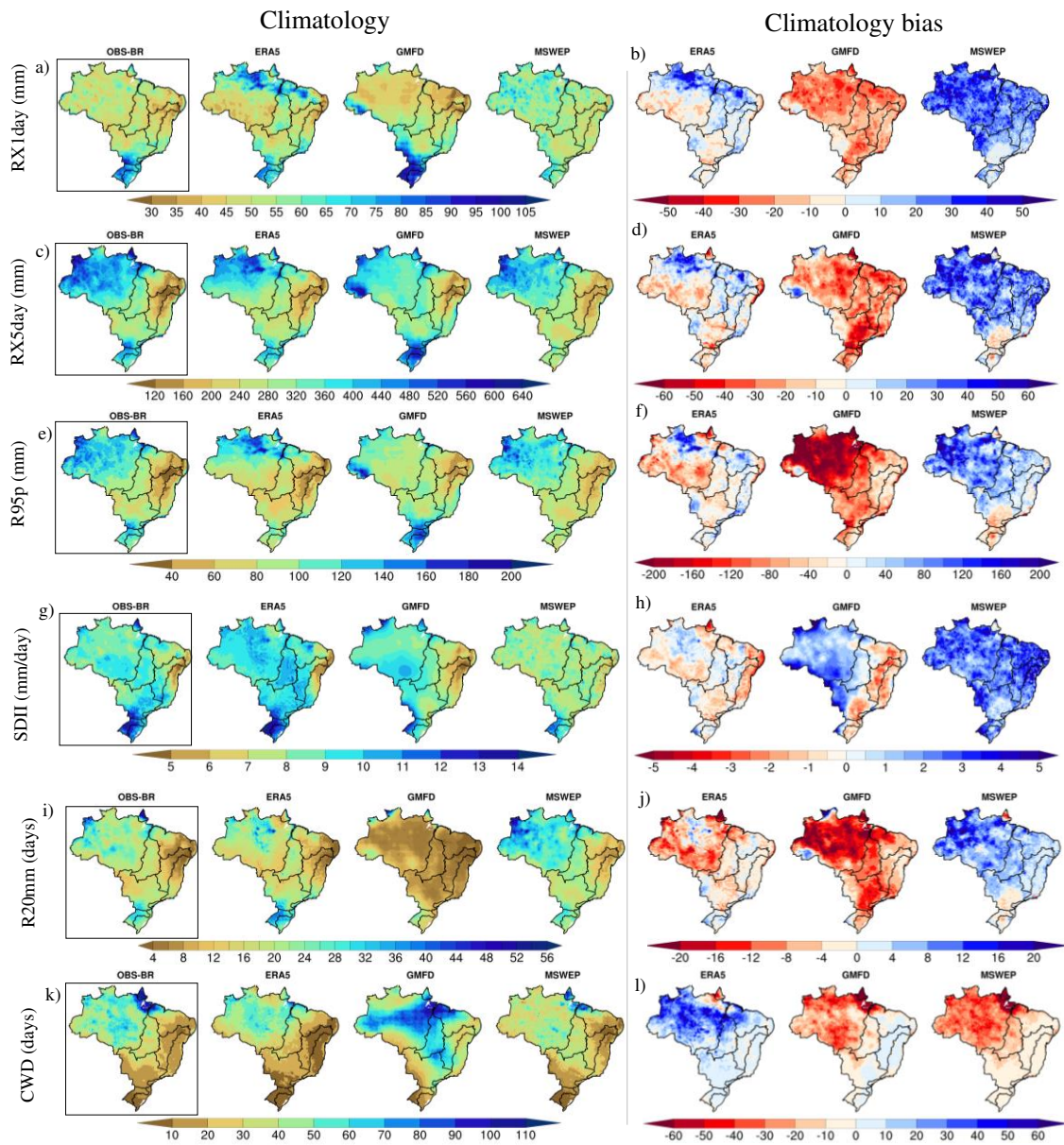


Figure S3.2 The 1980-2016 climatology and bias of the RX1day (a-b), RX5day (c-d), R95p (e-f), SDII (g-h), R20mm (i-j) and CWD (k-l) for OBS-BR (black rectangle; gridded observations), ERA5, GMFD and MSWEP

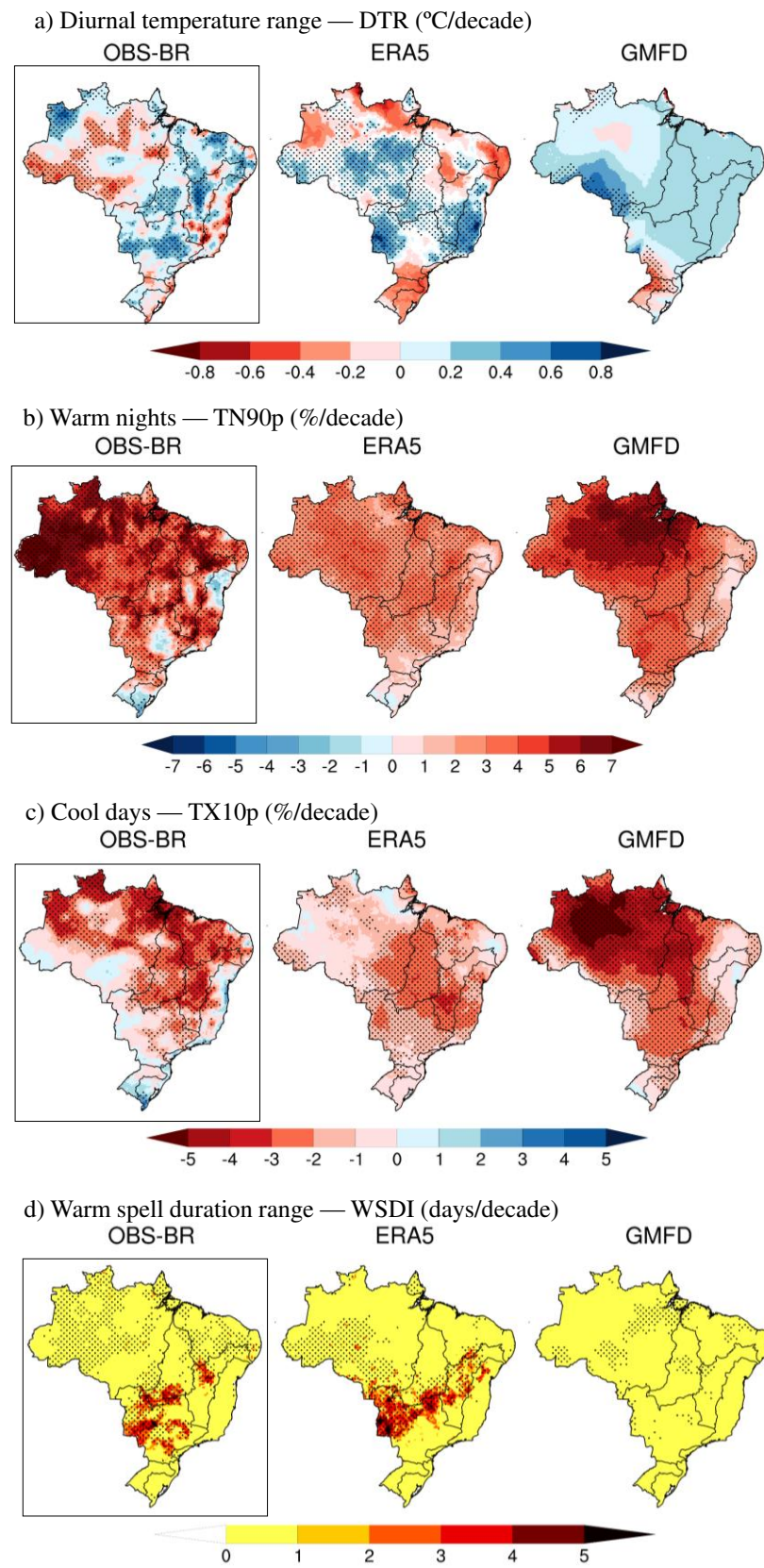


Figure S3.3 Decadal trends in DTR (c), TN90p (d), TX10p (a), and WSDI (b) during the period 1980–2016 for OBS-BR (black rectangle; gridded observations), ERA5 and GMFD. Hatching indicates where trends are significant at the 95% level

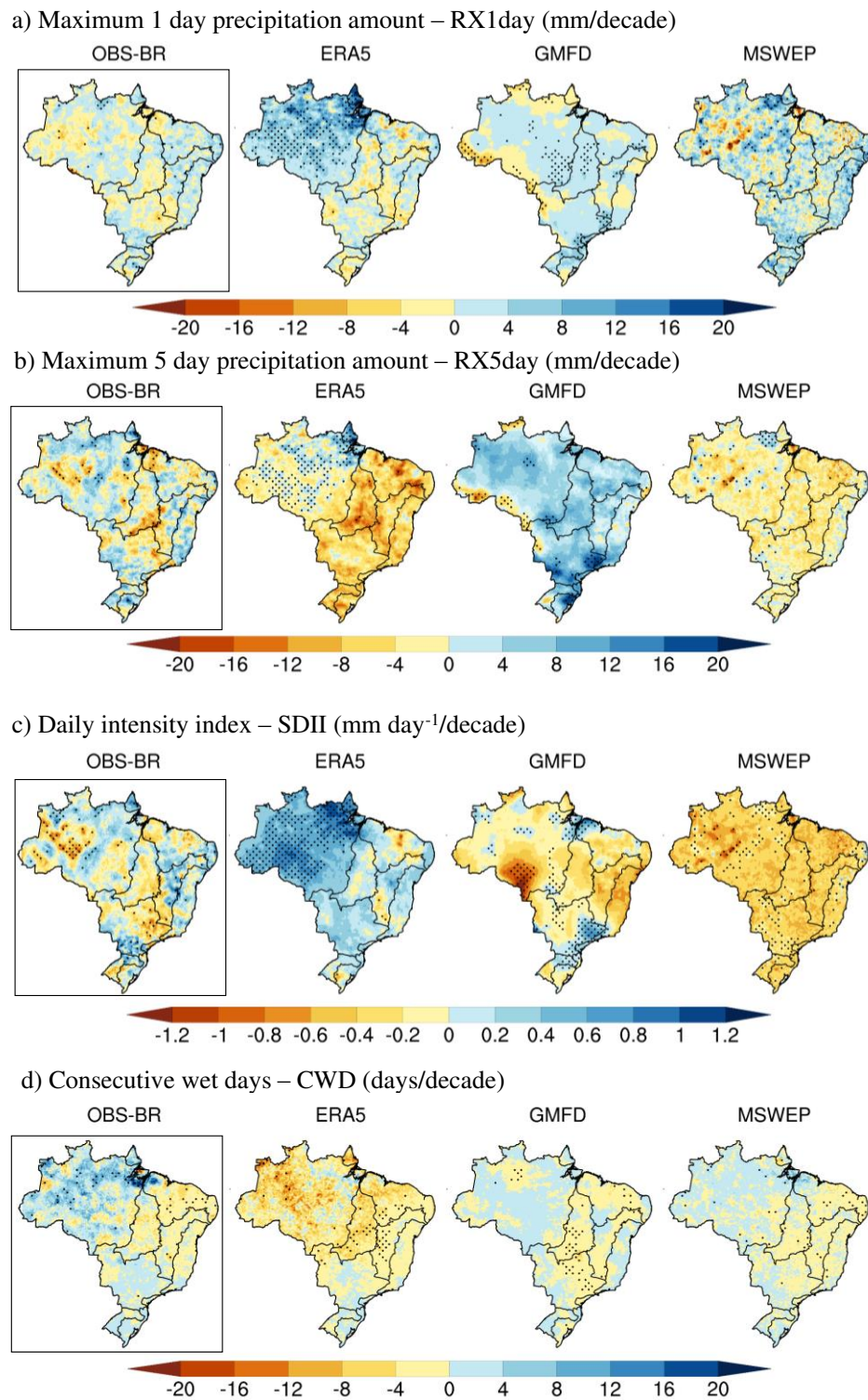


Figure S3.4 Decadal trends in RX1day (a), RX5day (b), R95p (c), and SDII (d) during the period 1980–2016 for OBS-BR (black rectangle; gridded observations), ERA5 and GMFD. Hatching indicates where trends are significant at the 95% level

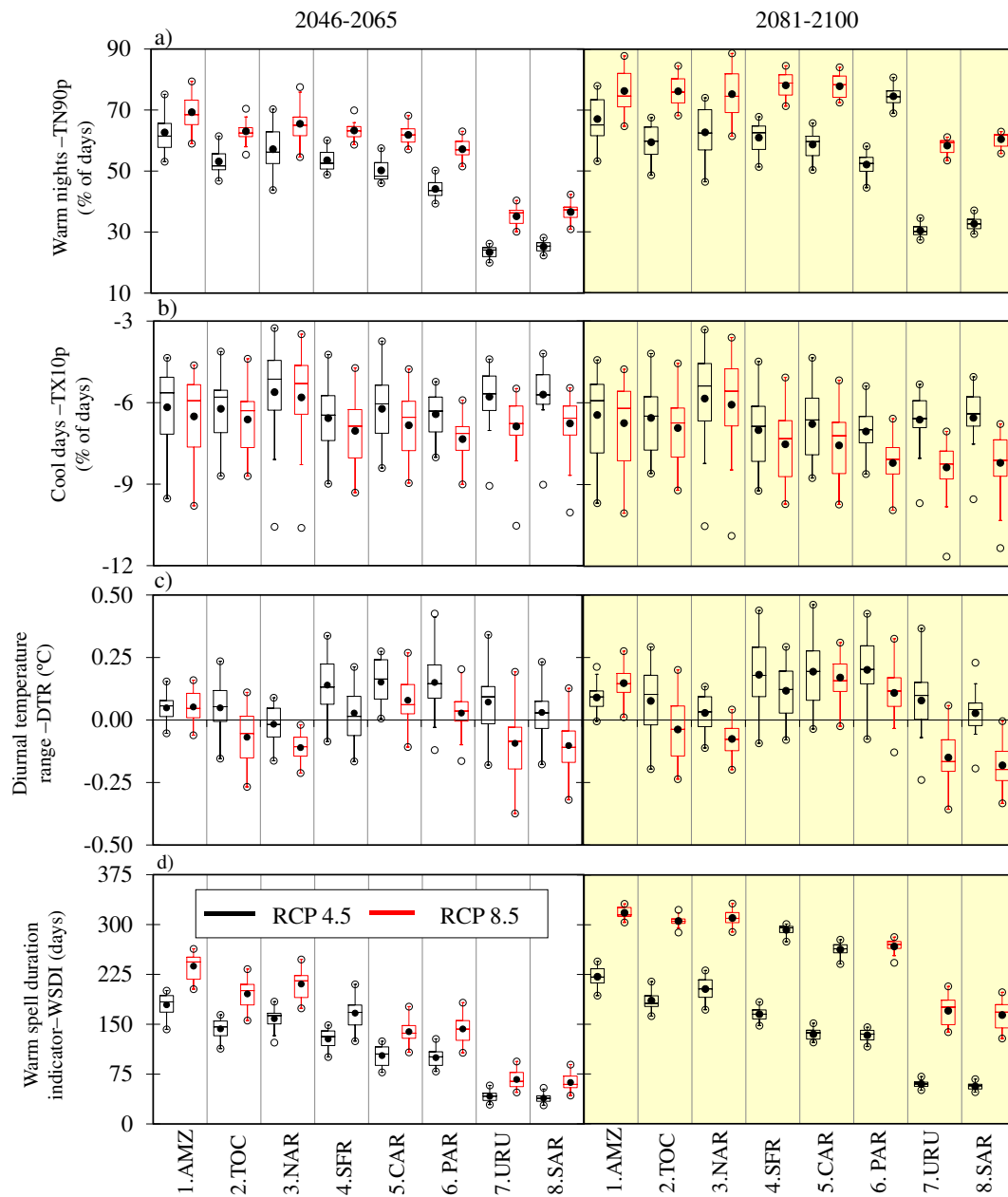


Figure S3.5 Projected changes in temperature indices (a-f) over the period 2046-2065 (white zone) and 2081-2100 (yellow zone) relative to the reference period (1986-2005) for RCP4.5 (black line) and RCP8.5 (red line). Regional mean changes are shown for each hydrological regions (Fig 1)

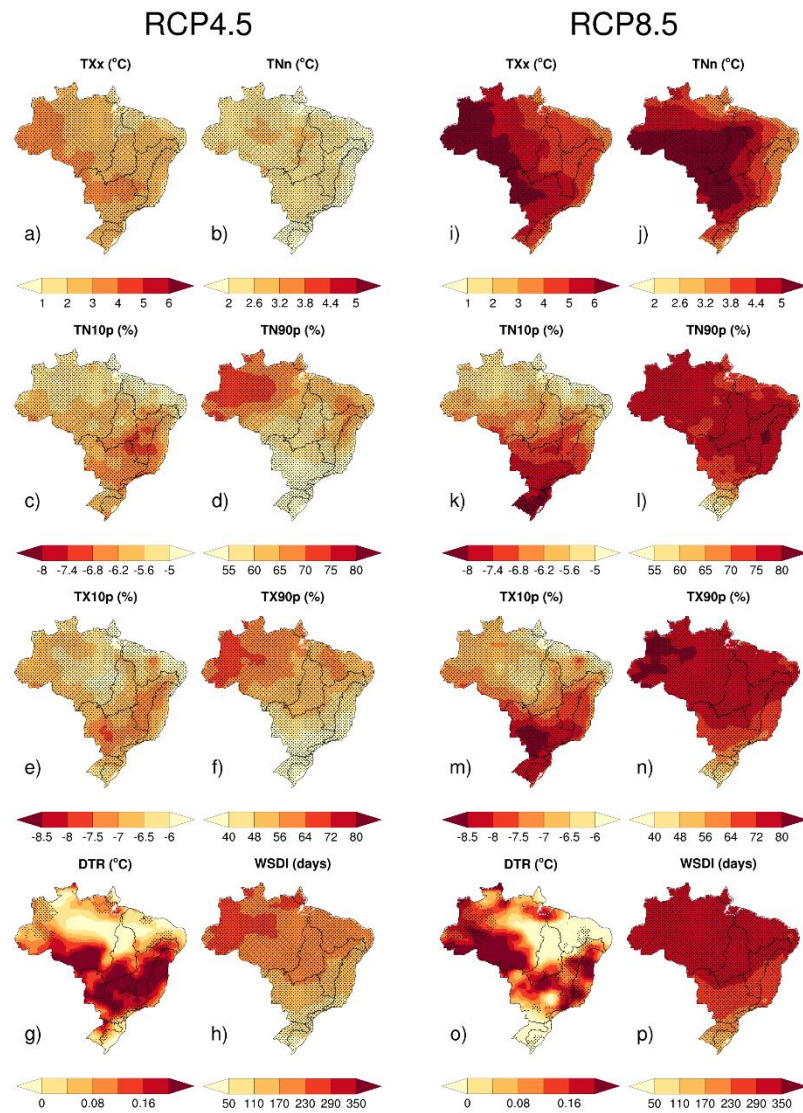


Figure S3.6 Future changes of multi-model ensemble in temperature extremes indices under the (a-h) RCP4.5 and (i-p) RCP8.5 scenarios for the period 2081-2100 relative to the reference period (1986–2005). Stippling indicates grid-points where more than 66 percent of the models agreed in change signal and in which more than 50 percent of the models show a significant change

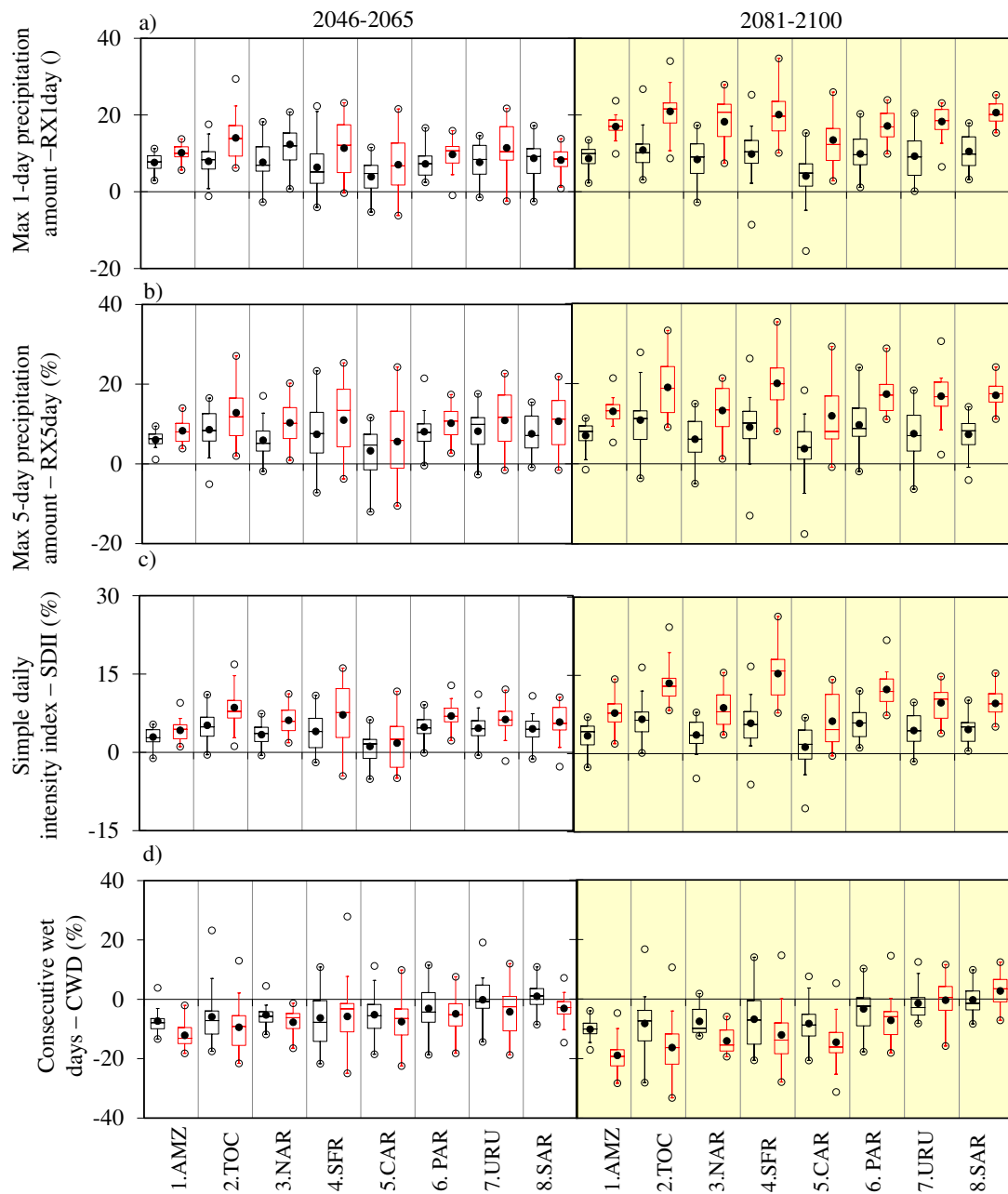


Figure S3.7 Projected changes in precipitation indices (a-f) over the period 2046-2065 (white zone) and 2081-2100 (yellow zone) relative to the reference period (1986–2005) for RCP4.5 (black line) and RCP8.5 (red line). Regional mean changes are shown for each hydrological regions (Fig. 3.1)

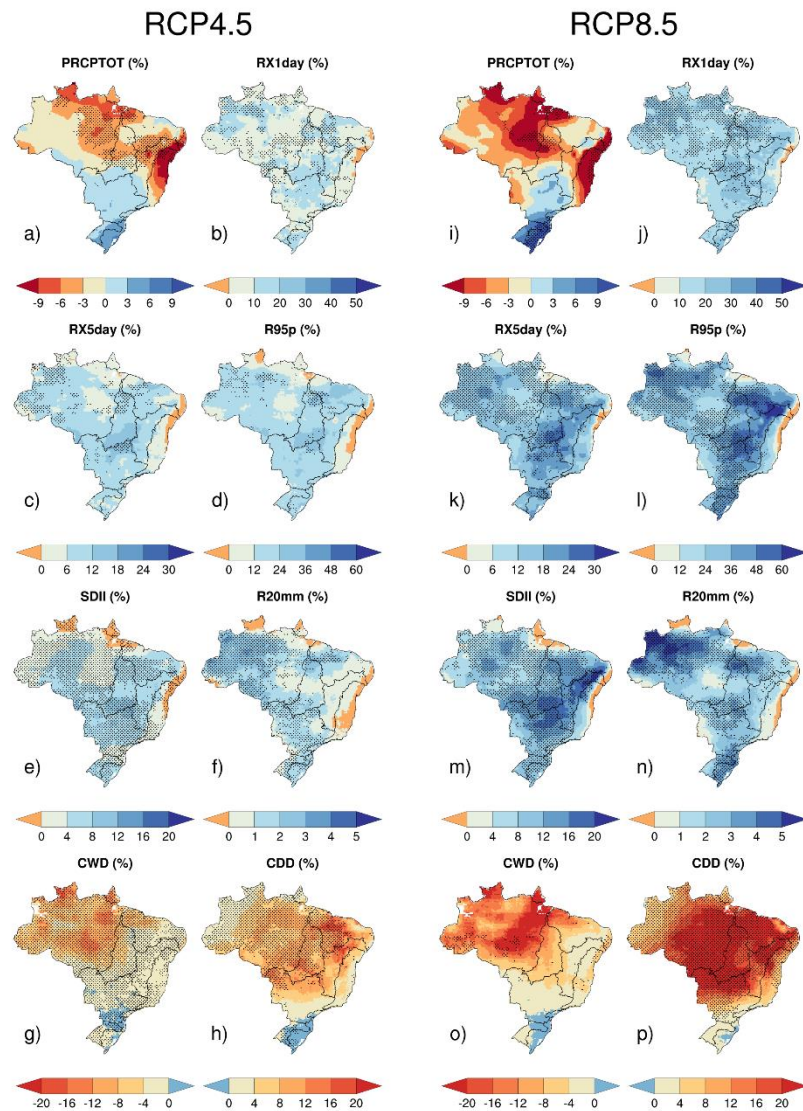


Figure S3.8 Future changes of multi-model ensemble in precipitation extremes indices under the (a-h) RCP4.5 and (i-p) RCP8.5 scenarios for the period 2081–2100 relative to the reference period (1986–2005). Stippling indicates grid-points where more than 66 percent of the models agreed in change signal and in which more than 50 percent of the models show a significant change

4. GENERAL CONCLUSIONS

This thesis has identified, on regional/local scale, the current and future changes on daily extremes events of temperature and precipitation across Brazil in gridded datasets at the high horizontal resolution (0.25° latitude/longitude~25 km x 25 km). Specifically, it was employed fourth different periods: I) 1986-2005, to evaluate the performance of the downscaled models; II) 1980-2016, to study the changes over the last fourth decades, and test the utility of the observations, reanalysis, and other merged products; III) to characterize the future changes in extreme climate indices are analyzed over mid-21st century (2046-2065); and IV) end-of-21st century (2081-2100). The latest two periods, relative to the reference period 1986–2005 through MME (multi-model ensemble) from 20 statistically downscaled Earth System Models (ESMs).

For the study described in Chapter 2, we developed a methodology to rank 25 downscaled ESMS and their MMEs (MMEs-Dyn(amical) and MMEs-Sta(tistically)) using fourth metrics for evaluating the simulated observed extreme climate indices during 1980-2005. The comprehensive ranked include, namely, Percent Bias (PBIAS), RMSE- observations standard deviation ratio (RSR), refined index of agreement (dr), and the Pearson correlation coefficient (CORR). Our results demonstrate that the multi-model ensembles of downscaled ESMs, showing the best skill in most hydrological basins at the annual and seasonal scale than individual models. In addition, the best options in representing the observed patterns of extreme climate events are, in order, MMEs-Sta, CNRM-CM5, CCSM4, and MRI-CGCM3. However, the majority of downscaled ESMs have poor representation of climate extremes over the Amazon basin for annual and seasonal indices. Also, almost all downscaled ESMs have some difficulty in simulating the warm spell duration index (WSDI), diurnal temperature range (DTR) over the majority of hydrological basins.

Chapter 3 considers the limitations of the gridded observational and downscaled products, we assess the historical and projected changes on daily extremes of temperature and precipitation. Based on the sequence of findings presented in Chapter 2, we selected the MME-Sta from 20 statistically downscaled Earth System Models (ESMs). In most of the hydrological basins, the new generation of reanalysis ERA5 exhibits good agreement with the observed climate extremes at the annual during the last four decades (1980-2016). The performance metrics show a better correspondence of the larger events in ERA5 compared to GMFD that is based on merged from several products (e.g., observation, reanalysis, and satellite). For precipitation indices the best option to capture spatial patterns (climate variability and trends) is ERA5 followed by MSWEP. Our findings reduce the uncertainties relative to accurate climate information in the tropical regions as Brazil, also, could be useful to meteorology, climatology, hydrological and climate-based studies (e.g., impacts from climate change).

The extreme temperature indices (e.g., TXx, TNn, TN10p, TX90p and WSDI) reveal significant warming trends across all datasets (e.g., OBS-BR, ERA5 and GMFD) over Brazil during 1980-2016. For precipitation indices, results show positive trends in annual total wet-day precipitation (PRCPTOT) in northern and southern basins and dry patterns in duration indices (e.g., CDD and CWD) over northern and central basins. Climate projections based on a multi-model ensemble of downscaled indicate that the more extreme temperature/precipitation events will intensify. For example, by the end of the 21st century, the maximum and minimum temperature may increase over Brazil by a wide range up to ~ 1.6 to 3.0 °C (RCP4.5), and from ~ 3.7 to 5.9 °C (RCP8.5), with consequent changes in reduction of cold night (TN10p) and cold days (TX10p) and increasing frequency of warm days (TX90p) and warm nights (TN90p) by the middle and end of the 21st century. In terms of precipitation indices, intensity indices such as RX5day and R95p, and SDII are projected to increase for future scenarios in the majority

areas; on the other hand, total precipitation and consecutive dry days reveals a dry pattern, especially over Amazon, Tocantins, North Atlantic, São Francisco, and Central Atlantic basins

The results of this work will be a breakthrough in understanding and diminishing the uncertainty about the possible impacts of climate extremes events, because an increase in extreme climatic events directly affects people who live in areas vulnerable to hydrometeorological hazards.

In preparing this thesis it became apparent that future research efforts should focus:

- It is necessary for a comprehensive global literature review (e.g., meta-analysis), to establish the current changes of climate extremes to focus in South America, including the robust presence indices to study fires and droughts events.
- Beyond the multi-model ensemble modeling, are there other robust methodologies to reduce the uncertainty of future climate projections?
- Based on the uncertainty of observations, reanalysis, satellite, merged products and Earth System models it is necessary evaluation of the consistency of extremes in gridded temperature/precipitation datasets, with a focus on products with high horizontal resolution.
- Add new projects for future climate projections from regional climate models (RCMs) from the Coordinated Regional Climate Downscaling Experiment (CORDEX), and also include the outputs of Coupled Model Intercomparison Project Phase 6 (CMIP6).
- Establish a composite climate index for quantifying observed/future changes in climate for Brazil, such as the Climate Extremes Index (CEI) developed to study the multidimensional climate changes in the United States

5. REFERENCES

- Aerenson T, Tebaldi C, Sanderson B, Lamarque JF (2018) Changes in a suite of indicators of extreme temperature and precipitation under 1.5 and 2 degrees warming. *Environ Res Lett* 13:. doi: 10.1088/1748-9326/aaafd6
- Aguilar E, Peterson T, Obando P, et al (2005) Changes in precipitation and temperature extremes in Central America and northern South America, 1961–2003. *J Geophys Res* 110:D23107. doi: 10.1029/2005JD006119
- Alexander L (2016) Global observed long-term changes in temperature and precipitation extremes: A review of progress and limitations in IPCC Assessments and beyond. *Weather Clim Extrem* 11:4–16. doi: <http://dx.doi.org/10.1016/j.wace.2015.10.007>
- Alexander L, Arblaster J (2017) Historical and projected trends in temperature and precipitation extremes in Australia in observations and CMIP5. *Weather Clim Extrem* 15:34–56. doi: 10.1016/j.wace.2017.02.001
- Alexander L, Zhang X, Peterson T, et al (2006) Global observed changes in daily climate extremes of temperature and precipitation. *J Geophys Res* 111:1–22. doi: 10.1029/2005jd006290
- Almagro A, Oliveira P, Nearing M, Hagemann S (2017) Projected climate change impacts in rainfall erosivity over Brazil. *Sci Rep* 7:1–12. doi: 10.1038/s41598-017-08298-y
- Almazroui M, Islam M, Saeed F, et al (2017) Assessing the robustness and uncertainties of projected changes in temperature and precipitation in AR5 Global Climate Models over the Arabian Peninsula. *Atmos Res* 194:202–213. doi: 10.1016/j.atmosres.2017.05.005
- Almeida C, Oliveira-Júnior J, Delgado R, et al (2017) Spatiotemporal rainfall and temperature trends throughout the Brazilian Legal Amazon, 1973–2013. *Int J Climatol* 37:2013–2026. doi: 10.1002/joc.4831
- Ambrizzi T, Reboita M, da Rocha R, Llopart M (2019) The state-of-the-art and fundamental aspects of regional climate modeling in South America. *Ann N Y Acad Sci* 1436:98–120. doi: 10.1111/nyas.13932
- Amorim P, Barfus K, Weiss H, Bernhofer C (2014) Trend analysis and uncertainties of mean surface air temperature, precipitation and extreme indices in CMIP3 GCMs in Distrito Federal, Brazil. *Environ Earth Sci* 72:4817–4833. doi: 10.1007/s12665-014-3301-y
- Aragão L, Malhi Y, Roman-Cuesta R, et al (2007) Spatial patterns and fire response of recent Amazonian droughts. *Geophys Res Lett* 34:1–5. doi: 10.1029/2006GL028946
- Avila A, Guerrero F, Escobar Y, Justino F (2019) Recent precipitation trends and floods in the Colombian Andes. *Water* 11:379. doi: 10.3390/w11020379
- Avila A, Justino F, Wilson A, et al (2016) Recent precipitation trends, flash floods and landslides in southern Brazil. *Environ Res Lett* 11:114029. doi: 10.1088/1748-9326/11/11/114029
- Bador M, Donat MG, Geoffroy O, Alexander L V. (2018) Assessing the robustness of future extreme precipitation intensification in the CMIP5 ensemble. *J Clim* 31:6505–6525. doi: 10.1175/JCLI-D-17-0683.1
- Beck H, Pan M, Roy T, et al (2019a) Daily evaluation of 26 precipitation datasets using Stage-IV gauge-radar data for the CONUS. *Hydrol Earth Syst Sci* 23:207–224. doi: 10.5194/hess-23-207-2019
- Beck H, Van Dijk A, Levizzani V, et al (2017a) MSWEP: 3-hourly 0.25° global gridded precipitation (1979–2015) by merging gauge, satellite, and reanalysis data. *Hydrol Earth Syst Sci* 21:589–615. doi: 10.5194/hess-21-589-2017
- Beck H, Vergopolan N, Pan M, et al (2017b) Global-scale evaluation of 22 precipitation datasets using gauge observations and hydrological modeling. *Hydrol Earth Syst Sci* 21:6201–6217. doi: 10.5194/hess-21-6201-2017

- Beck H, Wood E, Pan M, et al (2019b) MSWEP V2 global 3-hourly 0.1° precipitation: methodology and quantitative assessment. *Bull Am Meteorol Soc* 100:473–500. doi: 10.1175/BAMS-D-17-0138.1
- Betts A, Köhler M, Zhang Y (2009) Comparison of river basin hydrometeorology in ERA-Interim and ERA-40 reanalyses with observations. *J Geophys Res Atmos* 114:D02101. doi: 10.1029/2008JD010761
- Betts R, Alfieri L, Caesar J, et al (2018) Changes in climate extremes , fresh water availability and vulnerability to food insecurity projected at 1.5 ° C and 2°C global warming with a higher-resolution global climate model. *Philos Trans A Math Phys Eng Sci* 1–27. doi: 10.1098/rsta.2016.0452
- Bezerra B, Silva L, Santos e Silva C, de Carvalho G (2019) Changes of precipitation extremes indices in São Francisco River Basin, Brazil from 1947 to 2012. *Theor Appl Climatol* 135:565–576. doi: 10.1007/s00704-018-2396-6
- Boulanger J, Martinez F, Segura E (2006) Projection of future climate change conditions using IPCC simulations, neural networks and Bayesian statistics. Part 1: Temperature mean state and seasonal cycle in South America. *Clim Dyn* 27:233–259. doi: 10.1007/s00382-006-0182-0
- Boulanger J, Martinez F, Segura E (2007) Projection of future climate change conditions using IPCC simulations, neural networks and Bayesian statistics. Part 2: Precipitation mean state and seasonal cycle in South America. *Clim Dyn* 27:233–259. doi: 10.1007/s00382-006-0182-0
- Brito S, Cunha A, Cunningham C, et al (2018) Frequency, duration and severity of drought in the Semiarid Northeast Brazil region. *Int J Climatol* 38:517–529. doi: 10.1002/joc.5225
- Burger G, Murdock Q, Werner A, et al (2011) Downscaling Extremes - An Intercomparison of Multiple Statistical Methods for Present Climate. *J Clim* 25:4366–4388. doi: 10.1175/JCLI-D-11-00408.1
- Campozano L, Vázquez-Patiño A, Tenelanda D, et al (2017) Evaluating extreme climate indices from CMIP3&5 global climate models and reanalysis data sets: a case study for present climate in the Andes of Ecuador. *Int J Climatol* 37:363–379. doi: 10.1002/joc.5008
- Carvalho J, Assad E, de Oliveira A, Pinto H (2014) Annual maximum daily rainfall trends in the midwest, southeast and southern Brazil in the last 71 years. *Weather Clim Extrem* 5:7–15. doi: 10.1016/j.wace.2014.10.001
- CEPED-UFSC (2016) Relatório de danos materiais e prejuízos decorrentes de desastres naturais no Brasil: 1995 – 2014. Florianópolis
- CEPED-UFSC (2013) Atlas Brasileiro de Desastres Naturais 1991 a 2012-Volume Brasil, 2nd edn. Florianópolis
- Chaney N, Sheffield J, Villarini G, Wood E (2014) Development of a high-resolution gridded daily meteorological dataset over sub-Saharan Africa: Spatial analysis of trends in climate extremes. *J Clim* 27:5815–5835. doi: 10.1175/JCLI-D-13-00423.1
- Cheng C, Knutson T (2008) On the verification and comparison of extreme rainfall indices from climate models. *J Clim* 21:1605–1621. doi: 10.1175/2007JCLI1494.1
- Chou S, Lyra A, Mourão C, et al (2014a) Evaluation of the Eta Simulations Nested in Three Global Climate Models. *Am J Clim Chang* 03:438–454. doi: 10.4236/ajcc.2014.35039
- Chou S, Lyra A, Mourão C, et al (2014b) Assessment of Climate Change over South America under RCP 4.5 and 8.5 Downscaling Scenarios. *Am J Clim Chang* 03:512–527. doi: 10.4236/ajcc.2014.35043
- Coelho C, Cardoso D, Firpo M (2016a) Precipitation diagnostics of an exceptionally dry event in São Paulo, Brazil. *Theor Appl Climatol* 125:769–784. doi: 10.1007/s00704-015-1540-9

- Coelho C, de Oliveira C, Ambrizzi T, et al (2016b) The 2014 southeast Brazil austral summer drought: regional scale mechanisms and teleconnections. *Clim Dyn* 46:3737–3752. doi: 10.1007/s00382-015-2800-1
- Collins M, Knutti R, Arblaster J, et al (2013) Long-term Climate Change: Projections, Commitments and Irreversibility. In: *Climate Change 2013: The Physical Science Basis. Contribution of Working Group I to the Fifth Assessment Report of the Intergovernmental Panel on Climate Change*. pp 1029–1136
- Cornes R, Jones P (2013) How well does the ERA-Interim reanalysis replicate trends in extremes of surface temperature across Europe? *J Geophys Res Atmos* 118:10,262–10,276. doi: 10.1002/jgrd.50799
- da Silva V, da Silva B, Albuquerque W, et al (2013) Crop coefficient, water requirements, yield and water use efficiency of sugarcane growth in Brazil. *Agric Water Manag* 128:102–109. doi: 10.1016/j.agwat.2013.06.007
- Darela-Filho J, Lapola D, Torres R, Lemos M (2016) Socio-climatic hotspots in Brazil: how do changes driven by the new set of IPCC climatic projections affect their relevance for policy? *Clim Change* 136:413–425. doi: 10.1007/s10584-016-1635-z
- de Lima J, Alcântara C (2019) Comparison between ERA Interim/ECMWF, CFSR, NCEP/NCAR reanalysis, and observational datasets over the eastern part of the Brazilian Northeast Region. *Theor Appl Climatol* 138:2021–2041. doi: 10.1007/s00704-019-02921-w
- Debortoli N, Camarinha P, Marengo J, Rodrigues R (2017) An index of Brazil's vulnerability to expected increases in natural flash flooding and landslide disasters in the context of climate change. *Nat Hazards* 86:557–582. doi: 10.1007/s11069-016-2705-2
- Dee D, Balmaseda M, Balsamo G, et al (2014) Toward a consistent reanalysis of the climate system. *Bull Am Meteorol Soc* 95:1235–1248. doi: 10.1175/BAMS-D-13-00043.1
- Dee D, Uppala S, Healy S, et al (2011) The ERA-Interim reanalysis: configuration and performance of the data assimilation system. *Q J R Meteorol Soc* 137:553–597. doi: 10.1002/qj.828
- Dereczynski C, Silva W, Marengo J (2013) Detection and projections of climate change in Rio de Janeiro, Brazil. *Am J Clim Chang* 02:25–33. doi: 10.4236/ajcc.2013.21003
- Donat M, Alexander L, Yang H, et al (2013a) Updated analyses of temperature and precipitation extreme indices since the beginning of the twentieth century: The HadEX2 dataset. *J Geophys Res Atmos* 118:2098–2118. doi: 10.1002/jgrd.50150
- Donat M, Alexander L, Yang H, et al (2013b) Global land-based datasets for monitoring climatic extremes. *Bull Am Meteorol Soc* 94:997–1006. doi: 10.1175/BAMS-D-12-00109.1
- Donat M, Lowry A, Alexander L, et al (2016) More extreme precipitation in the world's dry and wet regions. *Nat Clim Chang* 6:508–513. doi: 10.1038/nclimate2941
- Donat M, Sillmann J, Wild S, et al (2014) Consistency of temperature and precipitation extremes across various global gridded in situ and reanalysis datasets. *J Clim* 27:5019–5035. doi: 10.1175/JCLI-D-13-00405.1
- Dosio A, Jones R, Jack C, et al (2019) What can we know about future precipitation in Africa? Robustness, significance and added value of projections from a large ensemble of regional climate models. *Clim Dyn*. doi: 10.1007/s00382-019-04900-3
- Dufek A, Ambrizzi T (2008) Precipitation variability in São Paulo State, Brazil. *Theor Appl Climatol* 93:167–178. doi: 10.1007/s00704-007-0348-7
- Dufek A, Ambrizzi T, Da Rocha R (2008) Are reanalysis data useful for calculating climate indices over South America? *Ann N Y Acad Sci* 1146:87–104. doi: 10.1196/annals.1446.010
- Espinoza J, Marengo J, Ronchail J, et al (2014) The extreme 2014 flood in south-western

- Amazon basin: the role of tropical-subtropical South Atlantic SST gradient. *Environ Res Lett* 9:1–9. doi: 10.1088/1748-9326/9/12/124007
- Feron S, Cordero R, Damiani A, et al (2019) Observations and Projections of Heat Waves in South America. *Sci Rep* 9:1–15. doi: 10.1038/s41598-019-44614-4
- Fischer E, Beyerle U, Knutti R (2013) Robust spatially aggregated projections of climate extremes. *Nat Clim Chang* 3:1033–1038. doi: 10.1038/nclimate2051
- Fotso-Nguemo T, Chamani R, Yepdo Z, et al (2018) Projected trends of extreme rainfall events from CMIP5 models over Central Africa. *Atmos Sci Lett* 19:1–8. doi: 10.1002/asl.803
- Fundação Brasileira para o Desenvolvimento Sustentável - FBDS (2009) Climate change and extreme events in Brazil. DaGema Comunicação
- Gao L, Bernhardt M, Schulz K (2012) Elevation correction of ERA-Interim temperature data in complex terrain. *Hydrol Earth Syst Sci* 16:4661–4673. doi: 10.5194/hess-16-4661-2012
- Geirinhas J, Trigo R, Libonati R, et al (2018) Climatic and synoptic characterization of heat waves in Brazil. *Int J Climatol* 38:1760–1776. doi: 10.1002/joc.5294
- Giorgi F (2006) Climate change hot-spots. *Geophys Res Lett* 33:1–4. doi: 10.1029/2006GL025734
- Giorgi F, Raffaele F, Coppola E (2019) The response of precipitation characteristics to global warming from global and regional climate projections. *Earth Syst Dyn Discuss* 10:73–89. doi: 10.5194/esd-2018-64
- Gloor M, Barichivich J, Ziv G, et al (2015) Recent Amazon climate as background for possible ongoing and future changes of Amazon humid forests. *Global Biogeochem Cycles* 29:1384–1399. doi: 10.1002/2014GB005080
- Grant PR (2017) Evolution, climate change, and extreme events. *Science* (80-) 357:3–5. doi: 10.1126/science.aao2067
- Gulizia C, Camilloni I (2014) Comparative analysis of the ability of a set of CMIP3 and CMIP5 global climate models to represent precipitation in South America. doi: 10.1002/joc.4005
- Gupta H, Sorooshian S, Yapo P (1999) Status of automatic calibration for hydrologic models: Comparison with multilevel expert calibration. *J Hydrol Eng* 4:135–143. doi: 10.1061/(ASCE)1084-0699(1999)4:2(135)
- Guyennon N, Romano E, Portoghesi I, et al (2013) Benefits from using combined dynamical-statistical downscaling approaches - Lessons from a case study in the Mediterranean region. *Hydrol Earth Syst Sci* 17:705–720. doi: 10.5194/hess-17-705-2013
- Haylock M, Peterson T, Alves L, et al (2006) Trends in total and extreme South American rainfall in 1960–2000 and links with sea surface temperature. *J Clim* 19:1490–1512. doi: 10.1175/JCLI3695.1
- Hersbach H, Rosnay P, Bell B, et al (2018) Operational global reanalysis: progress, future directions and synergies with NWP. ECMWF Report. 65 pp
- Hoegh-Guldberg O, Jacob D, Taylor M, et al (2018) Impacts of 1.5°C global warming on natural and human systems. In: *Global Warming of 1.5°C. An IPCC Special Report on the Impacts of Global Warming of 1.5°C above Pre-Industrial Levels*
- Hoeppe P (2016) Trends in weather related disasters - Consequences for insurers and society. *Weather Clim Extrem* 11:70–79. doi: 10.1016/j.wace.2015.10.002
- Hoffmann L, Günther G, Li D, et al (2019) From ERA-Interim to ERA5: The considerable impact of ECMWF's next-generation reanalysis on Lagrangian transport simulations. *Atmos Chem Phys* 19:3097–3214. doi: 10.5194/acp-19-3097-2019
- IPCC (2018) Summary for Policymakers. In: *Global Warming of 1.5°C. An IPCC Special Report on the impacts of global warming of 1.5°C above pre-industrial levels and related*

- global greenhouse gas emission pathways. Geneva, Switzerland
- Jiang Z, Li W, Xu J, Li L (2015) Extreme precipitation indices over China in CMIP5 models. Part I: Model evaluation. *J Clim* 28:8603–8619. doi: 10.1175/JCLI-D-15-0099.1
- Jones PW (1999) First- and Second-Order Conservative Remapping Schemes for Grids in Spherical Coordinates. *Mon Weather Rev* 127:2204–2210. doi: 10.1175/1520-0493(1999)127<2204:FASOCR>2.0.CO;2
- Jong P, Augusto C, Tanajura S, et al (2018) Hydroelectric production from Brazil's São Francisco River could cease due to climate change and inter-annual variability. *Sci Total Environ* 634:1540–1553. doi: 10.1016/j.scitotenv.2018.03.256
- Kendall M (1975) Rank correlation methods, 4th edn. London
- Knutti R, Furrer R, Tebaldi C, et al (2010) Challenges in combining projections from multiple climate models. *J Clim* 23:2739–2758. doi: 10.1175/2009JCLI3361.1
- Kusunoki S, Arakawa O (2015) Are CMIP5 models better than CMIP3 models in simulating precipitation over East Asia? *J Clim* 28:5601–5621. doi: 10.1175/JCLI-D-14-00585.1
- Lelieveld J, Proestos Y, Hadjinicolaou P, et al (2016) Strongly increasing heat extremes in the Middle East and North Africa (MENA) in the 21st century. *Clim Change* 137:245–260. doi: 10.1007/s10584-016-1665-6
- Liao X, Xu W, Zhang J, et al (2019) Global exposure to rainstorms and the contribution rates of climate change and population change. *Sci Total Environ* 663:644–653. doi: 10.1016/j.scitotenv.2019.01.290
- Liebmann B, Allured D (2006) Daily precipitation grids for South America. *Bull Am Meteorol Soc* 87:1095. doi: 10.1175/1520-0477(2006)87[1095:DPGFSA]2.0.CO;2
- Lin L, Wang Z, Xu Y, et al (2018) Larger Sensitivity of Precipitation Extremes to Aerosol Than Greenhouse Gas Forcing in CMIP5 Models. *J Geophys Res Atmos* 123:8062–8073. doi: 10.1029/2018JD028821
- Liu W, Zhang M, Wang S, et al (2013) Changes in precipitation extremes over Shaanxi Province, northwestern China, during 1960–2011. *Quat Int* 313–314:118–129. doi: 10.1016/j.quaint.2013.06.033
- Llopart M, Simões M, Rosmeri R (2019) Assessment of multimodel climate projections of water resources over South America CORDEX domain. *Clim Dyn*. doi: 10.1007/s00382-019-04990-z
- López-Franca N, Zaninelli P, Carril A, et al (2016) Changes in temperature extremes for 21st century scenarios over South America derived from a multi-model ensemble of regional climate models. *Clim Res* 68:151–167. doi: 10.3354/cr01393
- Luo H, Ge F, Yang K, et al (2019) Assessment of ECMWF reanalysis data in complex terrain: Can the CERA-20C and ERA-Interim data sets replicate the variation in surface air temperatures over Sichuan, China? *Int J Climatol* 1–16. doi: 10.1002/joc.6175
- Lyra A, Tavares P, Chou S, et al (2018) Climate change projections over three metropolitan regions in Southeast Brazil using the non-hydrostatic Eta regional climate model at 5-km resolution. *Theor Appl Climatol* 132:663–682. doi: 10.1007/s00704-017-2067-z
- Mann HB (1945) Nonparametric tests against trend. *Econometrica* 13:245–259. doi: 10.2307/1907187
- Marelle L, Myhre G, Hodnebrog Ø, et al (2018) The Changing Seasonality of Extreme Daily Precipitation. *Geophys Res Lett* 45:352. doi: 10.1029/2018GL079567
- Marengo J, Alves L, Alvala R, et al (2018a) Climatic characteristics of the 2010–2016 drought in the semiarid Northeast Brazil region. *An Acad Bras Cienc* 90:1973–1985. doi: 10.1590/0001-3765201720170206
- Marengo J, Ambrizzi T, da Rocha R, et al (2010a) Future change of climate in South America in the late twenty-first century: Intercomparison of scenarios from three regional climate models. *Clim Dyn* 35:1089–1113. doi: 10.1007/s00382-009-0721-6

- Marengo J, Camargo C (2008) Surface air temperature trends in Southern Brazil for 1960–2002. *Int J Climatol* 28:893–904. doi: 10.1002/joc.1584
- Marengo J, Chou S, Kay G, et al (2012) Development of regional future climate change scenarios in South America using the Eta CPTEC/HadCM3 climate change projections: Climatology and regional analyses for the Amazon, São Francisco and the Paraná River basins. *Clim Dyn* 38:1829–1848. doi: 10.1007/s00382-011-1155-5
- Marengo J, Jones B, Alves L, et al (2009) Future change of temperature and precipitation extremes in south america as derived from the PRECIS regional climate modeling system. *Int J Climatol* 29:2241–2255. doi: 10.1002/joc.1863
- Marengo J, Rusticucci M, Penalba O, Renom M (2010b) An intercomparison of observed and simulated extreme rainfall and temperature events during the last half of the twentieth century: Part 2: Historical trends. *Clim Change* 98:509–529. doi: 10.1007/s10584-009-9743-7
- Marengo J, Souza C, Thonicke K, et al (2018b) Changes in Climate and Land Use Over the Amazon Region: Current and Future Variability and Trends. *Front Earth Sci* 6:1–21. doi: 10.3389/feart.2018.00228
- Marengo J, Torres R, Alves L (2017) Drought in Northeast Brazil—past, present, and future. *Theor Appl Climatol* 129:1189–1200. doi: 10.1007/s00704-016-1840-8
- McPhillips LE, Chang H, Chester M V., et al (2018) Defining Extreme Events: A Cross-Disciplinary Review. *Earth's Futur* 6:441–455. doi: 10.1002/2017EF000686
- MCTI (2016) Third National Communication of Brazil to the United Nations framework convention on climate change, Ministry o. Brasilia
- Missirian A, Schlenker W (2017) Asylum applications respond to temperature fluctuations. *Science* (80-) 358:1610–1614. doi: 10.1126/science.aao0432
- Mora C, Spirandelli D, Franklin E, et al (2018) Broad threat to humanity from cumulative climate hazards intensified by greenhouse gas emissions. *Nat Clim Chang* 8:1062–1071. doi: 10.1038/s41558-018-0315-6
- Moriassi D, Arnold J, Van Liew M, et al (2007) Model evaluation guidelines for systematic quantification of accuracy in watershed simulations. *Trans ASABE* 50:885–900. doi: 10.13031/2013.23153
- Murara P, Acquavotta F, Garzena D, Fratianni S (2018) Daily precipitation extremes and their variations in the Itajaí River Basin, Brazil. *Meteorol Atmos Phys* 131:1145–1156. doi: 10.1007/s00703-018-0627-0
- Mysiak J, Torresan S, Bosello F, et al (2018) Climate risk index for Italy. *Phil Trans R Soc A* 376:. doi: 10.1098/rsta.2017.0305
- Nguyen P, Thorstensen A, Sorooshian S, et al (2017) Evaluation of CMIP5 Model Precipitation Using PERSIANN-CDR. *J Hydrometeorol* 18:2313–2330. doi: 10.1175/JHM-D-16-0201.1
- Oliveira P, Silva C, Lima K (2017) Climatology and trend analysis of extreme precipitation in subregions of Northeast Brazil. *Theor Appl Climatol* 130:77–90. doi: 10.1007/s00704-016-1865-z
- Oliveira P, Silva C, Lima K (2014) Linear trend of occurrence and intensity of heavy rainfall events on Northeast Brazil. *Atmos Sci Lett* 15:172–177. doi: 10.1002/asl2.484
- Ongoma V, Chen H, Gao C (2018a) Evaluation of CMIP5 twentieth century rainfall simulation over the equatorial East Africa. *Theor Appl Climatol* 135:893–910. doi: 10.1007/s00704-018-2392-x
- Ongoma V, Chen H, Gao C, et al (2018b) Future changes in climate extremes over Equatorial East Africa based on CMIP5 multimodel ensemble. *Nat Hazards* 90:901–920. doi: 10.1007/s11069-017-3079-9
- Parker WS (2013) Ensemble modeling, uncertainty and robust predictions. Wiley Interdiscip

- Rev Clim Chang. doi: 10.1002/wcc.220
- Raghavan S, Hur J, Liong S (2018) Evaluations of NASA NEX-GDDP data over Southeast Asia: present and future climates. *Clim Change* 148:503–518. doi: 10.1007/s10584-018-2213-3
- Rao V, Franchito S, Santo C, Gan M (2016) An update on the rainfall characteristics of Brazil: Seasonal variations and trends in 1979–2011. *Int J Climatol* 36:291–302. doi: 10.1002/joc.4345
- Ray D, Gerber J, Macdonald G, West P (2015) Climate variation explains a third of global crop yield variability. *Nat Commun* 6:1–9. doi: 10.1038/ncomms6989
- Rosso F, Boiaski N, Ferraz S, et al (2015) Trends and decadal variability in air temperature over Southern Brazil. *Am J Environ Eng* 5:85–95. doi: 10.5923/s.ajee.201501.12
- Rozante J, Moreira D, de Goncalves LG, Vila D (2010) Combining TRMM and Surface Observations of Precipitation: Technique and Validation over South America. *Weather Forecast* 25:885–894. doi: 10.1175/2010waf2222325.1
- Rusticucci M, Marengo J, Penalba O, Renom M (2010) An intercomparison of model-simulated in extreme rainfall and temperature events during the last half of the twentieth century. Part 1: Mean values and variability. *Clim Change* 98:493–508. doi: 10.1007/s10584-009-9742-8
- Santos M, Fonseca A, Fragoso M, Santos JA (2018) Recent and future changes of precipitation extremes in mainland Portugal. *Theor Appl Climatol* 2012:1–15. doi: 10.1007/s00704-018-2667-2
- Santos M, Fragoso M, Santos J (2017) Regionalization and susceptibility assessment to daily precipitation extremes in mainland Portugal. *Appl Geogr* 86:128–138. doi: 10.1016/j.apgeog.2017.06.020
- Schoof J, Robeson S (2016) Projecting changes in regional temperature and precipitation extremes in the United States. *Weather Clim Extrem* 11:28–40. doi: 10.1016/j.wace.2015.09.004
- Seinfeld J, Bretherton C, Carslaw K, et al (2016) Improving our fundamental understanding of the role of aerosol–cloud interactions in the climate system. *Proc Natl Acad Sci* 113:5781–5790. doi: 10.1073/pnas.1514043113
- Sen PK (1968) Estimates of the regression coefficient based on Kendall's tau. *J Am Stat Assoc* 63:1379–1389. doi: 10.2307/2285891
- Sheffield J, Goteti G, Wood E, et al (2006) Development of a 50-Year High-Resolution Global Dataset of Meteorological Forcings for Land Surface Modeling. *J Clim* 19:3088–3111. doi: <https://doi.org/10.1175/JCLI3790.1>
- Sillmann J, Kharin V, Zhang X, et al (2013a) Climate extremes indices in the CMIP5 multimodel ensemble: Part 1. Model evaluation in the present climate. *J Geophys Res Atmos* 118:1716–1733. doi: 10.1002/jgrd.50203
- Sillmann J, Kharin V, Zwiers W, et al (2013b) Climate extremes indices in the CMIP5 multimodel ensemble: Part 2. Future climate projections. *J Geophys Res Atmos* 118:2473–2493
- Silva Dias M, Dias J, Carvalho L, et al (2013) Changes in extreme daily rainfall for São Paulo, Brazil. *Clim Change* 116:705–722. doi: 10.1007/s10584-012-0504-7
- Silva P, Silva C, Spyrides M, Andrade L (2018) Precipitation and air temperature extremes in the Amazon and northeast Brazil. *Int J Climatol* 1–17. doi: 10.1002/joc.5829
- Silva W, Dereczynski C, Chou S, Cavalcanti I (2014) Future Changes in Temperature and Precipitation Extremes in the State of Rio de Janeiro (Brazil). *Am J Clim Chang* 3:353–365
- Skansi M, Brunet M, Sigró J, et al (2013) Warming and wetting signals emerging from analysis of changes in climate extreme indices over South America. *Glob Planet Change*

- 100:295–307. doi: 10.1016/j.gloplacha.2012.11.004
- Soares D, Lee H, Loikith P, et al (2017) Can significant trends be detected in surface air temperature and precipitation over South America in recent decades? *Int J Climatol* 37:1483–1493. doi: 10.1002/joc.4792
- Son J-Y, Gouveia N, Bravo M, et al (2016) The impact of temperature on mortality in a subtropical city: effects of cold, heat, and heat waves in São Paulo, Brazil. *Int J Biometeorol* 60:113–121. doi: 10.1007/s00484-015-1009-7
- Tang J, Niu X, Wang S, et al (2016) Statistical downscaling and dynamical downscaling of regional climate in China: Present climate evaluations and future climate projections. *J Geophys Res Atmos* 121:2110–2129. doi: 10.1002/2015JD023977
- Taylor K, Stouffer R, Meehl G (2012) An overview of CMIP5 and the experiment design. *Bull Am Meteorol Soc* 93:485–498. doi: 10.1175/BAMS-D-11-00094.1
- Tebaldi C, Arblaster JM, Knutti R (2011) Mapping model agreement on future climate projections. *Geophys Res Lett* 38:1–5. doi: 10.1029/2011GL049863
- Thrasher B, Maurer E, McKellar C, Duffy P (2012) Technical Note: Bias correcting climate model simulated daily temperature extremes with quantile mapping. *Hydrol Earth Syst Sci* 16:3309–3314. doi: 10.5194/hess-16-3309-2012
- Tomasella J, Pinho P, Borma L, et al (2013) The droughts of 1997 and 2005 in Amazonia: Floodplain hydrology and its potential ecological and human impacts. *Clim Change* 116:723–746. doi: 10.1007/s10584-012-0508-3
- Torres R, Marengo J (2013) Uncertainty assessments of climate change projections over South America. *Theor Appl Climatol* 112:253–272. doi: 10.1007/s00704-012-0718-7
- Torres R, Marengo J (2014) Climate change hotspots over South America: from CMIP3 to CMIP5 multi-model datasets. *Theor Appl Climatol* 117:579–587. doi: 10.1007/s00704-013-1030-x
- Valverde M, Marengo J (2014) Extreme rainfall indices in the hydrographic basins of Brazil. *Open J Mod Hydrol* 4:10–26. doi: <http://dx.doi.org/10.4236/ojmh.2014.41002>
- Vincent L, Peterson T, Barros V, et al (2005) Observed trends in indices of daily temperature extremes in South America 1960–2000. *J Clim* 18:5011–5023. doi: 10.1175/JCLI3589.1
- Wang R, Li C (2015) Spatiotemporal analysis of precipitation trends during 1961–2010 in Hubei province, central China. *Theor Appl Climatol* 124:385–389. doi: 10.1007/s00704-015-1426-x
- Wang S, Zhang X, Liu Z, Wang D (2012) Trend analysis of precipitation in the Jinsha River Basin in China. *J Hydrometeorol* 14:290–303. doi: 10.1175/JHM-D-12-033.1
- Wilby R, Dawson C (2013) The statistical downscaling model: Insights from one decade of application. *Int J Climatol* 33:1707–1719. doi: 10.1002/joc.3544
- Willmott C, Robeson S, Matsuura K (2012) A refined index of model performance. *Int J Climatol* 32:2088–2094. doi: 10.1002/joc.2419
- Willmott C, Robeson S, Matsuura K, Ficklin D (2015) Assessment of three dimensionless measures of model performance. *Environ Model Softw* 73:167–174. doi: 10.1016/j.envsoft.2015.08.012
- Xavier A, King C, Bridget S (2017) An update of Xavier, King and Scanlon (2016) daily precipitation gridded data set for the Brazil. pp 562–569
- Xavier A, King W, Scanlon B (2015) Daily gridded meteorological variables in Brazil (1980–2013). *Int J Climatol* 36:2644–2659. doi: 10.1002/joc.4518
- Xu K, Wu C, Hu B (2019) Projected changes of temperature extremes over nine major basins in China based on the CMIP5 multimodel ensembles. *Stoch Environ Res Risk Assess* 33:321–339. doi: 10.1007/s00477-018-1569-2
- Yhang Y Bin, Sohn SJ, Jung IW (2017) Application of Dynamical and Statistical Downscaling to East Asian Summer Precipitation for Finely Resolved Datasets. *Adv*

- Meteorol 2017:. doi: 10.1155/2017/2956373
- Yin L, Fu R, Shevliakova E, Dickinson RE (2013) How well can CMIP5 simulate precipitation and its controlling processes over tropical South America? *Clim Dyn* 41:3127–3143. doi: 10.1007/s00382-012-1582-y
- You Q, Jiang Z, Wang D, et al (2017) Simulation of temperature extremes in the Tibetan Plateau from CMIP5 models and comparison with gridded observations. *Clim Dyn* 51:355–369. doi: 10.1007/s00382-017-3928-y
- Yue S, Pilon P, Cavadas G (2002) Power of the Mann–Kendall and Spearman’s rho tests for detecting monotonic trends in hydrological series. *J Hydrol* 259:254–271. doi: 10.1016/S0022-1694(01)00594-7
- Zhang X, Alexander L, Hegerl G, et al (2011) Indices for monitoring changes in extremes based on daily temperature and precipitation data. *Wiley Interdiscip Rev Clim Chang* 2:851–870. doi: 10.1002/wcc.147
- Zhang X, Yang F (2004) *RClimDex (1.0)—User Manual*. 1–22
- Zhang X, Zwiers F, Hegerl G, et al (2007) Detection of human influence on twentieth-century precipitation trends. *Nature* 448:461–465. doi: 10.1038/nature06025
- Zhang Y, You Q, Chen C, et al (2018) Evaluation of Downscaled CMIP5 Coupled with VIC Model for Flash Drought Simulation in a Humid Subtropical Basin, China. *J Clim* 31:1075–1090. doi: 10.1175/JCLI-D-17-0378.1
- Zhou B, Wen Q, Xu Y, et al (2014) Projected changes in temperature and precipitation extremes in China by the CMIP5 multimodel ensembles. *J Clim* 27:6591–6611. doi: 10.1175/JCLI-D-13-00761.1
- Zhou M, Zhou G, Lv X, et al (2018) Global warming from 1.5°C to 2°C will lead to increase in precipitation intensity in China. *Int J Climatol* 1–11. doi: 10.1002/joc.5956
- Zilli M, Carvalho L, Liebmann B, Silva Dias M (2017) A comprehensive analysis of trends in extreme precipitation over southeastern coast of Brazil. *Int J Climatol* 37:2269–2279. doi: 10.1002/joc.4840